Towards Engineering *Rhodococcus* for Biodiesel Production from Lignin

Hannah Gulzar Somani

Department of Chemistry
Imperial College London

Submitted in partial fulfilment of the requirements for the degree of Doctor of Philosophy

June 2018

Declaration

All work presented in this thesis is my own, unless otherwise stated. Any that is not my own has been appropriately referenced.

The copyright of this thesis rests with the author and is made available under a Creative Commons Attribution Non-Commercial No Derivatives licence. Researchers are free to copy, distribute or transmit the thesis on the condition that they attribute it, that they do not use it for commercial purposes and that they do not alter, transform or build upon it. For any reuse or redistribution, researchers must make clear to others the licence terms of this work.

Abstract

There is a pressing need for sustainable liquid transportation fuels to address climate change concerns and meet increasing global energy demand. Biofuels offer a low carbon alternative to fossil fuels, and microbial biodiesel has the potential to play a key role in their future.

This thesis first assesses the economic and environmental considerations associated with producing biodiesel from lignin on a large scale. The analysis concludes that it could be commercially viable by sourcing underutilised waste lignin as a feedstock and using existing pulp mill or biorefinery infrastructure in the process, bringing costs in line with current cellulosic bioethanol production at around $140 per barrel of oil equivalent.

Based on this conclusion the oleaginous bacteria *Rhodococcus opacus* PD630 was then selected to explore the potential use of this genus of microorganisms to carry out this process. We demonstrate its capacity to metabolise, and accumulate intracellular lipids, when provided with lignin breakdown model compounds as a sole carbon source under nitrogen limiting conditions. Cells reached 22% lipid content (dry weight) after 36 hours when grown on 4-hydroxybenzoic acid, 14% after 48 hours on vanillic acid and were able to grow on, but not synthesise lipids from, vanillin.

Although this demonstrated that the strain could use lignin breakdown products for lipid biosynthesis it was unable use untreated Kraft lignin for this purpose. To remedy this we sought to express the DypB lignin peroxidase from the ligninolytic strain, *R. jostii* RHA1, in *R. opacus* PD630 to catalyse depolymerisation. Attempts at plasmid construction, cloning and protein expression were challenging, and creating a single organism able to perform the whole bioconversion pathway proved elusive.

A mixed enzymatic and microbial approach using *T. versicolor* laccase was more successful. The laccase catalysed lignin depolymerisation, in the presence of syringaldehyde as a redox mediator, allowing *R. opacus* PD630 to metabolise the breakdown products and accumulate lipids. A 96-hour depolymerisation reaction followed by fermentation yielded 20% cell lipid content after 60 hours. Combining these steps into a simultaneous process slowed culture growth, but cells reached a higher lipid content of 23% after 72 hours.

These results demonstrate that a mixed approach of enzymatic lignin depolymerisation and microbial fermentation is a potential route for converting waste lignin, a renewable feedstock, into biodiesel, a sustainable alternative to fossil fuels.

Acknowledgements

My grateful thanks are due to Professor Tony Cass, my supervisor, for his guidance over the last four years. This PhD could not have been accomplished without his valuable knowledge and contribution, particularly in steering the project through ups and downs.

I would also like to thank Dr John Hassard, my co-supervisor and CEO of Q Analytica, for generously sponsoring and setting the wider context of the project.

Thanks to past and present members of the Cass group who were always on hand to provide help, both in and out of the lab, and who made my time at Imperial far more enjoyable.

And finally to my family for their unwavering support and encouragement.

Table of Contents

List of figures *8*

List of tables *10*

Abbreviations *11*

1 Literature Review ***13***

1.1 Introduction and motivation for lignin-based biofuels **13**

1.2 Biofuels **13**

1.2.1 Biofuels classification 14

1.3 Biofuel vs conventional fuel **15**

1.3.1 Fuel properties 15

1.3.2 Microbial biodiesel 18

1.4 Biomass composition **19**

1.4.1 Breakdown of lignocellulosic biomass 20

1.5 Lignin **21**

1.5.1 Structure and synthesis 21

1.5.2 Breakdown 23

1.6 Microbial lignin depolymerisation **24**

1.6.1 Peroxidases 24

1.6.2 Laccases 25

1.7 Aromatic degradation **28**

1.7.1 β-ketoadipate pathway 28

1.8 Microbial lipids **31**

1.8.1 Bacterial lipid synthesis 31

1.9 Lignin to lipid bioconversion by *Rhodococcus* species **32**

1.9.1 *Rhodococcus jostii* RHA1 32

1.9.2 *Rhodococcus opacus* PD630 33

1.10 Outline of project **34**

2 Feasibility of lignin-based biofuels ***36***

2.1 Introduction **36**

2.2 Demand for biofuels **37**

2.2.1 Current biofuel production 37

2.2.2 Biofuel production forecasts 38

2.3 Environmental considerations **38**

2.3.1 Climate change 38

2.3.2 Sustainability 40

2.4 Policy support **42**

2.5 Economics of biofuel production **43**

2.5.1 Fatty acid conversion 44

2.5.2 Lignocellulosic biomass conversion 45

2.5.3 Lignin conversion 46

2.5.4 Microbial lignin conversion 47

2.6 Lignin as a feedstock **48**

2.6.1 Challenges 48

2.6.2 Sources of lignin 48
2.6.3 Potential scale of biofuel production from lignin 50
2.6.4 Value of lignin in alternative uses 51
2.7 Companies pursuing advanced biofuels 53
2.8 Conclusions 54
3 Materials and methods 56
3.1 Materials 56
3.2 General cell techniques and growth media 56
3.2.1 Competent cell preparation and transformation 57
3.3 Microbial growth experiments 58
3.4 Lipid accumulation experiments 58
3.4.1 Lipid extraction 58
3.5 General DNA techniques 59
3.5.1 Plasmid DNA isolation 59
3.5.2 Gel electrophoresis and DNA purification 59
3.6 Plasmid construction 60
3.6.1 PCR 60
3.6.2 Gibson assembly 61
3.6.3 Annealing single stranded DNA 61
3.6.4 gBlock 61
3.6.5 Site directed mutagenesis 62
3.6.6 Sequence verification 62
3.7 Protein expression 64
3.7.1 Growth, induction and cell lysis 64
3.7.2 SDS-PAGE 64
3.8 Laccase experiments 65
3.8.1 Enzyme activity 65
3.8.2 Laccase treatment of Kraft lignin 65
3.8.3 Simultaneous depolymerisation and metabolism 66
4 PD630 growth on lignin and lignin breakdown model compounds 68
4.1 Introduction 68
4.2 Results and discussion 69
4.2.1 PD630 and lignin 69
4.2.2 PD630 and lignin breakdown model compounds 70
4.2.3 Relationship between growth and lipid storage 77
4.3 Conclusions 78
5 Expression of lignin peroxidase DypB in R. opacus PD630 80
5.1 Introduction 80
5.2 Results and discussion 80
5.2.1 Approach 80
5.2.2 Plasmid construction 81
5.2.3 Protein expression 85
5.2.4 Plasmid alteration: site directed mutagenesis 90
5.3 Conclusions 92

6 Degradation of Kraft lignin using laccase and PD630 94

6.1 Introduction 94

6.2 Results and discussion 95

6.2.1 Laccase activity 95
6.2.2 Laccase oxidation of Kraft lignin 96
6.2.3 PD630 growth on laccase-treated Kraft lignin 96
6.2.4 PD630 lipid accumulation on laccase-treated Kraft lignin 98
6.2.5 Simultaneous depolymerisation and metabolism 99

6.3 Conclusions 102

7 Conclusions and future work 104

7.1 Summary 104

7.2 Commercial potential 105

7.3 Future work 106

7.3.1 PD630 lignin depolymerisation 106
7.3.2 Combined enzymatic and microbial approach 106

7.4 Concluding remarks 108

8 References 109

9 Appendix 125

9.1 Plasmid DNA sequences 125

List of figures

Figure 1.1: Transesterification reaction 18
Figure 1.2: Representation of lignocellulosic biomass 20
Figure 1.3: Structure of lignin monomers 22
Figure 1.4: Common monomer linkages found in lignin 23
Figure 1.5: Structure of the DypB monomer from *R. jostii* RHA1 25
Figure 1.6: Copper ions in the laccase enzyme and their coordination 26
Figure 1.7: Structure of *T. versicolor* laccase 26
Figure 1.8: Schematic of a laccase mediator system 27
Figure 1.9: Structures of laccase mediators 27
Figure 1.10: Pathways involved in monolignol degradation in *Rhodococcus* bacteria 30
Figure 1.11: Electron microscopy image of *R. opacus* PD630 showing intracellular lipid inclusions 33
Figure 2.1: Global biofuel production 2006-2016 37
Figure 2.2: GREET biofuel life cycle analysis 39
Figure 2.3: Global land use for bioenergy 41
Figure 2.4: ICE Brent crude oil front month price ($ per barrel) from January 2008 to present 42
Figure 2.5: Biofuel production costs from various feedstocks. 45
Figure 2.6: Proposed manufacturing framework 47
Figure 2.7: Potential applications for lignin 51
Figure 2.8: Lignin production vs lignin utilisation potential 52
Figure 4.1: Structure of lignin model compounds 69
Figure 4.2: Growth of *R. opacus* PD630 on Kraft lignin and glucose as the sole carbon source 70
Figure 4.3: Growth of *R. opacus* PD630 on the lignin model compounds 4-HBA, VanA and vanillin as the sole carbon source 71
Figure 4.4: Growth of *R. opacus* PD630 cells already adapted to using lignin model compounds as a sole carbon source 73
Figure 4.5: Growth and lipid accumulation of *R. opacus* PD630 on glucose and lignin breakdown model compounds 74
Figure 4.6: *R. opacus* PD630 growth and lipid accumulation in minimal media supplemented with 0.25% glucose, 0.25% vanillin and 0.05% nitrogen 75
Figure 4.7: *R. opacus* PD630 growth and lipid accumulation in minimal media supplemented with 0.25% VanA, 0.25% vanillin and 0.05% nitrogen 76
Figure 4.8: *R. opacus* PD630 growth and lipid accumulation in minimal media supplemented with 0.5% 4-HBA and 0.05% nitrogen 77
Figure 5.1: Plasmid maps of pNV18.1 (the *E. coli – Rhodococcus* shuttle vector), and pUCIDT-AMP containing the *DypB* gene. 81
Figure 5.2: Gibson assembly method 82
Figure 5.3: Agarose gels of PCR products 83
Figure 5.4: Sequencing results 84
Figure 5.5: Plasmid map of pNV18.1-ptac-DypB 85
Figure 5.6: SDS-PAGE comparing wildtype (wt) and recombinant (DypB) TOP10 *E. coli* 86
Figure 5.7: SDS-PAGE comparing wildtype (wt) and recombinant (DypB) TOP10 *E. coli* with longer induction time 87
Figure 5.8: SDS-PAGE comparing wildtype (wt) and recombinant (DypB) BL21 *E. coli* 88
Figure 5.9: SDS-PAGE comparing wildtype (wt) and recombinant (DypB) BL21 *E. coli* 89
Figure 5.10: SDS-PAGE comparing wildtype (wt) and recombinant (DypB) PD630 90
Figure 5.11: DNA sequence of region targeted for site directed mutagenesis 90
Figure 5.12: SDM sequencing results 91
Figure 6.1: Structure of syringaldehyde 95
Figure 6.2: *T. versicolor* laccase enzyme activity 96
Figure 6.3: Growth of *R. opacus* PD630 on Kraft lignin treated with *T. versicolor* laccase 97
Figure 6.4: Growth of PD630 cultures already adapted to growth on Kraft lignin that has been treated with *T. versicolor* laccase 98

Figure 6.5: *R. opacus* PD630 growth and lipid accumulation in minimal media supplemented with 0.5% Kraft lignin that had been treated with *T. versicolor* laccase 98
Figure 6.6: Growth of *R. opacus* PD630 in minimal growth media supplemented with 0.5% Kraft lignin, 0.1% nitrogen, 1 U/ml *T. versicolor* laccase and 1 mM syringaldehyde. Error bars represent standard deviation (n=3). 100
Figure 6.7: *R. opacus* PD630 growth and lipid accumulation in minimal media supplemented with 0.5% Kraft lignin, 0.05% nitrogen, 1 U/ml *T. versicolor* laccase and 1 mM syringaldehyde 101
Figure 9.1: DNA sequence of pUCIDT-AMP-DypB 125
Figure 9.2: DNA sequence of pNV18.1 126

List of tables

Table 1.1: Comparison of fuel properties 17
Table 1.2: Composition of lignocellulosic biomass sources 19
Table 2.1: Cost of biodiesel production using different feedstocks and conversion technologies 44
Table 2.2: Forecast and potential lignin production volumes 49
Table 3.1: DNA sequences of primers and gBlocks 63

Abbreviations

4-HBA	4-hydroxybenzoic acid
AFDC	Alternative Fuels Data Center
B100	Biodiesel
DNA	Deoxyribonucleic acid
E10	10% ethanol, 90% gasoline blend
E100	Bioethanol
EDTA	Ethylenediaminetetraacetic acid
FAAE	Fatty acid alkyl ester
FAEE	Fatty acid ethyl ester
FAME	Fatty acid methyl ester
IEA	International Energy Agency
IPCC	Intergovernmental Panel on Climate Change
IPTG	Isopropyl-β-D-thiogalactoside
ktoe	Thousand tonnes of oil equivalent
LCA	Life cycle analysis
LDS	Lithium dodecyl sulphate
NMR	Nuclear magnetic resonance
NREL	National Renewable Energy Laboratory
OD	Optical Density
PAGE	Polyacrylamide gel electrophoresis
PCR	Polymerase chain reaction
RFA	Renewable Fuels Association
SDM	Site directed mutagenesis
SDS	Sodium dodecyl sulphate
TAE	Tris-acetate-ethylenediaminetetraacetic acid
TAG	Triacylglycerol
Tm	Melting temperature
UNFCCC	United Nations Framework Convention on Climate Change
VanA	Vanillic acid

Chapter 1

Literature review

1 Literature Review

1.1 Introduction and motivation for lignin-based biofuels

Climate change concerns and declining fossil fuel reserves are driving the need for alternative, sustainable energy sources. Solar, wind and other low carbon technologies have a growing role in electricity generation, but despite the predicted increase in electric cars, cannot meet fuel demand for transportation which is still more than 90% dependent on petroleum (International Energy Agency, 2018) and forecast to continue growing for many years (BP, 2018). Biofuels offer a low carbon alternative to conventional, petroleum-based liquid transportation fuels. Biodiesel has the additional benefits of high energy density and of being a 'drop-in' product that does not require blending or any modification to existing engines or delivery infrastructure.

Lignocellulosic biomass from agricultural and forestry wastes are a source of biofuel feedstock that do not necessitate land use change or compete with food crops (Timilsina and Shrestha, 2010). Lignin in biomass is a heterogenous, aromatic polymer that is plentiful, renewable and largely wasted. It can be converted to hydrocarbon fuels, albeit at a relatively high cost, and has been shown to yield carbon chain lengths suitable for making jet-fuel and diesel (Wang *et al*., 2015). Though many challenges remain, ongoing research efforts combined with rising oil prices and policy support (to reduce dependence on fossil fuels for climate change and energy security) should help the commercial deployment of lignin-based biofuels.

1.2 Biofuels

Biofuel is an umbrella term referring to solid, liquid or gaseous fuels derived from biomass through agriculture and conversion processes, rather than geological processes like fossil fuels. Biofuels provided 4% of world road transport fuel demand in 2016, of which most was bioethanol produced in Brazil and the U.S. Low carbon transportation fuel has reached a market share of 27% in Brazil, around 10% in the U.S. and 5% in the E.U. (which mainly uses biodiesel) (Low Carbon Technology Partnerships, 2015).

Biofuels are often added to conventional fuels, with more than 50 countries blending 5 to 27% ethanol in gasoline. The U.S. limits ethanol content to 10%, and reaching this so called "blend wall" has contributed to the slowing growth of the industry. The national average in 2016 was 10.02% (Wang *et al*., 2016; Renewable Fuels Association, 2018), and any further increase would require legislation related to fuel vapour pressure to be amended. Technology development and engine modifications

allow newer vehicles to use gasoline with a higher ethanol content, so there is potential for raising the blend limit (Souza *et al*., 2015b; Bracmort, 2018).

1.2.1 Biofuels classification

Liquid biofuels are conventionally classified into three generations based on feedstock and production processes, outlined below (Nagarajan et al, 2012). However, while these were useful in the early stages of biofuel development, newer technologies are not readily categorised using this terminology and are often referred to as advanced biofuels. Indeed, the work presented in this thesis contains elements of both second and third generation biofuels.

1.2.1.1 First generation

The majority of biofuel today is bioethanol produced from the fermentation of crops that contain high levels of easily accessible carbohydrates. These include cane- or corn-based sugar grown specifically for bioethanol production, or oils pressed from seeds and other edible plant products to produce biodiesel. The use of food crops as a fuel source for first generation biofuels has been controversial, as has the deforestation caused by palm oil production (Mekhilef, Siga and Saidur, 2011). Furthermore, energy used in the production process (including use of oil and fertiliser) means that a significant portion of first generation biofuels is far from carbon neutral (Searchinger and Heimlich, 2015).

1.2.1.2 Second generation

These are derived from non-food feedstocks such as agricultural waste, or energy crops grown specifically for the purpose, allowing the selection of crops with high yield and desirable biomass composition. These tend to have lower agricultural input requirements (such as fertiliser) and can grow on land of lower quality, for example the perennial grass *Miscanthus* widely grown in Europe (Lewandowski *et al*., 2000; Mohr and Raman, 2013). The sugars in lignocellulosic feedstocks are far less accessible than sugar crops, being in the form of cellulose polymers and complexed to hemicellulose and lignin. Pre-treatment and processing often requires high temperature, pressure, catalysts or chemicals. Although environmental performance is better than first generation biofuels, processing and feedstock logistical challenges have made second generation lignocellulosic biofuels expensive to produce, explaining the slow development of the sector (Balan, 2014).

1.2.1.3 Third generation

Third generation generally refers to biodiesel produced from the intracellular lipid stores of photosynthetic algae and cyanobacteria. It has higher oil productivity per unit of land area, fast growth rates, limited nutritional requirements, no competition for arable land and can be used as a drop-in fuel. However, the technologies need further development and costs are high due to expensive photobioreactors or open ponds. Although not fitting the conventional third generation classification, other microorganisms beside algae and cyanobacteria can produce large quantities of lipids, as discussed in section 1.3.2.

As well as biodiesel, some microorganisms can produce other biofuels including biobutanol, which possesses similar properties to gasoline and does not require engine modifications as ethanol does (Kim *et al*., 2011). *Clostridium acetobutylicum* naturally produces butanol, but production levels are limited by its toxicity. Metabolic engineering approaches have been used to overcome this (Lee *et al*., 2008), and butanol synthesis has been engineered into other organisms such as *Escherichia coli* (Atsumi *et al*., 2008) and *Saccharomyces cerevisiae*, which shows tolerance to higher concentrations (Generoso *et al*., 2015). Green Biologics Limited have repurposed a commercial bioethanol plant in Minnesota to produce n-butanol from biomass using species of *Clostridia* (www.greenbiologics.com).

1.3 Biofuel vs conventional fuel

To be widely employed bioderived fuels must be competitive with petroleum-based fuels, therefore compatibility with existing infrastructure and comparable fuel performance are important factors.

1.3.1 Fuel properties

Table 1.1 compares important characteristics of gasoline blended with 0 to 10% ethanol, low-sulphur petroleum-derived diesel, bioethanol (E100) and biodiesel (B100). Detailed specifications and test procedures have been set out for ethanol (ASTM D4806 in the U.S. and EN15376 in the E.U.) and biodiesel (ASTM D6751 in the U.S., EN14214 in the E.U.) in transport fuel (Costenoble, 2017).

Ethanol has lower energy density than gasoline by more than 30% per gallon, but has a higher octane number (Balat, Balat and Öz, 2008). Octane number is defined as "a measure of the quality of a [gasoline] expressed as the percentage of isooctane in a mixture of isooctane and n-heptane that gives a fuel with the same antiknock qualities as the given [gasoline]" (Collins English Dictionary) in a spark ignition engine. Ethanol's impact on fuel economy depends on the percentage blended in the fuel, and whether an engine is optimised to run on ethanol. E10 burns more slowly and completely than gasoline

due to the oxygen content in ethanol, resulting in reduced emissions of some pollutants, however it vaporises more readily which could increase ozone pollution in warm weather (Demirbas, 2008).

In contrast with ethanol which is a specific compound, biodiesel is made from various sources (such as fatty acid methyl esters or hydrotreated vegetable oils) so can have differing chemical properties. It has similar physical properties to conventional diesel and can be blended with or even replace it. Blending improves the lubricity of diesel and raises the cetane number, which helps engine start up and reduces idling noise. Cetane number is defined "as a measure of the quality of a diesel fuel expressed as the percentage of cetane in a mixture of cetane [hexadecane] and 1-methylnapthalene of the same quality as the given fuel" (Collins English Dictionary) in a compression ignition engine. Biodiesel is safer than conventional diesel due to its higher flashpoint of 130 °C (compared with 52 °C), however it has slightly lower energy content (33,321 vs 35,812 kJ/l) and a higher pour point, so may need a cold flow improver in very cold conditions (Gebremariam and Marchetti, 2018). Biodiesel has no sulphur, produces less carbon monoxide, particulate matters, smoke and hydrocarbons and has more free oxygen than conventional diesel which helps achieve complete combustion and reduces emissions. However it has higher nitrogen oxide emissions than conventional diesel (Gebremariam and Marchetti, 2018).

Table 1.1: Comparison of fuel properties of petroleum-based gasoline (petrol) and diesel vs bioethanol and biodiesel. E10 is a 90/10 blend of gasoline/ethanol, E100 is 100% bioethanol, B100 is 100% biodiesel. The term gasoline is used for petrol since energy density of petroleum fuels is typically quoted in U.S. gasoline gallon equivalent for comparison purposes; 42 U.S. gallons make up a barrel of oil; 1 tonne of oil equivalent is approximately 7 barrels of oil. Adapted with permission from the Alternative Fuels Data Center, National Renewable Energy Laboratory, U.S. Department of Energy, 2014.

	Gasoline/E10	**Low Sulphur Diesel**	**Ethanol/E100**	**Biodiesel/B100**
Chemical Structure	C4 to C12 and ethanol ≤ 10%	C8 to C25	CH_3CH_2OH	Methyl esters of C12-C22 fatty acids
Fuel Material (feedstocks)	Crude Oil	Crude Oil	Corn, grains, or agricultural waste (cellulose)	Fats and oils from sources such as soy beans, waste cooking oil, animal fats, and rapeseed
Gasoline Gallon Equivalent	97% - 100%	One gallon of diesel has 113% of the energy of one gallon of gasoline.	One gallon of E85 has 73% to 83% of the energy of one gallon of gasoline (variation due to ethanol content in E85). One gallon of E10 has 96.7% of the energy of one gallon of gasoline.	B100 has 103% of the energy in one gallon of gasoline or 93% of the energy of one gallon of diesel. B20 has 109% of the energy of one gallon of gasoline or 99% of the energy of one gallon of diesel.
Energy Content (Lower heating value)	112,114 - 116,090 Btu/gal or 31,248 – 32,357 kJ/l	128,488 Btu/gal or 35,812 kJ/l	76,330 Btu/gal or 21,275 kJ/l	119,550 Btu/gal or 33,321 kJ/l
Energy Content (Higher heating value)	120,388 - 124,340 Btu/gal or 33,555 – 34,656 kJ/l	138,490 Btu/gal or 38,600 kJ/l	84,530 Btu/gal or 23,560 kJ/l	127,960 Btu/gal or 35,665 kJ/l
Cetane Number	N/A	40-55	0-54	48-65
Pump Octane Number	84-93	N/A	110	N/A

1.3.2 Microbial biodiesel

Some microorganisms can store excess carbon as lipids within the cells. Those that can accumulate more than 20% of their dry cell weight as lipids are termed "oleaginous" and offer an alternative route to biodiesel production. These lipids are often in the form of triacylglycerols (TAGs) which are triesters of glycerol with three fatty acid chains. They are not directly suitable for use as biodiesel due to high viscosity (Knothe and Steidley, 2005) and must therefore undergo transesterification to mono-alkyl esters. Glycerol is replaced with an alcohol on each fatty acid chain, as illustrated in figure 1.1 (using methanol as the example alcohol).

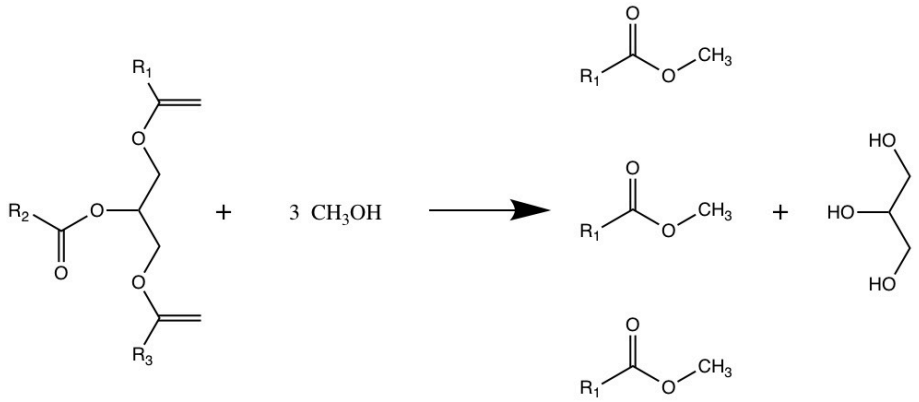


Figure 1.1: Transesterification reaction of triacylglycerols and methanol to glycerol and fatty acid methyl esters i.e. biodiesel.

The transesterification reaction is already widely employed for the processing of plant oils to biodiesel. Methanol is added in excess to drive the reaction, glycerol is removed, and the methanol is recovered to be reused. Alkali catalysts may be added to accelerate the reaction (Meher, Vidyasagar and Naik, 2006). Enzymatic transesterification has the added benefit of easy glycerol removal, but is uncommon due to the high cost (Fukuda, Kondo and Noda, 2001).

There have been metabolic engineering approaches to intracellular transesterification, creating a microbe that produces fatty acid alkyl esters directly. This was achieved in *S. cerevisiae* (Yu *et al.*, 2012; Valle-Rodríguez *et al.*, 2014) and *E. coli* (Kalscheuer, Stölting and Steinbüchel, 2006; Duan *et al.*, 2011; Guo, Pan and Li, 2015), which also requires the expression of ethanol production pathways.

1.3.2.1 Ideal biodiesel

Structural variations greatly influence the properties of the resultant fuel. Fatty acid chain length, degree of unsaturation, chain branching and the alcohol used in transesterification all impact fuel performance by affecting the cetane number (ignition quality), lubricity, viscosity, cold flow and oxidative stability among others. Varying one characteristic may improve one property while causing another to worsen, making trade off necessary (Knothe, 2005, 2008; Islam *et al*., 2013). It is suggested that straight chain, mono-unsaturated fatty acids of C10-16 chain length transesterified with 2-propanol may possess the most desirable properties. However, fatty acid features are difficult to control and methanol is the most widely used alcohol (despite often coming from fossil fuel sources) due to its low cost (Knothe, 2008).

1.4 Biomass composition

Lignocellulosic biomass is composed of cellulose, hemicellulose and lignin. The proportions of each of these polymers vary depending on the type of plant, part of the plant and even the location in which the plant is grown (Malherbe and Cloete, 2002). Table 1.2 shows the typical composition of hardwood (angiosperm), softwood (gymnosperm) and grasses.

Table 1.2: Composition of lignocellulosic biomass sources. Data from Betts et al., 1991.

	Cellulose %	**Hemicellulose %**	**Lignin %**
Hardwood	45 – 55	24 – 40	18 – 25
Softwood	45 – 50	24 – 35	25 – 35
Grasses	25 – 40	25 – 50	10 – 30

The most abundant component, cellulose, is a linear polymer of D-glucose molecules linked by β-1-4-glycosidic bonds (therefore their orientation alternates along the chain and the repeating unit is cellobiose). The degree of polymerisation is high, though it varies widely between 500 and 25,000 (Kuhad, Singh and Eriksson, 1997), and the chains are packed together and bonded through hydrogen bonds and van der Waals forces, providing strength and resistance to hydrolysis (Malherbe and Cloete, 2002). Plants typically contain 25-55% cellulose (Betts *et al*., 1991).

Hemicellulose is more complex and consists of shorter polymers of various five (such as xylose) and six (such as glucose, mannose and galactose) carbon sugars. There may be branching, with a degree of polymerisation in the region of 100 to 200 (Kuhad, Singh and Eriksson, 1997) making it more easily hydrolysed than cellulose. Hemicellulose content ranges from 24-50% (Betts *et al*., 1991).

Lignin is more complex still, and is a heterogenous, aromatic polymer with no regular defined structure. It accounts for 10-35% of the plant (Betts *et al*., 1991) and is detailed further below. Biomass also contains other components in small quantities, such as proteins, fatty acids, terpenes and inorganic materials (Lange, 2007).

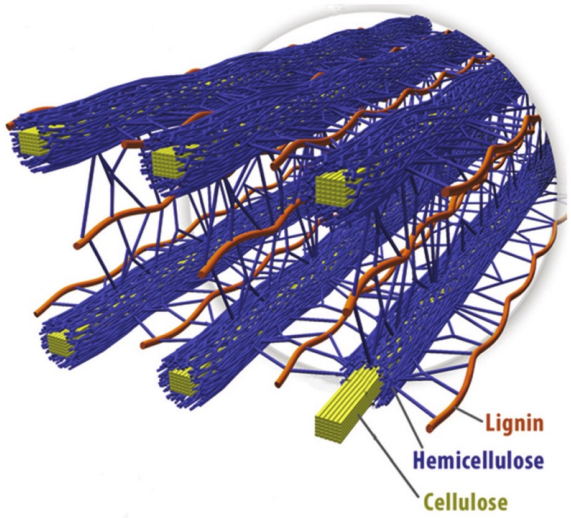


Figure 1.2: Representation of lignocellulosic biomass, showing cellulose (yellow), hemicellulose (blue) and lignin (brown). Reprinted with permission from U.S. Department of Energy Genome Programs image gallery.

Figure 1.2 shows the structure of lignocellulosic biomass. The three main polymers are complexed together through hydrogen and covalent bonding, with hemicellulose acting as a glue between cellulose and lignin (Malherbe and Cloete, 2002). These interactions add to its resistance to enzymatic degradation.

1.4.1 Breakdown of lignocellulosic biomass

Lignocellulosic biomass requires pre-treatment to liberate the components before efficient enzymatic hydrolysis can occur. Pre-treatment can involve physical, chemical or biological methods (Mosier *et al*., 2005).

Physical treatments include mechanical processes that expose greater surface area for hydrolysis, though these tend to be highly energy intensive. For example, steam explosion involves rapidly heating biomass with high pressure steam (Mosier *et al*., 2005). Chemical pre-treatments expose the biomass to acidic or alkaline conditions of varying strength and pH. The conditions affect to what extent each of the three polymers are broken down and the quality of the resulting sugars or aromatics for downstream processing (Ragauskas *et al*., 2014).

There are various thermochemical methods including pyrolysis, gasification and high-pressure liquefaction (Kan, Strezov and Evans, 2016). Pyrolysis involves exposing biomass to high temperature in the absence of oxygen to produce pyrolysis oil or char, depending on temperature and reaction time.

Ionic liquids are salts that contain poorly coordinated, often bulky ions and are liquid at room temperature. They are considered "green" solvents due to their low volatility and recyclability. Treatment with ionic liquids allows the fractionation of lignocellulosic biomass, with the choice of ion combinations determining which component is dissolved. Suitable solvents include 1-ethyl-3-methylimidazolium acetate and 1-allyl-3-methylimidazolium chloride (Mäki-Arvela *et al*., 2010). The ionoSolv process effectively uses ionic liquids to liberate cellulose for fermentation, then recover the lignin and other biomass components (Brandt-Talbot *et al*., 2017).

Biological treatment methods use depolymerisation enzymes such as β-glucosidase (cellulose) or peroxidases/laccases (lignin). However, their action on whole biomass is slow due to is recalcitrance and would therefore benefit from initial pre-treatment by other methods (Balan, 2014).

1.5 Lignin

Lignin is the second most abundant polymer on earth, after cellulose. It is a highly complex, heterogenous, aromatic polymer with no defined subunits and high levels of crosslinking. These characteristics convey structural rigidity and strength in plants and make it resistant to degradation by both chemical and biological means (Liu, Luo and Zheng, 2018).

Kraft lignin is a by-product of the Kraft process, which removes lignin from biomass in the pulp and paper industries. It involves heating the biomass with sodium hydroxide and sodium sulphide to fragment and increase solubility of the lignin polymer, leaving cellulosic fibres intact (Chakar and Ragauskas, 2004). The residual Kraft lignin is soluble only above pH 10 and has low reactivity compared to other lignins (Froass, Ragauskas and Jiang, 1996).

1.5.1 Structure and synthesis

Lignin is found mainly in the plant cell wall where it protects cellulose and hemicellulose from degradation and provides rigidity and resistance to microbial attack. It is also produced in response to stresses on the plant such as drought, extreme temperatures, infection or physical damage (Vanholme *et al*., 2010; Liu, Luo and Zheng, 2018).

Lignin is a three-dimensional aromatic polymer composed of three primary subunits: sinapyl, coniferyl and *p*-coumaryl alcohols (figure 1.3). Once these monolignols are incorporated into the lignin polymer they are known as syringyl (S), guaiacyl (G) and *p*-hydroxyphenyl (H) units respectively. Lignin composition varies between species, and between cell types within a single plant (Vanholme *et al*., 2010). The monomer composition influences the polymer's molecular structure (branching) and its interaction with cellulose and hemicellulose, therefore affecting the susceptibility to degradation (Constant *et al*., 2016). In general, hardwood lignin contains mostly coniferyl and sinapyl alcohols, softwoods contains exclusively coniferyl alcohol and grasses contain all three (Gellerstedt and Henriksson, 2008).

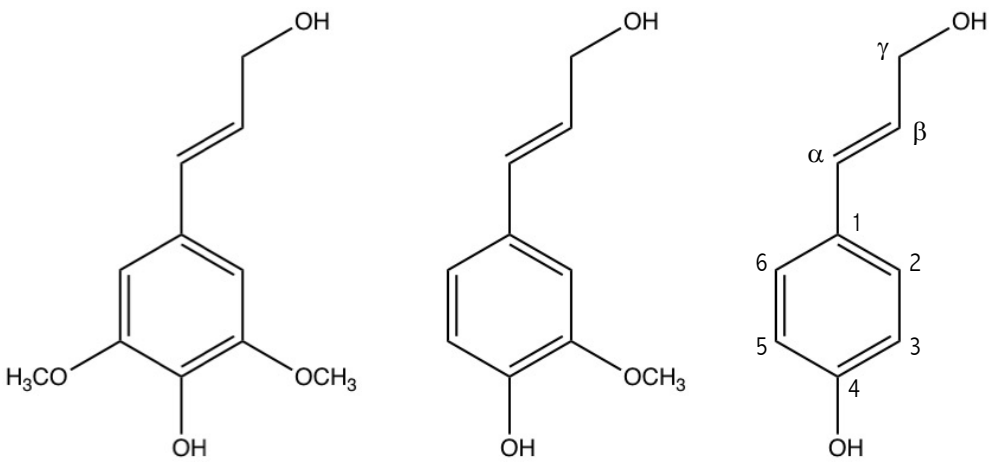


Figure 1.3: Structure of lignin monomers - sinapyl, coniferyl and p-coumaryl alcohols. Ring carbon atoms are labelled 1-6 and aliphatic carbon atoms α, β and γ for describing linkages between units.

Linkages between monolignols are named by labelling the ring carbon atoms 1-6, and the aliphatic carbon atoms α, β and γ (figure 1.3). The main linkage between adjacent monolignols is β-O-4 (β-aryl ether), though others include β-β, β-5, β-1, 5-5, α-O-4 and 4-O-5 (Munk et al., 2015), shown in figure 1.4. Again, frequencies vary and the proportions affect susceptibility to degradation, as bond dissociation energies are higher for C-C linkages than C-O-C ether linkages (Heitner, Dimmel and Schmidt, 2010).

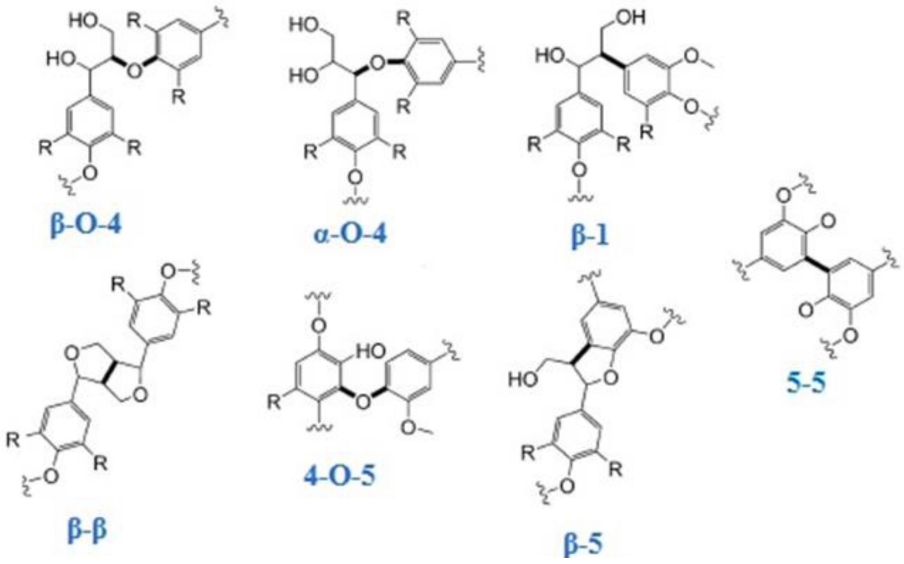


Figure 1.4: Common monomer linkages found in lignin. Reprinted with permission from Diop *et al*., 2015.

Lignin biosynthesis is a complex process. Monolignols are synthesised in the cytoplasm, involving eleven enzymes and a great number of steps, before being transported across the cell membrane to the cell wall where polymerisation occurs (Humphreys and Chapple, 2002). This involves their dehydrogenation and is facilitated by peroxidase and laccase enzymes (Lewis, Davin and Sarkanen, 1998; Boerjan, Ralph and Baucher, 2003; Heitner, Dimmel and Schmidt, 2010). Both these enzyme families include many members with varying activities, even including the depolymerisation of lignin. The conditions under which this occurs are discussed later.

As biomass degradation depends so heavily on the particular characteristics of the lignin, there is much interest into its modification to allow easier breakdown. With greater understanding of the biosynthetic pathways come opportunities for their genetic manipulation. Downregulating lignin biosynthesis to reduce lignin content (when cellulose is the desired product), altering the monolignol composition or even introducing alternative monolignols has been investigated (Weng *et al*., 2008; Mansfield, 2009). However, disrupting these pathways can have far reaching effects on gene expression, as well as have consequences for plant development and durability (Vanholme *et al*., 2010).

1.5.2 Breakdown

The breakdown products of lignin include high value compounds such as flavourings (vanillin) and phenols that feed into the chemicals industry (Rinaldi *et al*., 2016), hence there is considerable interest in its fragmentation and depolymerisation. Chemical and mechanical methods are similar to those used

for whole biomass, including liquefaction and pyrolysis. Here we are interested in biological mechanisms for lignin breakdown, which are discussed in detail in the following sections.

1.6 Microbial lignin depolymerisation

Despite its recalcitrance, a number of microorganisms are able to degrade the lignin polymer. Most widely studied are white-rot and brown-rot fungi, which produce ligninolytic enzymes such as peroxidases and laccases. *Phanaerochaete chrysosporium* expresses a lignin peroxidase and a heme-dependent manganese peroxidase which act extracellularly to break down lignin. It also produces copper-dependent laccases which degrade lignin via the action of redox mediators (Miki, Renganathan and Gold, 1986; Pollegioni, Tonin and Rosini, 2015). Some bacteria can also degrade lignin, including species of *Streptomyces*, *Nocardia* and *Rhodococcus* (Bugg, Ahmad, Hardiman and Singh, 2011; Brown and Chang, 2014), also thought to be by producing peroxidase and laccase enzymes. The *Rhodococcus* species of interest to this project are discussed in more detail below.

1.6.1 Peroxidases

Peroxidases catalyse the oxidation of many different compounds, while reducing hydrogen peroxidase to water. Many fungal species secrete various types of heme-containing peroxidases that degrade lignin, such as lignin peroxidases, manganese peroxidases, versatile peroxidases and dye-decolourising peroxidases (DyPs). In bacteria only the latter has been identified (de Gonzalo *et al*., 2016), which we focus on here.

DyPs are categorised into five subgroups, A-E, and it is the B subtype that is implicated in lignin degradation (Singh and Eltis, 2015). The heme cofactor is contained between two ferroxidin-like folds consisting of anti-parallel β-pleated sheets and surrounded by α-helices. A distal channel allows solvent and hydrogen peroxide access to the heme, and a hydrophobic groove, which could be responsible for binding large substrates such as lignin, may be involved in long-range electron transfer (Roberts *et al*., 2011). These features are illustrated in figure 1.5, using the *R. jostii* RHA1 DypB as an example.

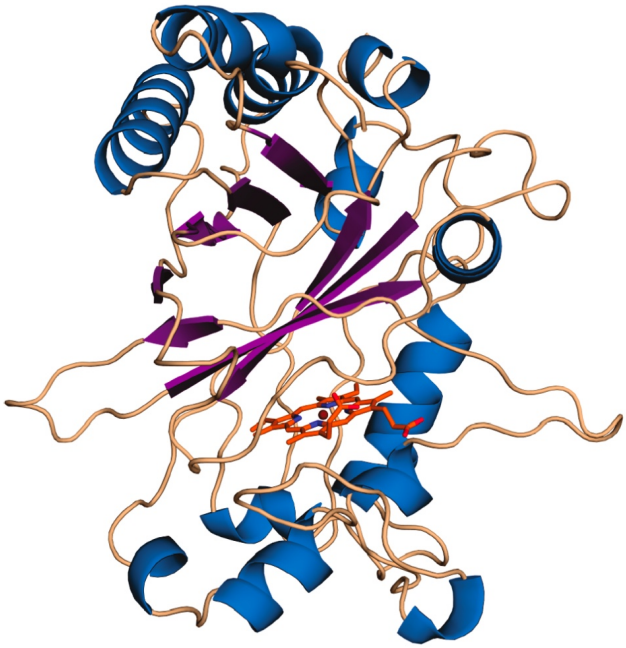


Figure 1.5: Structure of the DypB monomer from *R. jostii* RHA1. The heme cofactor is shown as a stick model surrounded by β-pleated sheets (purple) and α-helices (blue). Reprinted with permission from Roberts *et al*., 2011. Copyright 2011 American Chemical Society.

1.6.2 Laccases

Laccases are copper containing enzymes that can also catalyse the depolymerisation of lignin. They are ubiquitous across plant, fungal and bacterial species, oxidising a broad range of substrates while reducing oxygen to water. This makes them more industrially attractive than peroxidases, and as such they have been employed in various biotechnological applications including organic synthesis, bioremediation, food additive synthesis and indeed biofuel production (Mate and Alcalde, 2016).

Due to their diverse nature, laccases can catalyse very different reactions depending on their biological origin and environmental conditions. For example, plant laccases are involved in wound responses and lignin synthesis in young plants (Mayer and Staples, 2002), while fungal laccases may contribute to defence mechanisms and biomass (lignin) degradation (Alcalde, 2007). They are often highly glycosylated, contributing to their thermal stability, and may occur as monomeric or dimeric isozymes (Wong, 2009).

The four copper ions are located in the active site and are categorised into three types. Type 1 is responsible for substrate oxidation, after which electrons are shuttled to the trinuclear cluster of the remaining three copper ions (one type 2 and two type 3) where oxygen is reduced to water (Christopher, Yao and Ji, 2014). The copper ions and their coordinated residues are shown in figure 1.6.

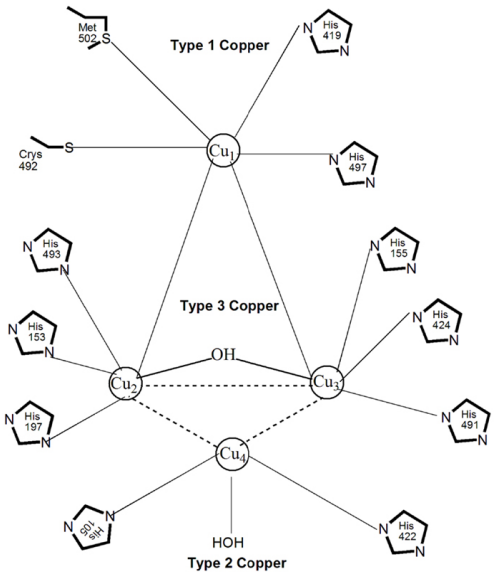


Figure 1.6: Copper ions in the laccase enzyme and their coordination. The substrate is oxidised at the type 1 site, then electrons are transferred to the trinuclear cluster where oxygen is reduced to water. Copyright Christopher, Yao and Ji, 2014.

One of the most well characterised microbial laccases is that of the white-rot fungi, *Trametes versicolor*. The structure is given in figure 1.7 (Piontek, Antorini and Choinowski, 2002).

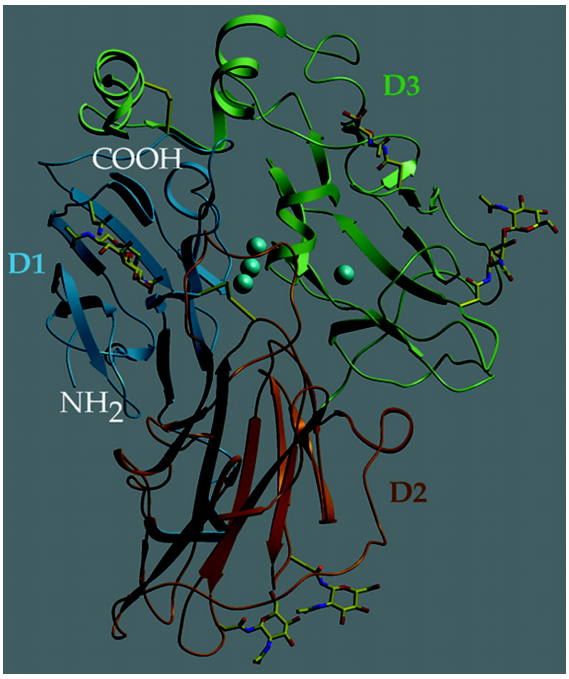


Figure 1.7: Structure of *T. versicolor* laccase. The three domains are labelled D1-3, copper ions are shown as blue spheres, carbohydrates and disulphide bonds are shown as stick models. Copyright 2002, by the American Society for Biochemistry and Molecular Biology (Piontek, Antorini & Choinowski, 2002).

The lignin polymer is too large to enter the enzyme active site, therefore laccases alone are unable to catalyse its oxidation. In addition, they have relatively low redox potential of 0.5-0.8 V so are only able to oxidise phenolic lignin subunits. A large proportion of lignin is made up of non-phenolic subunits, therefore redox mediators are required to facilitate their oxidation. Mediators are small molecules that shuttle between enzyme and substrate and are continuously oxidised and reduced, thereby enhancing the redox potential of the system (Christopher, Yao and Ji, 2014; Munk *et al*., 2015). Figure 1.8 shows a schematic of this mechanism.

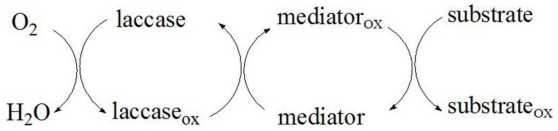


Figure 1.8: Schematic of a laccase mediator system, enhancing the redox potential of the enzyme and allowing oxidation of the large lignin polymer. The mediator continuously diffuses between the laccase, where it is oxidised, and substrate, where it is reduced. Copyright Christopher, Yao and Ji, 2014.

Both synthetic and natural mediator compounds have been described. The first identified artificial mediator was 2,2′-azinobis(3-ethylbenzothiazoline-6-sulfonic acid) (ABTS) (Bourbonnais and Paice, 1990), whose structure is shown in figure 1.9. 1-hydroxybenzotriazole (HBT), 2,2,6,6-tetramethylpiperidin-1-oxyl (TEMPO) and many others followed (Munk *et al*., 2015). However, these compounds can inhibit laccase activity at concentrations above 1 mM (Christopher, Yao and Ji, 2014), prompting research into how mediated systems occur in nature.

Naturally occurring mediators include the breakdown products of lignin itself, potentially creating an autocatalytic system. Laccases alone can oxidise phenolic subunits, which may then be released to penetrate the polymer and act as mediators for the oxidation of non-phenolic subunits and further bond cleavage (Christopher, Yao and Ji, 2014). Syringaldehyde (figure 1.9), acetosyringone and *p*-coumaric acid, among others, have been shown to mediate depolymerisation of Kraft lignin (Camarero *et al*., 2007; Gutiérrez *et al*., 2007).

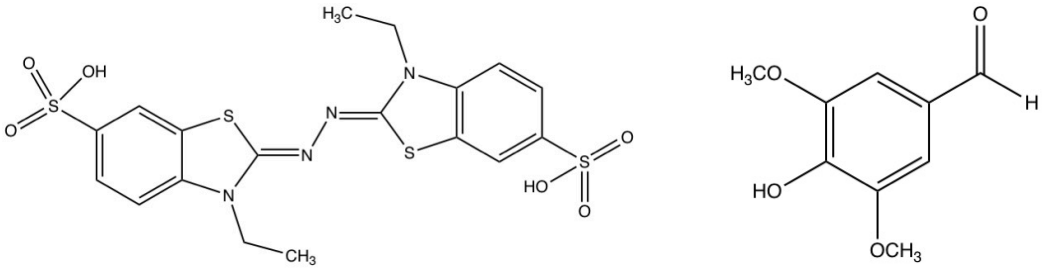


Figure 1.9: Structures of laccase mediators. Left: the synthetic mediator 2,2′-azinobis(3-ethylbenzothiazoline-6-sulfonic) acid (ABTS), right: natural mediator syringaldehyde.

Laccases catalyse both the polymerisation and depolymerisation of lignin (Shleev *et al*., 2006), therefore it is important to control conditions to favour the desired reaction. For instance, removal of monolignols by uptake and metabolism would drive the reaction towards depolymerisation (Munk *et al*., 2015). *T. versicolor* laccase has been shown to catalyse depolymerisation of Kraft lignin in the presence of ABTS, but polymerisation in the absence of a mediator (Bourbonnais *et al*., 1995).

1.7 Aromatic degradation

After depolymerisation, these aromatic monomers must then be metabolised further to be fed into central carbon metabolism and used for growth and energy production. There are numerous pathways employed throughout nature to achieve this, both aerobically and anaerobically. The pathways outlined here are those identified in soil bacteria and fungi, including species of *Rhodococcus*, that are exposed to the many aromatic compounds produced by plants and decaying plant matter (Harwood and Parales, 1996; Fuchs, Boll and Heider, 2011).

The aromatic is first modified to form a dihydroxylated benzene ring such as catechol or protocatechuate, which then undergoes cleavage of the aromatic ring. This can be *ortho*-cleavage between the two hydroxyl groups (intradiol) or *meta*-cleavage adjacent to one of the hydroxyl groups (extradiol). The *ortho*-cleavage route is also known as the β-ketoadipate pathway and is used by many species of bacteria, including the *Rhodococcus* species of interest here (Fuchs, Boll and Heider, 2011).

The lignin breakdown products used in this project are 4-hydroxybenzoic acid, vanillic acid and vanillin. These are all metabolised via protocatechuate and the β-ketoadipate pathway. In *R. jostii* RHA1, vanillin is converted to vanillic acid by vanillin dehydrogenase, then to protocatechuate by vanillate *O*-demethylase (Chen *et al*., 2012). 4-hydroxybenzoic acid is converted directly to protocatechuate by a single hydroxylation step. Figure 1.10 shows these preparatory steps and the relevant part of the β-ketoadipate pathway.

1.7.1 β-ketoadipate pathway

There are two branches to this pathway (protocatechuate and catechol) that both end in β-ketoadipate, which is then converted to acetyl-CoA and other Krebs cycle intermediates and fed into central carbon metabolism for the generation of energy (Harwood and Parales, 1996; Bugg, Ahmad, Hardiman and Rahmanpour, 2011). Different lignin-derived aromatics are channelled through each branch of the

pathway, but those of interest to this thesis follow the protocatechuate route, shown in figure 1.10 (Henson, Campbell, *et al*., 2018; Henson, Hsu, *et al*., 2018).

Protocatechuate is converted to β-carboxymuconate by protocatechuate 3,4-dioxygenase, then to γ-carboxymuconolactone by carboxymuconate lactonizing enzyme. This is then decarboxylated to β-ketoadipate enol-lactone by γ-carboxymuconolactone decarboxylase, before finally being converted to β-ketoadipate by enol-lactone hydrolase (Harwood and Parales, 1996). Although the pathway is broadly conserved between species, some steps do vary. For instance, the decarboxylase and hydrolase activities are likely to be performed by a single enzyme in *R. opacus* 1CP (Eulberg *et al*., 1998).

Two more steps are required to produce Krebs cycle intermediates from β-ketoadipate, which are carried out by β-ketoadipate:succinyl-CoA transferase and β-ketoadipyl-CoA thiolase. The final products are acetyl-CoA and succinyl-CoA. Acetyl-CoA is an important building block for fatty acid synthesis (Fuchs, Boll and Heider, 2011).

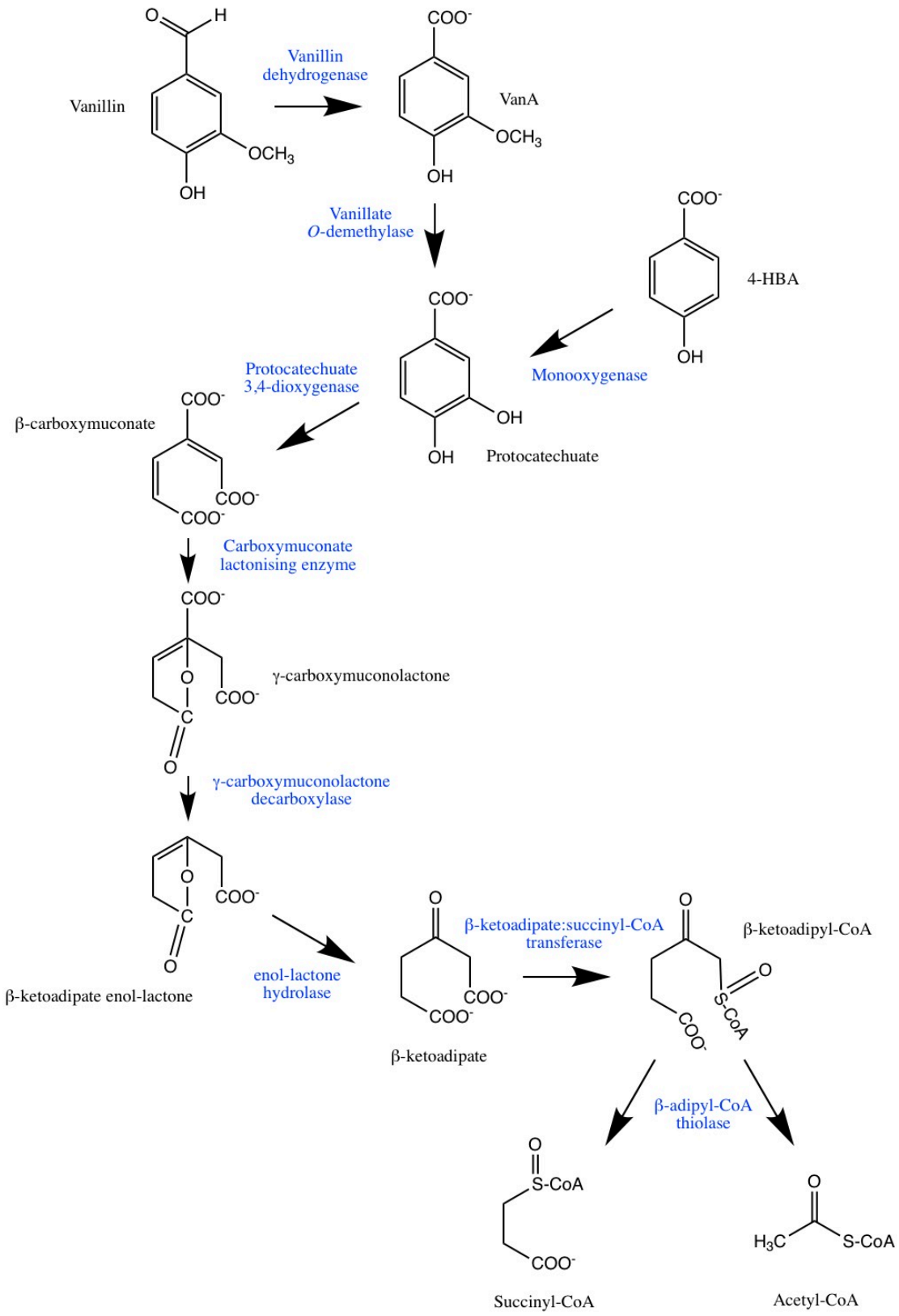


Figure 1.10: Pathways involved in monolignol degradation in *Rhodococcus* bacteria. Aromatic compounds are first converted to the dihydroxylated benzene, protocatechuate, which enters the β-ketoadipate pathway. Through several intermediates this culminates in β-ketoadipate, which then undergoes two more steps to produce succinyl-CoA and acetyl-CoA. See main text for details. Enzymes are shown in blue.

1.8 Microbial lipids

Oleaginous microorganisms accumulate fats as storage molecules when excess carbon is available, offering a source of lipids for biodiesel production. Much research has focussed on microalgae and cyanobacteria. Many species of these photosynthetic microorganisms are able to accumulate high quantities of lipids, such as the marine eustigmatophyte *Nannochloropsis* sp. F&M-M2 which can accumulate up to 60% (dry weight) lipid under certain conditions (Liliana *et al*., 2008). Some non-photosynthetic microorganisms are also capable of accumulating high levels of lipids, such as species of *Rhodococcus* (Alvarez *et al*., 1996), *Nocardia* (Alvarez *et al*., 2001) and *Streptomyces* (Olukoshi and Packter, 1994).

1.8.1 Bacterial lipid synthesis

Prokaryotic microorganisms can store excess carbon as lipids of various forms, including polyhydroxyalkanoic acids, wax esters and TAGs. Of interest here are bacteria that accumulate TAGs: energy-dense, water-insoluble molecules that do not affect cytoplasm osmolarity and release energy and carbon upon oxidation. They are stored in membrane-bound inclusion bodies (Alvarez and Steinbüchel, 2002).

These storage mechanisms allow carbon to be used even when other nutrients are limiting, assisting survival in the often harsh environments where these organisms are found. For instance, low nitrogen levels prohibit protein synthesis and therefore cell proliferation, so rather than leave any available carbon unused it is incorporated into TAGs. These are then oxidised when nitrogen becomes available, allowing growth on endogenous, stored carbon even if the exogenous supply is limited (Alvarez and Steinbüchel, 2002). This phenomenon can be exploited to enhance lipid production in these bacteria, and is a method employed throughout this project.

TAG biosynthesis pathways vary depending on the carbon source. For instance, carbon in the form of lipid-related molecules containing fatty acids will feed directly into TAG synthesis reactions. Unrelated carbon sources such as glucose must proceed via the cell's central metabolism to form acetyl-CoA and then undergo *de-novo* fatty acid synthesis. This involves the fatty acid synthase I multienzyme complex. TAG production then occurs via the Kennedy pathway, where glycerol-3-phosphate is sequentially acylated to replace the phosphate groups with fatty acid chains (Alvarez *et al*., 2013). A great number of enzymes are involved in TAG metabolism, with many different homologues seemingly catalysing the reaction of specific fatty acids. Mutants deficient in single enzymes can therefore still accumulate TAGs. The pathways and their regulation are still poorly understood (Alvarez *et al*., 2013).

1.9 Lignin to lipid bioconversion by *Rhodococcus* species

Rhodococcus species are a diverse group of actinobacteria with wide ranging habitats and metabolic activities. Their ability to grow on unusual substrates (such as polychlorinated biphenyls) and synthesise commercially interesting products (such as acrylamide) make them candidates for a range of technologies including bioremediation and industrial metabolite production (Bell *et al*., 1998; Van Der Geize and Dijkhuizen, 2004).

Rhodococcus are gram-positive, aerobic bacteria of rod or cocci morphology, with large genomes of high G+C content. Their cell envelope contains distinctive mycolic acids and an arabinogalactan polysaccharide covalently bonded to the cell wall peptigoglycan, making it very robust (Sutcliffe and Dover, 2010).

Two species of interest here are *R. jostii* RHA1, a known lignin degrader, and *R. opacus* PD630, which accumulates lipids.

1.9.1 *Rhodococcus jostii* RHA1

Rhodococcus jostii RHA1 is a soil bacterium that can degrade lignin, and a dye-decolourising, heme-containing peroxidase enzyme, DypB, has been identified. The structure is shown and described in figure 1.5, section 1.6.1. Gene deletion mutants show reduced degradation capability, and recombinant DypB has been shown to degrade Kraft lignin by catalysing cleavage of β-aryl ether bonds (Ahmad et al., 2011).

Lignin degradation by this strain was identified in the extracellular matrix (Ahmad *et al*., 2010), indicating that the DypB protein may be secreted from the cell. This is likely, as polymeric lignin must be broken down into smaller fragments before it can be transported into the cell and metabolised.

DypB is coexpressed with an encapsulin protein, thought to form intracellular nanocompartments that encapsulate DypB. This significantly increases DypB activity, and is hypothesised to aid localisation to the lignin surface where the compartment disassembles to release the peroxidase (Rahmanpour and Bugg, 2013). Activity is also enhanced by the presence of Mn^{2+} ions, and is dependent on the presence of hydrogen peroxide (Ahmad *et al*., 2011; Roberts *et al*., 2011; Singh *et al*., 2013).

RHA1 is able to store lipids under nitrogen limiting conditions, mostly as a mixture of glycogen, polyhydroxyalkanoates and TAGs, the relative levels of which vary depending on growth substrate (Hernández *et al*., 2008; Tajparast and Frigon, 2015). Differing levels of lipid product would make downstream processing to biodiesel more challenging, and the low accumulation levels compared to

other species make RHA1 a less attractive candidate for biodiesel production. The maximum total lipid content reported is 55% (dry cell weight) when grown on benzoate under nitrogen limiting conditions (Amara *et al*., 2016). This is not as high as reported in *Rhodococcus opacus* PD630, discussed below.

1.9.2 *Rhodococcus opacus* PD630

Rhodococcus opacus PD630 is a model prokaryotic oleaginous microbe that is capable of accumulating very large quantities of lipids in intracellular inclusion bodies (Alvarez *et al*., 1996). These lipids are in the form of triacylglyerides which can undergo transesterification to fatty acid alkyl esters, i.e. biodiesel (shown in figure 1.1 and detailed in section 1.3.2). Alvarez *et al*. showed that PD630 cells could accumulate up to 87% of their dry cell weight as lipid when grown on olive oil, and 76% when grown on gluconate under nitrogen-limiting conditions (figure 1.11). These extremely high levels make it a highly attractive species for industrial applications, and many of these lipids are TAGs composed of unusual straight chain, odd carbon fatty acids that are suitable for biodiesel production (Holder *et al*., 2011).



Figure 1.11: Electron microscopy image of *R. opacus* PD630 showing intracellular lipid inclusions. Cells were grown on gluconate under nitrogen limiting conditions, accumulating 76% dry cell weight as lipids. Length of bar is in mm, ET1 is an electron transparent inclusion body, B is the boundary layer. Reproduced with permission from Springer-Verlag Berlin Heidelberg (Alvarez *et al*., 1996).

Rhodococcus species are unusual in that they contain three lipid biosynthesis systems: fatty acid synthase type 1a (FAS I), mycocerosic acid synthase type 1b (MAS) and fatty acid synthase II (FAS II). FAS I initiates fatty acid chain synthesis, while MAS and FAS II elongate fatty acid chains by incorporating various different precursors. FAS I and II are responsible for producing shorter chains of up to 20 carbon atoms that are incorporated in cell membranes and storage lipids (TAGs). MAS-family synthases produce longer chains that are used to construct an extracellular protective layer. The highly complex lipid synthesis system in PD630 is not fully understood. However, the genome contains 8632 genes, of which 2017 are enzymatic reactions and 261 are implicated in TAG synthesis (Holder *et al*., 2011).

1.10 Outline of project

In this work we investigate the potential for bioconversion of lignin waste to biodiesel using oleaginous microorganisms that accumulate triacylglycerols (TAGs). The processing of TAGs to biodiesel by transesterification to fatty acid alkyl esters is well established, so we focus on the depolymerisation of lignin and its conversion to lipids by biological means.

First, we explore the demand for biofuels and the economic justification for such a project. We consider the costs and environmental implications of the whole production process, from sourcing feedstocks, to biomass processing, to downstream fuel processing.

Next, we assess the natural lignin degrading capability of wildtype *R. opacus* PD630, by monitoring growth on Kraft lignin as a sole carbon source. We then provide the lignin breakdown model compounds 4-hydroxybenzoic acid, vanillic acid and vanillin and monitor growth and intracellular lipid accumulation, demonstrating the strain's ability to metabolise monolignols and use them for lipid synthesis. We then attempt to enhance lignin depolymerisation by PD630 by expressing the DypB enzyme, a lignin peroxidase from *R. jostii* RHA1.

Finally, we investigate a combined enzymatic and microbial process for the bioconversion of lignin to lipid. Kraft lignin is pre-treated with *T. versicolor* laccase and redox mediators to cause depolymerisation, and the breakdown products are then accessible to PD630 for growth and lipid accumulation.

Chapter 2

Feasibility of lignin-based biofuels

2 Feasibility of lignin-based biofuels

2.1 Introduction

The United Nations Framework Convention on Climate Change (UNFCCC) recognises that global warming is directly related to the cumulative total carbon dioxide emitted into the atmosphere. The 195 member states of UNFCCC signed the legally binding Paris Agreement in 2015 to reduce greenhouse gas emissions, with the aim of holding the increase in the global average temperature to below 2 °C above pre-industrial levels and thus avoiding some of the worst effects of climate change.

Liquid biofuels could play a key role in meeting this ambitious target. This chapter presents a case for investigating lignin-derived biodiesel as an alternative to petroleum-based fuels, exploring increasing worldwide energy demand and the following three main areas of consideration:

- Environment: favourable emissions balance (energy required to grow, harvest and process biomass vs energy content of the biofuel), limited food competition (direct use of food crops or use of arable land), high water requirements.
- Economics: cost and source of feedstock, processing, price of the biofuel produced, opportunity to co-locate with existing plants (ethanol biorefineries or pulp and paper mills) to reduce capital and transportation costs.
- Policy: viability will be influenced by government policies, with many countries introducing subsidies or other incentives, with varying degrees of success.

A number of reviews have comprehensively analysed the economic viability of biofuel production, covering first- and second-generation bioethanol and biodiesel, as well as advanced biofuels and the use of lignin as a feedstock. The main studies referred to in this chapter are:

- Lignin: Technology, Applications and Markets – Special Market Analysis Study, RISI (Miller, 2016).
- Current Challenges in Commercially Producing Biofuels from Lignocellulosic Biomass (Balan, 2014).
- Economic Evaluation of Lignocellulosic Biofuel Manufacturing Considering Integrated Lignin Waste Conversion to Hydrocarbon Fuels (Ge, Dababneh and Li, 2017).

A low oil price in recent years has reduced interest in alternative technology development, but policy support, rising prices and the recognised urgency to limit global warming should make advanced biofuels a more attractive investment in the coming years.

2.2 Demand for biofuels

At the end of 2016, worldwide proved oil reserves stood at 1.7 trillion barrels, which is equivalent to 50 years of consumption at today's rates (BP, 2017). The cost of producing these reserves is likely to increase over time as existing reserves are depleted and replaced by more difficult oil fields located in deep water or more difficult geological formations. The consequent increase in forecast oil price (U.S. Energy Information Administration, 2018) should help biofuels become more competitive (Crooks, 2018).

2.2.1 Current biofuel production

Production of biofuels has grown at a rapid rate of 14% per annum over the past decade, and in 2016 provided 4% of world road transport fuel demand. Over 1.5 million barrels of oil equivalent per day was produced, of which some 36% was biodiesel and the rest bioethanol (figure 2.1). The latter is mostly produced in US and Brazil (although China and India are setting up cellulosic ethanol plants) while the largest biodiesel producer is Europe, with significant contributions from the Americas and Asia (BP, 2017).

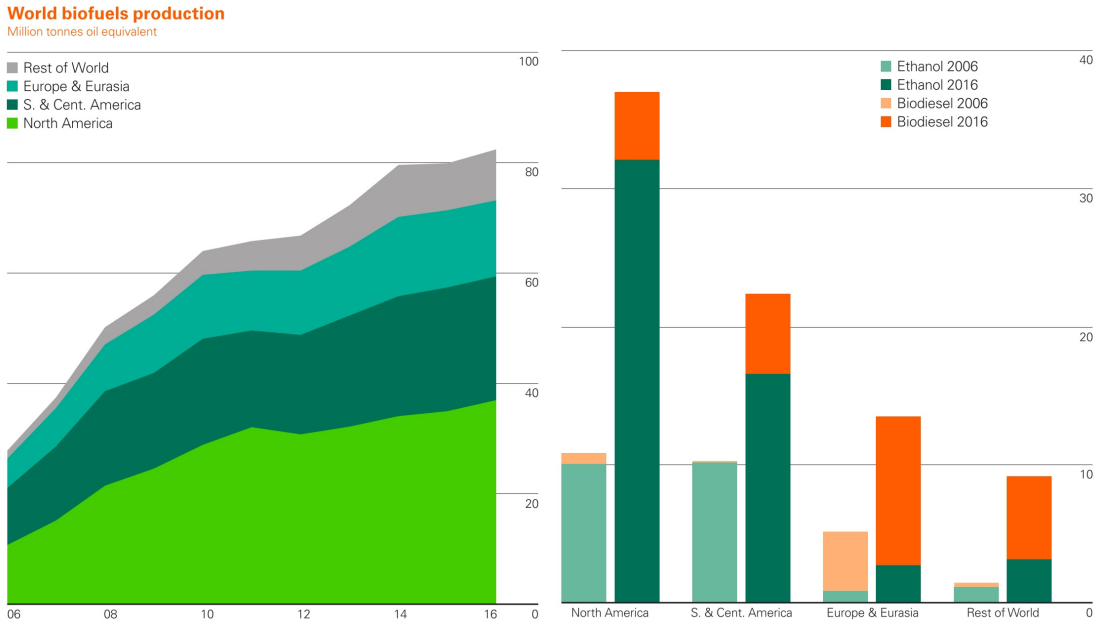


Figure 2.1: Global biofuel production 2006-2016. Left – total annual production by region. Right – regional ethanol and biodiesel production in 2006 and 2016.

"Global biofuels production rose by 2.6% in 2016, well below the 10-year average of 14.1%, but faster than in 2015 (0.4%). The US provided the largest increment (1930 thousand tonnes of oil equivalent, or ktoe). Global ethanol production increased by only 0.7%, partly due to falling production in Brazil. Biodiesel production rose by 6.5% with Indonesia providing more than half of the increment (1149 ktoe)." Figure and caption reprinted from BP Statistical Review of World Energy, 2017.

2.2.2 Biofuel production forecasts

Various biofuel production forecasts for the coming years all agree that they will play an increasingly important role in global fuel supply. Three examples are given here:

- BP's "Evolving Transition" scenario expects production to more than double by 2040 to between 3 and 4 million barrels of oil equivalent per day. Whilst crude oil demand will peak, BP sees biofuel demand continue to grow annually by 80,000 barrels per day, which is the equivalent of adding 20 of today's largest biorefineries every year (BP, 2018).

- The International Energy Agency (IEA) "2 °C scenario" forecasts annual biofuel production to rise to 1 billion barrels (or 2.7 million barrels per day) in five years' time and to play a particularly important role in the long-term decarbonisation of long-haul transport (aviation, marine and road freight) (International Energy Agency, 2017).

- Shell's ambitious "Sky" scenario (designed to hold global average temperature increase below 2 °C) sees overall liquid hydrocarbon fuel demand falling in the second half of the century as passenger vehicles electrify, but biofuel demand reaching some 30 million barrels per day. It predicts a decline in first generation biofuel use, but an increase in drop-in alternatives for aviation, road freight and shipping, produced from a wider range of bio-feedstocks and so reducing dependency on food crops (Shell, 2018).

2.3 Environmental considerations

While biofuels can provide a "green" alternative to fossil fuels, there are a number of factors to consider regarding the environmental impact of their use. Energy input is required for their production, and controversy has surrounded the use of food crops as feedstock, deforestation to clear land for feedstock growth, use of land otherwise used for food production, high water requirements and soil nutrient depletion among other factors discussed in this section.

2.3.1 Climate change

The 2015 Paris Agreement aims to limit global warming to below 2 °C above pre-industrial levels. According to the International Energy Agency, achieving this without compromising economic growth will require 10% of all transport fuels to be low carbon by 2030 and 30% by 2050. This will reduce greenhouse gas emissions by around 2 billion tonnes per year (Low Carbon Technology Partnerships, 2015), which is significant since transport accounted for 8 billion tonnes of CO_2 out of a total 34 billion

tonnes emitted in 2015 (Shell, 2018). For biofuels to have a meaningful impact on emissions, the net energy balance must be positive, i.e. the energy required for production should be significantly less than the energy content of the fuel itself.

2.3.1.1 Emissions balance

Biofuels are carbon neutral in the sense that CO_2 emitted during burning is offset by carbon fixed during plant photosynthesis. However the production, harvesting, transporting and processing of biomass to biofuel consumes energy and produces direct and indirect emissions (such as using fertiliser from the energy intensive Haber Bosch process, which itself uses large amounts of fossil fuels).

Several models have been developed to analyse the broader emissions and sustainability impact of various fuels and conversion pathways, including estimated effects of indirect land use change. Examples of Life Cycle Analysis (LCA) models include the GREET model (Greenhouse gases, Regulated Emissions and Energy use in Transportation) (Argonne National Laboratory, 2017) and BioGrace (Harmonised Calculations of Bioenergy Greenhouse Gas Emissions in Europe) (BioGrace Project, 2012). A schematic example of factors considered in the GREET model are shown in figure 2.2.

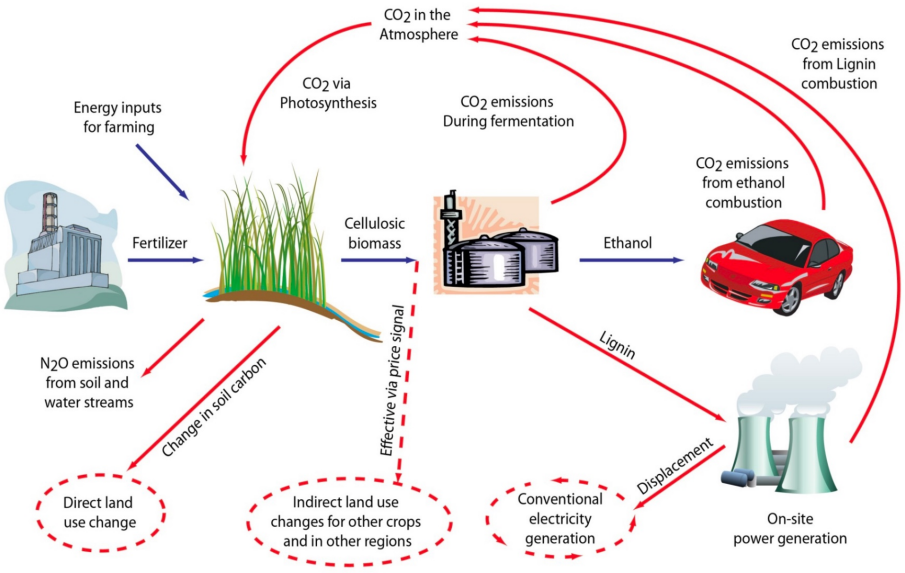


Figure 2.2: GREET biofuel life cycle analysis. Example showing switchgrass to ethanol conversion, including both direct and indirect factors. Reprinted with permission from Wang, 2018. Copyright Argonne National Laboratory, U.S. Department of Energy.

For first generation biofuels, ethanol from sugarcane shows the largest average net emissions mitigation. According to Shell, Brazilian sugar cane ethanol can reduce CO_2 emissions by 70% compared with gasoline (which emits 92g CO_2 equivalent per MJ) (Shell Energy and Innovation, no date). A 2006 review (Hammerschlag, 2006) suggested that corn-based ethanol used some 60-75% of its energy content during production: 20-25% for growth and harvesting of the crop and 40-50% for conversion to ethanol, including the energy required for extraction from fermentation cultures (Valentine *et al*., 2012). Growth Energy, the U.S. biofuels trade body, has stated that the use of ethanol reduces emissions by 43%, and is improving due to production process innovations and precision agriculture (Growth Energy, 2018). The Alternative Fuels Data Center (Vehicle Technologies Office, U.S. Department of Energy) shows a lower reduction of 34% for corn ethanol from dry mills, but up to 108% for cellulosic ethanol on a life cycle basis (Alternative Fuels Data Center, 2018b).

LCA has shown that biodiesel derived from palm oil may even result in higher emissions than fossil fuels, after considering the indirect land use impact of deforestation on carbon sequestration (Carrington, 2012). Biodiesel from Europe provides 30-60% mitigation compared with diesel (Souza *et al*., 2015a). The AFDC quotes 74% mitigation for biodiesel, based on analysis by Argonne National Laboratory (Alternative Fuels Data Center, 2018a).

Second and third generation biofuels (using lignocellulosic biomass from agricultural and forestry wastes and algae-based biodiesel) have greater potential for emissions reduction, but numbers will vary depending on processes and have yet to be verified at commercial scale.

2.3.2 Sustainability

2.3.2.1 Food competition and land use

The use of food crops as a feedstock for biofuel production is controversial, especially with a fast-growing global population and rising food prices (Valentine *et al*., 2012). The U.S. produced 40% of the world's corn in 2013, and used 40% of it to produce 10% of its own gasoline supply (Conca, 2014). A 5% displacement of gasoline and diesel in the E.U. requires about 5% and 15% respectively of available cropland to produce biofuel. The equivalent numbers for the U.S. are 8% for ethanol and 13% for diesel (Demirbas, 2008).

Although second generation biofuels do not compete directly with food, finite land resources still raise concern. A notable example is deforestation to clear land for the growth of sugar cane and palm oil crops exclusively for biofuel production, with negative consequences for biodiversity and carbon sequestration. Use of lignocellulosic biomass from agricultural and forestry wastes do not require land use change (beyond that needed for food production and existing forestry activities).

The Intergovernmental Panel on Climate Change (IPCC) reports that "land availability for bioenergy will depend on how much of the biomass can be grown on areas with little current production, and that trade-offs with water and biodiversity are crucial to avoid adverse effects" (Souza *et al.*, 2015a). From 2000 to 2010 the net increase in land area associated with biofuels was 13.5 million hectares, which was divided equally between bioethanol and biodiesel. Figure 2.3 illustrates current and future required global land used for food and bioenergy production.

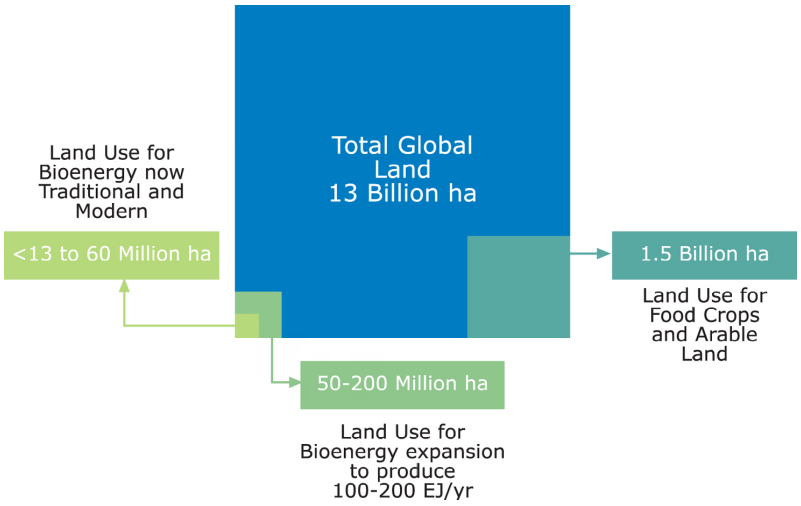


Figure 2.3: Global land use for bioenergy. Reprinted with permission from SCOPE Scientific Committee on Problems with the Environment. Copyright 2015.

Globally, around 0.9 billion hectares of land is suitable for fuel crop growth, being either unused or lightly used pastureland (Souza *et al.*, 2015a). Much of this is in Latin America and Sub-Saharan Africa. Some 50-200 million hectares of this could provide a 10-20% share of total primary energy by 2050 (and an additional 130-220 million hectares of good quality land would be required for food production). This corresponds to 0.4-1.5% of total global land or 5-20% of the underutilised land. Biomass for liquid biofuels would use up some 10-40% of this land, the higher number corresponding to the most ambitious emissions reduction scenarios (Shell, 2018).

2.3.2.2 Water requirements

Water is needed for both biomass growth and its processing to biofuel. The requirements vary significantly by crop, cultivation practice and location, but several hundred to several thousand litres of water can be consumed per litre of biofuel (Souza *et al.*, 2015a). Biomass growth therefore needs careful management in water-constrained areas, though it has been argued that the impact of this water

use should be compared with the alternative of the impact of global warming on water supplies (Souza *et al*., 2015a).

Processing of biomass into biofuel typically requires 1-6 litres of water per litre of fuel. An estimated 2.7 litres of water were used to produce a litre of bioethanol in 2012, which is a reduction of more than 50% in 20 years. This has been due to improved water recovery and recycling, with some facilities now able to use municipal wastewater (Souza *et al*., 2015a).

2.4 Policy support

For the widespread use of biofuels to be feasible, they must be cost competitive with petroleum-based fuels. However, few biofuel systems are currently economically viable, and advanced biofuels in particular need support for sustained technology development to deliver emissions reductions, energy security, rural economy development and other promised benefits. The low oil price over recent years (Brent crude averaged only $43.73 per barrel in 2016 (BP, 2017)) made biofuel production less commercially attractive, and led to reduced interest and investment into the development of new technologies (Reboredo *et al*., 2016). Figure 2.4 plots the price of Brent crude over the last decade, showing a high of $140 per barrel 2008 and a recent rise that should help to reverse this trend.

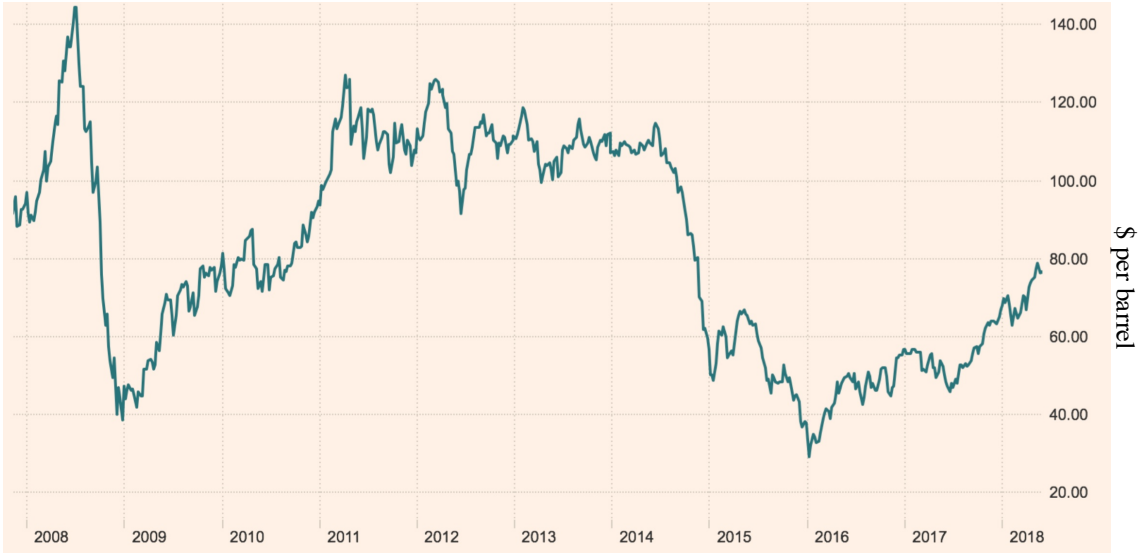


Figure 2.4: ICE Brent crude oil front month price ($ per barrel) from January 2008 to present. Source: ft.com.

Economists refer to the harmful effects of greenhouse gas emissions as negative externalities that are not internalised or reflected in the cost of fossil fuel use. To correct this market failure and encourage emissions reductions, 57 jurisdictions worldwide had introduced carbon pricing policies in 2016 including carbon taxes and emissions trading systems (REN21, 2017). Targeted policies have also been introduced to promote energy efficiency (e.g. building insulation regulations and grants, and fuel efficiency standards) and renewable energy production (e.g. feed-in tariffs and renewable power obligations), particularly for technologies that are currently not economically viable such as offshore wind.

Policy support to encourage biofuel production includes aid for the cultivation of feedstock, grants for the capital cost of biorefineries, and systems to encourage demand for biofuels (such as excise tax credits, effectively taxpayer subsidies, which lower the cost for consumers). The other widely used approach to boost demand is biofuel obligations or blending mandates, where fuel retailers must blend a certain percentage of biofuels into their gasoline or diesel regardless of cost, which is borne by consumers (Demirbas, 2008). Most countries incentivised biofuels regardless of net carbon reduction, though the U.S. and E.U. have specific mandates or provide additional benefits for second generation biofuels. However, these are set low in the E.U. and waivers can be purchased at low cost to offset (and effectively negate) mandated volumes in the U.S. (Skolrud *et al*., 2016).

Regional biofuel regulations include the E.U. Renewable Fuel Directive, the U.K. Renewable Transport Fuel Obligation, the California Low Carbon Fuel Standard and the U.S. Renewable Fuel Standard. More than 50 countries have blending mandates. The policy environment in which biofuels are produced, consumed and traded is complex as policies evolve rapidly in many countries (Carriquiry et al, 2011).

2.5 Economics of biofuel production

Estimations of biofuel production costs vary significantly between studies, as the economics are dependent on specific circumstances. These include:

- type of biofuel and local demand
- type of feedstock and local supply
- conversion process technology
- scale of production
- value of by-products
- jurisdiction (i.e. subsidy, regulation and tax systems)
- location (cost of transportation, logistics, utilities, labour and construction)
- prevalent oil price (on which some of the above will depend)

A variety of feedstocks, fuel types and processing technologies could be viable depending on these specific parameters, as reviewed in the following sections using several cost analyses (Paulson and Ginder, 2007; International Energy Agengy, 2008; Carriquiry, Du and Timilsina, 2011; Dutta *et al*., 2011; Humbird *et al*., 2011; Brownbridge *et al*., 2013; Davis *et al*., 2013, 2014; Nagarajan *et al*., 2013; Gebremariam and Marchetti, 2018). Differences in the date of these cost estimates are ignored, as the effect of inflation is likely to be countered by cost reductions from technology improvements. Furthermore, some costs have dropped due the recent low oil price, and any corrections applied would be within the accuracy range of most cost estimates.

2.5.1 Fatty acid conversion

Table 2.1 (Gebremariam and Marchetti, 2018) reviews the large cost variation of producing biodiesel from oil feedstocks using different technologies (waste cooking oil estimates range from $580 to $1048 per ton, or $77 to $140 per barrel). The very high cost of palm oil conversion is due to the high cost of palm oil feedstock. While there are no cost analyses for the bacterial biodiesel production we are concerned with, the estimates shown for algal biodiesel are lower than other methods ($560 to $620 per ton, or $74 to $83 per barrel). It is likely that bacterial biodiesel would be less costly still, due to the reduced requirement for expensive equipment and new technologies.

Table 2.1: Cost of biodiesel production using different feedstocks and conversion technologies. Reprinted with permission from Gebremariam & Marchetti, 2018. Copyright Elsevier.

Production technology type	Capacity	Feedstock	Production cost $/ton
KOH Catalyzed transesterification with methanol	8000 ton per year	Waste cooking oil	868,60
H_2SO_4 Catalyzed transesterification with methanol		Waste cooking oil	750,38
Lipase (Novozym-435) Catalyzed transesterification		Waste cooking oil	1047,97
Alkali catalyst process	Batch mode with a production capacity of 1000 tons	Palm oil	1166,67
Soluble lipase catalyst process		Palm oil	7821,37
Immobilized lipase catalyst process		Palm oil	2414,63
Homogeneous H_2SO_4 catalyzed and using purchased feedstock	Continuous reactor operating at 30 °C	Microalgae oil	620
Homogeneous H_2SO_4 catalyzed and using self-produced feedstock from recycled glycerol		Microalgae oil	580
Homogeneous KOH catalyst and hot water purification process	Batch mode with a production capacity of 1452 tons per year biodiesel	Waste cooking oil	921
Homogeneous KOH catalyst and vacuum FAME distillation process		Waste cooking oil	984
Heterogeneous CaO catalyst and hot water purification process		Waste Cooking Oil	911
Heterogeneous CaO catalyst and vacuum FAME distillation process		Waste cooking oil	969
Homogeneous KOH catalyst and hot water purification process	Batch mode with a production capacity of 7260 tons per year biodiesel.	Waste cooking oil	598
Homogeneous KOH catalyst and vacuum FAME distillation process		Waste cooking oil	641
Heterogeneous CaO catalyst and hot water purification process		Waste cooking oil	584
Heterogeneous CaO catalyst and vacuum FAME distillation process		Waste cooking oil	622

Other estimates for algal biodiesel include the U.S. National Renewable Energy Laboratory (NREL) who showed $180 per barrel (of which 70% was the cost of feedstock algae) (Davis *et al*., 2014), Brownbridge *et al*. who showed 80-160 pence per kg or $150-300 per barrel (Brownbridge *et al*., 2013), and Nagarajan *et al*. who showed $0.42-0.97 per litre or $67-$154 per barrel (Nagarajan *et al*., 2013).

Carriquiry *et al*., 2011 did a comprehensive review of numerous studies on the cost of producing biofuels (Paulson and Ginder, 2007; International Energy Agengy, 2008; Carriquiry, Du and Timilsina, 2011), shown in figure 2.5. The vertical axis scale can be converted to $ per barrel of oil equivalent by multiplying by 5.7 (so the scale goes up to $570 per barrel) (Staffel, 2011).

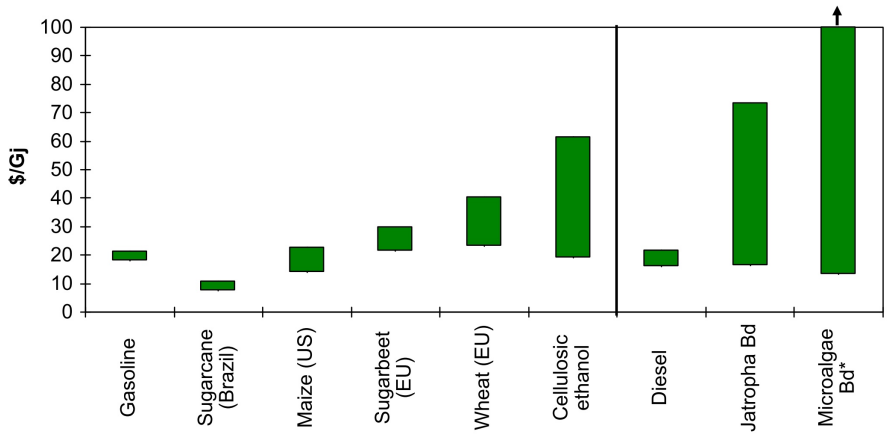


Figure 2.5: Biofuel production costs from various feedstocks.

Source: International Energy Agency (IEA), (2008). For gasoline and diesel prices, the range is given by wholesale prices (excluding taxes) in years 2007 and 2008 in the U.S. The assumed energy contents are as follows: ethanol 21.1 MJ/L; gasoline 32 MJ/L; biodiesel 33.3 MJ/L; and diesel 36.4 MJ/L. Capital and operating costs for processing algae oil into biodiesel were assumed equal to those of converting other vegetable oils into biodiesel and set to $0.122/L (Paulson & Ginder, 2007). First generation ethanol costs are from International Energy Agency (IEA), (2008). *The upper values for feedstock costs would imply costs of production per GJ in the thousands for algae biodiesel.

Figure and caption reprinted with permission from Carriquiry, Du & Timilsina, 2011. Copyright Elsevier.

2.5.2 Lignocellulosic biomass conversion

The US National Renewable Energy Laboratory (NREL) has published three relevant technical reports on alternative pathways for biomass to biofuel conversion: thermochemical, biochemical and biological, which use common assumptions (feedstock quantity of 2000 metric tonnes per day and detailed capital and operating cost estimates). A discounted cash flow analysis was used to derive the unit cost of fuel assuming 60% debt finance over 10 years at an interest rate of 8% to achieve an internal rate of return of 10% for equity investors over a plant life of 30 years.

The first report (TP-5100-51400 (Dutta *et al*., 2011)) considers thermochemical conversion by indirect gasification and mixed alcohol synthesis using forestry products as feedstock. The resulting 65 million gallons per year (or 4200 barrels per day) of ethanol are produced at a unit cost of $2.05 per gallon (or $3.11 per gallon of gasoline equivalent or $130 per barrel of oil, based on 42 gallons in a barrel).

The second report (TP-5100-47764 (Humbird *et al*., 2011)) considers a biochemical process of dilute acid pre-treatment and enzymatic hydrolysis of corn stover, followed by fermentation to ethanol. The resulting 61 million gallons per year (or 4000 barrels per day) of ethanol are produced at a unit cost of $2.15 per gallon ethanol (or $3.27 per gallon of gasoline equivalent or $137 per barrel of oil). This is slightly lower than the minimum selling price quoted in Balan's 2014 review of challenges in commercially producing biofuels from lignocellulosic biomass, which is $2.25 per gallon of cellulosic bioethanol (or $3.42 per gallon of gasoline equivalent or $144 per barrel of oil) (Balan, 2014).

The third report (TP-5100-60223 (Davis *et al*., 2013)) also considers acid pre-treatment and enzymatic hydrolysis, but instead of fermentation the resulting sugars are fed into a bioreactor for microbial conversion of cellulose and xylose to free fatty acids. These are recovered and hydrotreated to make a product suitable for blending with diesel. The resulting 31 million gallons per year (or 2000 barrels of hydrocarbons per day, equivalent in energy terms to around 3000 barrels of ethanol per day) of fuel are produced at a unit cost of $5.10 per gallon of gasoline equivalent or $214 per barrel of oil.

The higher cost of this third conversion process is mainly due to lower yield (hence production rate) and higher capital cost (due to the addition of bioreactors and hydrotreating).

2.5.3 Lignin conversion

The NREL states that lignin utilisation is of "paramount importance" in improving the economic viability of lignocellulosic biomass conversion. Only their thermochemical pathway currently does this, while the biochemical and biological pathways burn the lignin to generate low value energy. Ge *et al*. consider the economic benefit of such lignin utilisation, integrated into a cellulosic ethanol plant (Ge, Dababneh and Li, 2017) using NREL's biochemical process as a baseline (Humbird *et al*., 2011).

Without increasing the feedstock quantity, 16 million gallons of biodiesel could be produced in addition to the ethanol, although coal is imported to replace the lignin burnt as fuel which somewhat undermines the environmental motivation for such an endeavour. Integration into an existing biorefinery eliminates the first two steps of lignin conversion (depolymerisation), which are achieved during biomass pre-treatment for ethanol production. High purity lignin is separated when cellulose and hemi-cellulose are converted into fermentable sugars. The final step of upgrading lignin monomer into biofuels uses noble-metal catalysed hydrodeoxygenation (HDO in figure 2.6) to reduce the oxygen content for transportation fuel application.

The resulting cost on an energy equivalent basis is just over 0.1 $/MCal or $140 per barrel of oil equivalent, virtually the same as that of cellulosic ethanol produced from the same site (Ge, Dababneh and Li, 2017).

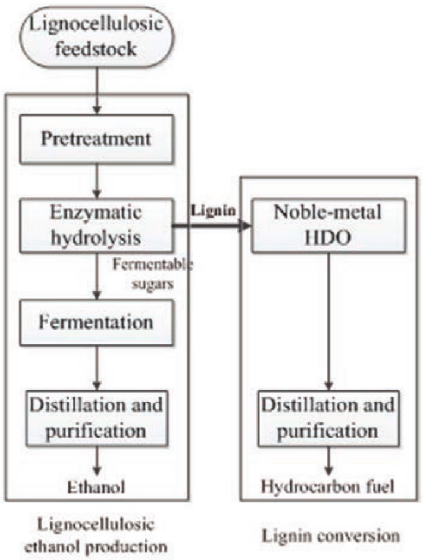


Figure 2.6: Proposed manufacturing framework, where lignin conversion is integrated into a conventional bioethanol plant. Reprinted with permission from Ge, Dababneh & Li, 2017. Copyright Elsevier.

2.5.4 Microbial lignin conversion

Though Ge *et al*. showed lignin utilisation in this way to be viable, costs are increased significantly by the requirement for high temperature, catalysts and hydrogen. Microbial lignin breakdown and metabolism could avoid these costs (though with a possible impact on productivity) and potentially offer an alternative conversion route:

- use lignin as obtained from pulp mills or bioethanol plants without the need for pre-treatment
- conversion at ambient temperature and pressure (to avoid energy, catalyst and hydrogen cost)
- production of biodiesel requiring limited processing to useable fuel

Many microorganisms are able to break down lignocellulosic biomass via the action of cellulolytic, hemicellulolytic and ligninolytic enzymes. These are discussed in chapter 1, but one recent advancement is the NREL's characterisation of CelA from the anaerobic bacteria *Caldicellulosiruptor bescii*. This multi catalytic domain cellulase degrades cellulose regardless of its degree of crystallinity by creating cavities in the plant cell wall, and acts much faster than most identified cellulases (Brunecky *et al*., 2013, 2017). This demonstrates that high profile research institutions are already working towards the commercial application of microbial cellulose conversion. The same technologies could be used for converting the remaining components of lignocellulosic biomass.

2.6 Lignin as a feedstock

Lignin is the world's second most abundant natural polymer after cellulose and is estimated to represent 20-30% of total carbon contained in the earth's biomass. The quantity of biomass available worldwide is thought to exceed 1 billion tonnes per year and is expected to more than double by 2030 (Miller, 2016). The U.S. Department of Energy's 2016 Billion-Ton Report concludes that the U.S. could more than double annual lignocellulosic biomass production to 1 billion tons by 2040 (including energy crops) without adversely affecting the environment or food production. This could produce enough biofuel, power and other products to displace 6 million barrels per day of oil consumption (or 300 million tonnes per year) (U.S. Department of Energy, 2016).

2.6.1 Challenges

Although lignin is plentiful, renewable and cheap, there are many challenges in using lignocellulosic biomass and lignin itself in biofuel production, due to the inherent complexity and recalcitrance of this feedstock (discussed in chapter 1). Producing, harvesting and transporting low density biomass poses logistical issues, and conversion processes including pre-treatment, hydrolysis and fuel separation are challenging once at the biofuel production site (Balan, 2014). All of this increases the cost of producing biofuels, making it significantly more expensive than petroleum-based fuels (Carriquiry, Du and Timilsina, 2011). DuPont's Iowa biorefinery, for example, has a capacity of 30 million gallons per year (2000 barrels per day) and cost more than $200 million to build (Lane, 2012).

However, biofuel processing costs are likely to come down as technology matures and with economies of scale (Balan 2014), as happened in the early days of the petroleum refining industry. Modern petroleum refineries are built to produce 1 million barrels per day (or 50 million tonnes per year) compared to a typical biorefinery producing 2000 barrels per day (or 30 million gallons or 100 thousand tonnes per year).

The cost of feedstock for second generation biofuels is lower than for first generation (food crops), but can still be up to 50% of the total cost. In contrast with cellulosic ethanol, feedstock cost is the main issue for biodiesel economics (Carriquiry 2010), which necessitates finding cheaper options (Gebremariam and Marchetti 2018).

2.6.2 Sources of lignin

Whilst biomass is abundant, dedicated sourcing of lignin (biomass production, collection, transportation and extraction) is unlikely to be economically viable on its own. A more feasible

approach is to target residual lignin from paper and bioethanol industries, less than 1% of which is recovered for processing into value added materials. The rest is wasted or burned, and the energy generated is used to power the plant itself. The potential supply of lignin from these sources is estimated to be 140 million tonnes per year (Miller, 2016), as shown in table 2.2 and detailed below.

Table 2.2: Forecast and potential lignin production volumes from different sources (in thousand tonnes). Data from Miller, 2016 (RISI Special Market Analysis Study) and Gosselink, 2011.

Kilo tonnes	2015 production	2020 forecast	2025 forecast	Potential
Kraft lignin	75	200	250	78,000
Lignosulfonate	1100	1400	1,550	3,000
Biorefinery	3	50	100	60,000

Kraft lignin is a product of the pulp and paper industry, which uses the Kraft process to isolate cellulose from biomass. During the process, "black liquor" containing the lignin fraction is incinerated, regenerating the inorganic pulping agents (NaS/NaOH) and producing steam for internal use and to generate (typically low efficiency) electricity (Ragnar *et al*., 2014). Seven tonnes of black liquor are produced for every tonne of pulp, and the lignin could have higher value uses (Biermann, 1993).

Kraft lignin is only soluble at alkaline pH and can be readily precipitated from black liquor using sulphuric acid. More environmentally friendly treatments such as Organosolv processes (no sulphur or extreme conditions), LignoBoost (using only CO_2) and LignoForce (using less acid and CO_2) are not currently economical for use on a commercial scale (Laskar *et al*., 2013; Miller, 2016; Rinaldi *et al*., 2016 and references therein).

The outdated sulphite pulping process produces smaller quantities of pulp (some 8 million tonnes versus 130 million tonnes from the Kraft process), but still the largest quantities of lignin, in the form of lignosulphonate (table 2.1). It is water soluble and therefore has more commercial applications, such as in the construction and agricultural chemicals industries. Hence some Kraft lignin is converted and sold as lignosulphonate (Miller, 2016).

By-products of ethanol biorefineries include various lignins, along with sugars, cellulose, hemicellulose and other chemicals. Most biorefineries burn lignin as a low value waste product, though some produce lignin co-products that can be sold for higher value (such as Lignol's Organosolv lignin, DuPont's lignin-rich solid or syrup, and Dong Imbicon's lignin pellets for fuel) (Miller, 2016).

A major source of lignin that does not require collection and transportation of bulky biomass (but does require lignin separation from cellulose and hemicellulose) is waste from the forestry and sawmill

industries, where up to 60% of the harvested fibre is discarded. Minor sources include the olive and olive oil industries, and the date palm industry. Olive harvest was 17 million tonnes in 2007 (Matos, Barreiro and Gandini, 2010), and the stones and olive husk have a lignin content of 26% and 48% respectively (Demirbaş, 2002). The date palm harvest amounts to 1 million tonnes in Saudi Arabia alone, and the waste has a lignin content of 30% (Hossain *et al*., 2014). Both these industries generally burn the waste for heat and electricity, and though their combined lignin quantity is estimated at just 1-2 million tonnes per year, they are examples of potential underutilised lignin sources (Demirbaş, 2002).

2.6.3 Potential scale of biofuel production from lignin

The potentially available quantity of lignin from the pulp industry and biorefineries is 140 million tonnes per year (table 2.1), which is enough to produce some 68 million tonnes of biodiesel per year (or 1.3 million barrels per day). This is based on calculations by Ge *et al*. (330 tons per day of lignin produces 16 million gallons per year or 1044 barrels per day of biodiesel; 1 ton of lignin with energy content of 22 GJ, slightly less than coal, is converted to 3.2 barrels of biodiesel with energy content of around 17 GJ or 4.7 MWh) (Ge, Dababneh and Li, 2017).

This assumes operation at full capacity, which is currently not the case for cellulosic ethanol plants that have struggled with the low oil price in recent years (but should pick up with regulatory support and as oil prices rise). It also assumes that less than 5% of potentially available lignin is used for higher value applications (discussed in section 2.6.4) and that no lignin is used for heat or power generation in pulp mills or biorefineries. This is unrealistic for the pulp industry, which burns waste to power the plant and also has excess energy supply. A modern pulp mill can produce surplus energy equivalent to some 30% of its lignin production potential (ABB Communications, 2011), so 20% may be a reasonable estimate of the lignin available from pulp mills for biofuel production in the medium term.

In theory, it could make economic sense to import cheap energy to power the plant, freeing up lignin for the production of higher value liquid fuels (for example DuPont's Iowa biorefinery). This would be especially beneficial from an emissions perspective if the energy were renewable (e.g. solar steam or photovoltaics) and if the biofuel produced from the freed-up lignin were used to displace fossil fuels. However, it is more likely that readily-available, low-cost natural gas would be used in the short term, giving a smaller net benefit (still preferable to dirty coal or lignite).

If only the 20% excess lignin from the pulp and bioethanol industries were available for biofuel production, it would amount to 28 million tonnes per year, which is enough to produce some 13 million tonnes of biodiesel per year (or 260 thousand barrels per day). This number could increase if additional lignin is freed up by (1) pulp mills and biorefineries finding it profitable to import energy and (2) bioethanol production expanding as forecasted.

Hence, assuming biofuel use doubles by 2040 (as in BP's "Evolving Transition" scenario (BP, 2018)), biodiesel production using excess lignin from pulp and ethanol biorefineries alone could reach 500 thousand barrels per day, which would account for some 15% of liquid biofuels used for transportation. This ignores the potential for producing biodiesel from lignin extracted from other waste biomass sources such as forestry and sawmill waste, albeit at high cost using today's technologies.

2.6.4 Value of lignin in alternative uses

Given its aromatic nature, there is extensive research into the use of lignin as a sustainable feedstock for valuable chemicals, as an alternative to the petrochemical industry (Stewart, 2008). Many institutions and companies are interested in commercialising lignin, driven by efforts to improve the economics of the paper industry (as demand decreases) and to replace plastics and other petroleum-based products with sustainable alternatives. The value of lignin in various potential applications is illustrated in figure 2.7 (Gosselink, 2011).

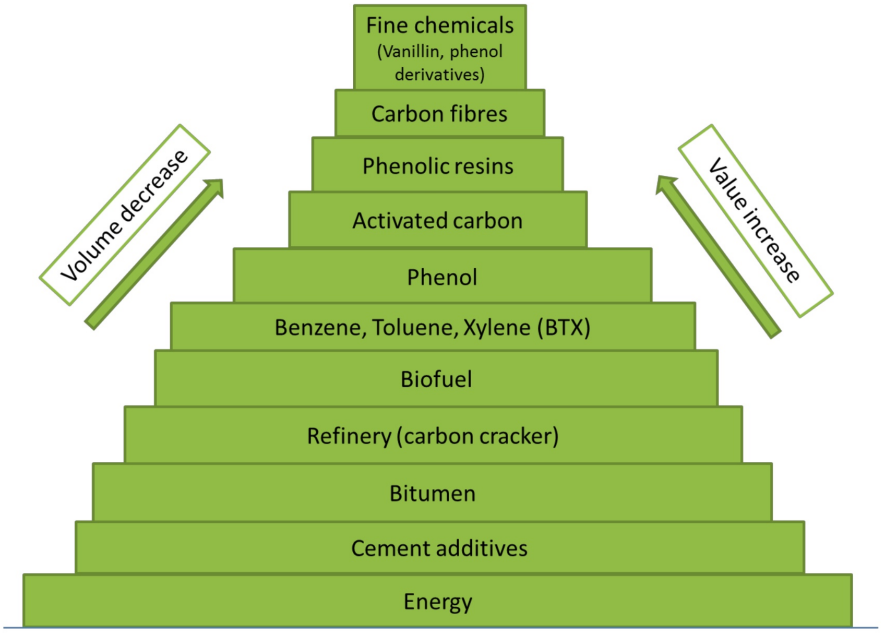


Figure 2.7: Potential applications for lignin, from high volume/low value such as combustion for energy generation to low volume/high value such as aromatic chemicals, including vanillin and other monolignols. Reprinted with permission from R. Gosselink, Wageningen University.

The flavouring vanillin is an example of a high value product that can be derived from lignin. Around 15% of vanillin is produced from lignin (Silva *et al*., 2009), for both the food and chemical industries. The RISI Special Market Analysis Study (Miller, 2016) reports the value of lignin for vanillin production to be $1200 per tonne. Such is the interest in vanillin that biological production methods are being researched. The lignin degrading bacteria, *Rhodococcus jostii* RHA1, has had its vanillin dehydrogenase gene deleted to prevent complete lignin degradation and encourage vanillin accumulation (Sainsbury *et al*., 2013).

However, the size of these markets is small, high-quality lignin is required and production costs are very high. The quantity of lignin therefore exceeds demand and is available for medium value applications such as biodiesel production, which could still be significantly more profitable than its current uses as fuel for electricity generation (Miller, 2016). This is illustrated in figure 2.8 (De Wild, Huijgen and Gosselink, 2014), indicating that lignin-based biodiesel could be economically viable if the conversion cost is kept below the value differential.

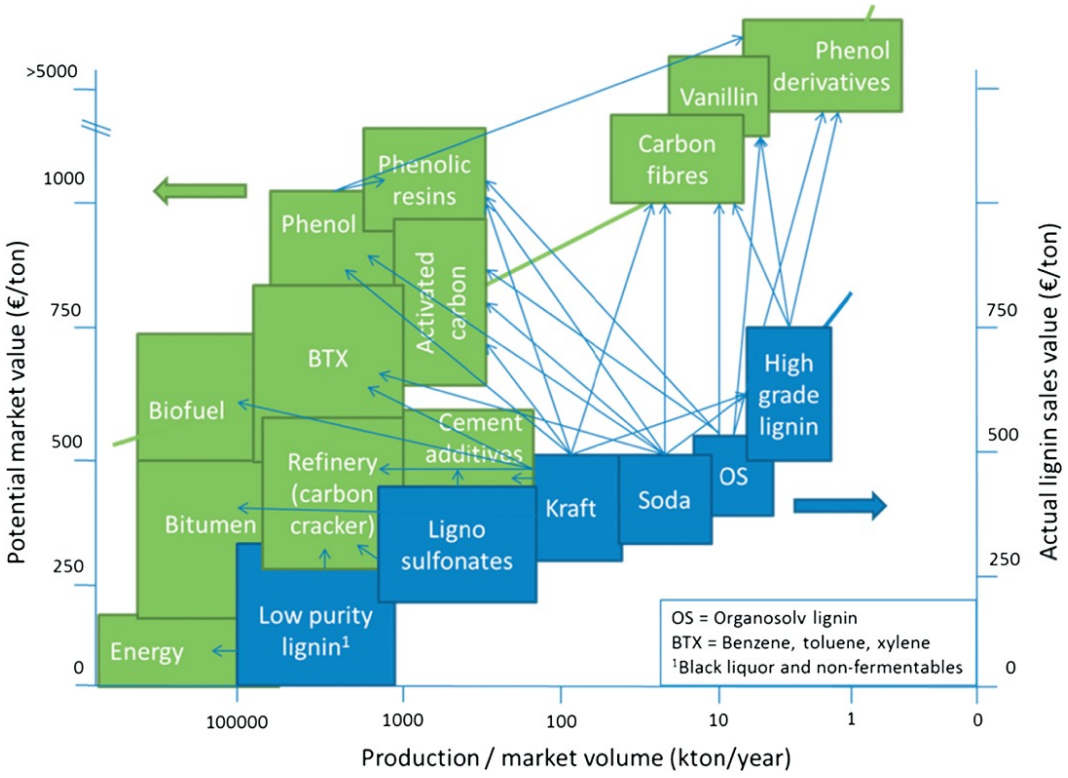


Figure 2.8: Lignin production vs lignin utilisation potential. Blue boxes and the secondary y-axis depict actual sales value, green boxes and the primary y-axis depict potential market value, with arrows indicating potential value-added application routes. Reprinted with permission from De Wild, Huijgen & Gosselink, 2014. Copyright John Wiley and Sons.

2.7 Companies pursuing advanced biofuels

There are a few companies that produce second generation bioethanol. Quad Counties (U.S.) has a co-process of conventional corn and cellulosic bioethanol production, and Borregaard (Norway) has been producing cellulosic ethanol from a legacy plant established when it was part of a pulp and paper company. Together these two companies produce more liquid fuel from cellulose and hemi-cellulose than everyone else in the world combined (Ethanol Europe Renewables, 2018). Other successful producers that supplement first generation with cellulosic bioethanol include Raizen (joint venture between Cosan and Shell) in Brazil and Enerkem in Canada. A handful of other advanced biorefineries have been built by companies including POET-DSM, Dupont, Abengoa and INEOS in U.S. (Skolrud *et al*., 2016), which have all struggled in the recent past due to low oil prices. Beta Renewables built a plant in Italy, Dong Inbicon has a demonstration plant in Denmark, Clariant in Germany. Lignocellulosic plant developers in Asia include Praj Industries in India and Jinan Shengquan and Shandong Longlive in China, both countries have announced government support.

Several companies such as BIOX, Forge Hydrocarbons, Inventure Renewables and REG Life Sciences produce biodiesel from waste oil. However, production of biodiesel from agricultural and other wastes is relatively new. Fulcrum BioEnergy has a thermochemical plant for conversion of household waste to biodiesel. UPM Norway produces biodiesel from conifer tall oil. Shell/CRI has a demonstration thermocatalytic waste to biofuel plant in Bangalore. Kaidi has a thermocatalytic wood to biodiesel pilot plant in China. RenFuel has announced the construction of a catalytic process plant for patented biocrude 'Lignol' from lignin in black liquor discharged by pulp mills owned by Rottneros in Norway. In addition, there are a number of technology companies focused on the development of technologies to convert lignin to biodiesel such as Steeper Energy, Red Rock Biofuels and Global Bioenergies.

In 2017, the high profile joint venture between ExxonMobil and Synthetic Genomics announced a modified algae strain that more than doubled oil content without significantly inhibiting growth, a key challenge along the path to commercial scalability (ExxonMobil, 2018). They recently announced an outdoor research study that will grow naturally occurring algae in several contained ponds to better understand fundamental engineering parameters including viscosity and flow, and how to scale the technology for potential commercial deployment. ExxonMobil believes that 10,000 barrels of algae biofuel per day could technically be produced by 2025 but additional work will be required to advance larger-scale production. Both companies are continuing with fundamental research on algae biology. Some smaller companies such as Pond Technologies and Algenol did pursue algal biofuels but have recently changed focus to carbon capture and high value bioproducts such as neutraceuticals.

In January 2019 ExxonMobil and REG signed a joint venture with Clariant with the aim of combining their technologies to convert cellulosic biomass to biodiesel. Clariant's process converts agricultural waste into sugars which provide a feedstock for REG and ExxonMobil's one-step fermentation technology for biodiesel production.

2.8 Conclusions

Climate change and other concerns are driving the need for biofuel as a low carbon alternative to petroleum-based liquid transportation fuels, which are likely to be needed for many decades. Lignin in biomass is abundant, renewable and potentially available from ethanol biorefineries and pulp mills in sufficient quantities to make a meaningful contribution to biofuel supply. Lignin does not compete with food crops like other feedstocks and can be converted to biodiesel, albeit at a relatively high cost.

Despite many challenges, the cost of biodiesel produced from the lignin by-product of a cellulosic ethanol biorefinery has potential to be economically viable (Ge, Dababneh and Li, 2017), costing virtually the same as ethanol produced from the same site. The cost on an energy equivalent basis for both products is calculated at just over 0.1 $/MCal or $140 per barrel of oil equivalent. This is higher than the current price of petroleum diesel (Brent crude oil $70-80 per barrel plus refinery margin of around $10 per barrel). However, policy support for low carbon fuels reduces this cost difference, with potential to fall further due to the following:

- the economics of combined lignocellulosic bioethanol/biodiesel refineries are improved by integration with existing first-generation bioethanol plants
- companies are profitably producing bioethanol from lignocellulosic biomass today (e.g. Quad Counties and Borregaard)
- some companies have quoted a breakeven oil price of $70 per barrel (DSM's Liberty cellulosic ethanol plant (Crooks, 2018) and Biochemtex PROESA™ process (Biochemtex, 2009))
- expected increase in oil price
- economies of scale
- process integration and design improvements
- operational optimisation
- technology improvements such as simplifying the lignin conversion process (catalysts and high temperature contribute significantly to lignin conversion cost (Ge, Dababneh and Li, 2017))

Microorganisms offer a potential route for lignin conversion that avoids processes requiring high temperatures, pressures, chemical and catalysts. Naturally occurring microbes are being discovered frequently that have ligninolytic capabilities (such as species of *Rhodococcus* (Ahmad *et al*., 2011)), and many others are able to accumulate high levels of lipid biodiesel precursors (Alvarez *et al*., 1996). Though currently in the early stages of research and expensive, the availability of underutilised lignin waste makes investigating and enhancing these microbial processes an interesting prospect, and one which we explore in the following chapters of this thesis.

Chapter 3

Materials and Methods

3 Materials and methods

3.1 Materials

All chemicals were purchased from Sigma-Aldrich, as were antibiotics, Luria-Bertani (LB) growth media, Hoagland solution and carbon sources. One Shot TOP10 chemically competent *E. coli* and One Shot BL21 chemically competent *E. coli* were purchased from Invitrogen. *Rhodococcus opacus* PD630 was purchased from DMSZ (strain 44193).

QIAprep Spin Miniprep Kit, QIAquick Gel Extraction Kit and QIAquick PCR Purification Kit were purchased from Qiagen. All enzymes used for plasmid construction were purchased from New England Biolabs, as was the Gibson Assembly Master Mix. SYBR Safe DNA Gel Stain and DNA Gel Loading Dye (6X) for gel electrophoresis were purchased from Thermo Fisher Scientific. The DNA molecular weight marker used was HyperLadder 1kb, purchased from Bioline.

The *E. coli – Rhodococcus* shuttle vector, pNV18.1, was kindly donated by Dr Jun Ishikawa at the National Institute of Infectious Diseases, Tokyo (Chiba *et al*., 2007). The *DypB* gene, all primers, DNA fragments and gBlocks were synthesised by Integrated DNA Technologies.

30 kDa Amicon Ultra 0.5 ml Centrifugal Filters and BugBuster Master Mix were purchased from Merck. NuPAGE LDS Sample Loading Buffer 4X, Reducing Agent 10X, 4-12% Bis-Tris Protein Gels and PageRuler Unstained Protein Ladder were all from Thermo Fisher Scientific.

3.2 General cell techniques and growth media

All cell work was carried out in sterile conditions next to a flame. LB media powder was dissolved in water at 25 g/l, then autoclaved and allowed to cool before the addition of filter sterilised antibiotic where appropriate. Minimal growth media was prepared with no carbon or nitrogen source to allow alteration between experiments, and filter sterilised. Per litre this contained 9g $Na_2HPO_4.12H_2O$, 1.5g KH_2PO_4, 0.2g $MgSO_4.7H_2O$, 1.2 mg $FeNH_4$-citrate, 20 mg $CaCl_2$, 2 ml Hoagland solution, 0.5 g $NaHCO_3$ (Schlegel, Kaltwasser and Gottschalk, 1961; Kosa and Ragauskas, 2013). Ammonium chloride was added as a nitrogen source at 0.1% for adaptation media and 0.05% for lipid accumulation media. Glucose or lignin breakdown model compounds (4-hydroxybenzoic acid, vanillic acid, vanillin) were also added at various concentrations. The pH was adjusted to 7.0 and the media was filter sterilised.

As Kraft lignin is insoluble in aqueous media at neutral pH, a different procedure was followed for this carbon source. The lignin was added to minimal media and the pH was adjusted to 12.5 using 1 M

sodium hydroxide. It was then shaken at 180 rpm for one hour and, once dissolved, the pH was readjusted to 7.0 with 1 M hydrochloric acid.

In the case of engineered strains with antibiotic resistance, the appropriate antibiotic was added to both liquid and solid media for selection purposes and to avoid contamination (100 µg/ml ampicillin, 50 µg/ml kanamycin or 50 µg/ml neomycin). 1000x stocks of antibiotic were prepared in water, filter sterilised and stored at -20 °C.

Stocks of all bacterial strains, wildtype and recombinant, were stored in 20% glycerol at -80 °C. These were used to streak LB agar plates (containing antibiotic where appropriate), which were incubated at 37 °C overnight (*E. coli*) or 30 °C for 2-3 days (*R. opacus*) until colonies formed. Single colonies were picked to inoculate liquid cultures, and plates were stored at 4 °C for two weeks, when fresh plates were prepared. LB media was used to grow initial cultures of all strains. *E. coli* and *R. opacus* liquid cultures were grown in a shaking incubator at 200 rpm and 37 °C or 30 °C respectively.

3.2.1 Competent cell preparation and transformation

3.2.1.1 E. coli

Chemically competent TOP10 and BL21 were purchased and transformed using the following protocol: 50 µl competent cells were thawed on ice, then 2 µl (0.05-0.1 µg) plasmid DNA was added and mixed by gently tapping. The tube was incubated on ice for 30 minutes, then at 42 °C for 30 seconds in a heat block, then back on ice for a further 2 minutes. 250 µl room temperature S.O.C. media was added aseptically (supplied with competent cells) and the tube incubated horizontally at 37 °C, 225 rpm for one hour. Two volumes of the cell suspension (20 µl and 200 µl) were spread onto two LB agar plates containing the appropriate antibiotic for selection of successful transformants. The plates were incubated, inverted, at 37 °C overnight or until colonies formed.

3.2.1.2 PD630

Electrocompetent PD630 cells were prepared as follows: 10 ml cultures were inoculated and grown overnight to OD_{600} 1.0, then the cells harvested by centrifugation at 4 °C, 4000 rpm for 10 minutes. The supernatant was discarded and the cells resuspend in 10 ml ice cold, sterile water. These were centrifuged as before, the supernatant discarded and cell resuspended in 10 ml ice cold, sterile 10% glycerol. After a final centrifugation the cells were resuspended in 400 µl ice cold, sterile 10% glycerol and kept on ice until transformation.

Competent cells were prepared fresh each time to ensure high transformation efficiency. The following transformation protocol was used: 400 µl competent cells and 0.5-1 µg DNA were mixed in a 2 mm electroporation cuvette, and the cells electroporated at 2.4 kV using a VWR ECM 399 Electroporation System. 600 µl room temperature LB media was added, mixed by pipetting and transferred to a 1.5 ml tube, which was incubated horizontally at 30 °C, 180 rpm for 4 hours. 100 µl was spread onto LB agar plates containing 50 µg/ml neomycin, which were incubated, inverted, at 30 °C for 2-3 days until colonies formed.

3.3 Microbial growth experiments

Before all experiments assessing *R. opacus* PD630 growth on different carbon sources, 10 ml LB media was inoculated with a single colony from an agar plate, and the culture incubated at 30 °C and 200 rpm until OD_{600} 1.0 was reached. 100 µl of this culture was used to inoculate 10 ml minimal media containing the relevant carbon source and 0.1% nitrogen. Samples were taken at various time intervals and absorbance at 600 nm measured to give cell density, using fresh media as the blank.

3.4 Lipid accumulation experiments

As with the growth experiments, 10 ml PD630 cultures were grown in LB media overnight to OD_{600} 1.0. Cells were harvested by centrifugation at 4000 rpm for 10 minutes, the supernatant discarded, and the pellet resuspended in 10 ml minimal media. This washing step was repeated to remove all rich media traces, before a final resuspension in 10 ml minimal media supplemented with the relevant carbon source and 0.1% nitrogen source (adaptation media). These cultures were incubated and grown to an OD_{600} of 0.6. This step allowed cells to adapt to growth on the particular substrate and avoids a long lag time during lipid accumulation experiments. After washing twice as before, the cells were resuspended in accumulation media (0.05% nitrogen) and incubated, once again, at 30 °C and 200 rpm. 1 ml samples were taken at various time points and frozen at -80 °C until analysis.

3.4.1 Lipid extraction

To extract the total lipids, these samples were thawed from -80 °C storage, and the cells harvested by centrifugation at 4000 rpm for 10 minutes. The cell pellets were washed twice in sterile 0.9% sodium chloride solution and then centrifuged at 13000 rpm for 10 minutes. The supernatant was discarded, and the remaining material was lyophilised overnight using a Heto Drywinner. The total mass was recorded before lipid extraction.

A modified Folch extraction (Folch, Lees and Sloane Stanley, 1957; Kosa and Ragauskas, 2012) was carried out: 2 ml chloroform and 1 ml methanol were added to the lyophilised cells, and the tubes shaken at room temperature for 2 hours. The tubes were then allowed to settle and separate overnight and the upper (aqueous) phase was discarded. The organic layer was pipetted into a fresh (weighed) tube, and the solvent was evaporated under a nitrogen stream. The mass was recorded and the lipid mass calculated, expressed as a percentage of the dry cell weight.

3.5 General DNA techniques

3.5.1 Plasmid DNA isolation

After each DNA transformation, colonies were picked from agar plates and used to inoculate 10 ml LB liquid culture containing the appropriate antibiotic. These cultures were grown overnight, and the plasmid DNA extracted using a QIAprep Spin Miniprep kit following the protocol provided, but with the final elution using 30 µl sterile water instead of PB buffer. For *R. opacus* the incubation time in lysis buffer (buffer P2) was extended to 5 minutes.

3.5.2 Gel electrophoresis and DNA purification

1% agarose gels containing SybrSafe gel stain were run to assess the size of DNA fragments after each stage of plasmid construction. They were prepared using tris-acetate-EDTA buffer, which was also used as the running buffer. 6X gel loading dye was added to each sample and a molecular weight marker (HyperLadder 1 kb) was used as a reference for DNA fragment size. For analytical gels, 5 µl of PCR product was loaded and run at 120 V for 1 hour. For gel extraction and purification, the full reaction volume was loaded (split between a few wells as necessary) and run at 80 V for 2 hours.

The Qiagen Gel Extraction kit was used to isolate the desired DNA bands, with the following protocol modifications: one QG buffer wash, two PE buffer washes, warmed water instead of buffer for elution and 30 µl elution volume to increase DNA yield. Gels were visualised using a Syngene Dyversity Imaging System or a benchtop UV transilluminator. DNA concentrations were determined using a NanoDrop 1000 Spectrophotometer.

3.6 Plasmid construction

ApE software was used to manipulate DNA sequences and aid primer design during the plasmid construction process. The *DypB* gene (sequence shown in blue in appendix 9.1) was synthesised by Integrated DNA Technologies and was received in their standard vector, pUCIDT-AMP. The *E. coli* – *Rhodococcus* shuttle vector pNV18.1 was provided by Dr Jun Ishikawa at the National Institute of Infectious Disease, Tokyo (Chiba *et al*., 2007). Both vectors were transformed into chemically competent TOP10 *E. coli* for glycerol freezer stocks, using the protocols described above. This strain was used for all steps in the plasmid construction procedure that required transformation.

3.6.1 PCR

The polymerase chain reaction (PCR) (Mullis *et al*., 1986) was used for many steps of the plasmid construction process, using an Eppendorf Mastercycler Gradient. Details of each stage are described in chapter 5, and the final, optimised conditions for each reaction are given here. All primer sequences are given in table 3.1.

DypB was amplified out of pUCIDT-AMP, and pNV18.1 was amplified using primers designed to give amplicons with overlapping sequences for Gibson assembly. The reactions were assembled on ice (10 µl GC buffer, 1 µl dNTPs, 0.5 µl template DNA, 0.5 µl forward primer, 0.5 µl reverse primer, 1.5 µl DMSO, 0.5 µl Phusion polymerase, 35.5 µl water), and the two-step cycle shown below was performed. A combined annealing and extension step was used due to the high T_m of the primers (NEB Phusion-specific T_m calculator https://tmcalculator.neb.com).

Amplify *DypB* from pUC-IDT-DypB

98 °C	30 s	
98 °C	10 s	30 cycles
72 °C	20 s	
72 °C	10 m	
4 °C	Hold	

Amplify pNV18.1

98 °C	30 s	
98 °C	10 s	30 cycles
72 °C	90 s	
72 °C	10 m	
4 °C	Hold	

1 µl DpnI was then added to the reaction mix to degrade methylated template DNA, which was incubated at 37 °C for 2 hours and heat inactivated at 80 °C for 20 minutes. The reactions were run on an agarose gel for band excision and purification.

3.6.2 Gibson assembly

NEB Gibson Assembly Master Mix was used to assemble pNV18.1 and *DypB*, and also pNV18.1-DypB and the ptac+RBS gBlock, as described in chapter 5. The recommended excess of insert compared to vector was used, and the volumes given here were determined by the gel purification DNA yield.

pNV18.1 and *DypB* assembly		**pNV18.1-DypB and ptac+RBS assembly**	
pNV18.1	8 µl	pNV18.1-DypB	9 µl
DypB	2 µl	ptac gBlock	1 µl
Master mix	10 µl	Master mix	10 µl

Reactions were incubated at 50 °C for 1 hour, and 2 µl transformed into chemically competent TOP10 *E. coli*, as per the manufacturer's instructions. Two volumes of cells were spread onto LB agar plates containing 50 µg/ml kanamycin, to ensure appropriate colony spacing.

3.6.3 Annealing single stranded DNA

As described in chapter 5, the tac promoter was initially synthesised as a linear, single stranded DNA fragment (119 base pairs) with a ribosome binding site and flanked by overhangs for subsequent Gibson assembly with pNV18.1-DypB (sequence given in table 3.1). The reverse complement sequence was also synthesised, and the two strands annealed as follows: Lyophilised DNA was resuspended in water to give a 100 µM stock, and 100 mM potassium acetate and 30 mM HEPES buffer was prepared and the pH adjusted to 7.5. 30 µl of buffer and 10 µl of each DNA strand were combined in a thermocycler tube and the thermocycler was programmed to heat to 94 °C for 2 minutes before decreasing by 1 °C every minute until reaching 4 °C. The reaction product was used for Gibson assembly with pNV18.1-DypB as described in chapter 5.

3.6.4 gBlock

The tac promoter was ordered from IDT as a 199 base pair gBlock (linear, double stranded DNA) with a ribosome binding site and overhangs complementary to the desired insert site of pNV18.1-DypB. The plasmid was linearised by digestion with fast digest XbaI, following the manufacturers protocol. A Gibson reaction was performed using the gBlock and linearised plasmid as above and transformed into *E. coli*.

3.6.5 Site directed mutagenesis

To remove 6 base pairs from pNV18.1-ptac-DypB between the ribosome binding site and start codon, inverse PCR was carried out using 5' phosphorylated primers that flank and amplify away from the desired deletion. The reaction was assembled on ice (5 µl GC buffer, 0.25 µl dNTPs, 0.25 µl template DNA, 0.25 µl forward primer, 0.25 µl reverse primer, 1 µl DMSO, 0.25 µl Phusion polymerase, 17.75 µl water) and the following reaction conditions used:

98 °C	1 m	
98 °C	10 s	30 cycles
72 °C	2m 30 s	
72 °C	10 m	
4 °C	Hold	

1 µl DpnI was then added to the reaction mix, which was incubated at 37 °C for 2 hours and heat inactivated at 80 °C for 20 minutes. Gel extraction and purification using the QIAquick Gel Extraction Kit yielded 5 ng/µl DNA. The plasmid was circularised by ligation by mixing the reaction components on ice (2 µl T4 ligase buffer, 17 µl DNA, 1 µl T4 ligase) and incubating for 2 hours at 25 °C, before the enzyme was heat inactivated for 10 minutes at 65 °C. 2 µl of the reaction was transformed into chemically competent TOP10 *E. coli* cells.

3.6.6 Sequence verification

After each plasmid construction step the resulting DNA was sequenced to confirm the modification. Plasmids were isolated from *E. coli* using the QIAprep Spin Miniprep Kit as above, and the DNA sent to GATC for sequencing on one or both strands. Universal primers were selected that bound 50-100 base pairs upstream of the sequence of interest. These were PCR1 and RPC for verifying *DypB* insertion into pNV18.1, PCR1 for ptac insertion and pUC-R for the site directed mutagenesis. These steps were always performed in triplicate to reduce the chance of false positive results.

Table 3.1: DNA sequences of primers and gBlocks used for the construction of plasmid pNV18.1-ptac-DypB. All sequences are written 5' to 3' as ordered from IDT DNA. Sequences in red indicate overlapping regions for DNA assembly.

Name	Description	Sequence
1. DypB F1	Amplify *DypB* from pUCIDT-AMP for Gibson assembly	GTCACGACGTTGTAAAACGATGCCAGGCCCAGTCGCGAG
2. DypB R2		CGTTCGAACCGTGACCGGCAAGTAACGCTATGAGGAAACTC
3. pNV18.1 F2	Amplify pNV18.1 for Gibson assembly	CTCAAAGGAGTATCGCAATGAACGGCCAGTGCCAAGCTTGC
4. pNV18.1 R1		GAGCGCTGACCCGGACCGTAGCAAAATGTTGCAGCACTG
5. DypB BamHI F1	Amplify *DypB* from pUCIDT-AMP for Gibson at BamHI site	CTGCAGGTCGACTCTAGAGATGCCAGGCCCAGTCGCGAG
6. DypB BamHI R2		GAGCTCGGTACCCGGGGATCTCATTGCGATACTCCTTTGAGACCACCG
7. pNV18.1 BamHI F2	Amplify pNV18.1 for Gibson at BamHI site	CTCAAAGGAGTATCGCAATGAGATCCCCGGGTACCGAGCTC
8. pNV18.1 BamHI R1		CTCGCGACTGGGCCTGGCATCTCTAGAGTCGACCTGCAGGCATG
9. pNV18.1 ptac F	Amplify pNV18.1-DypB for Gibson with ptac + RBS	ATTTCACACAGGAGATATCATATGCCAGGCCCAGTCGCGAG
10. pNV18.1 ptac R		TGATTAATTGTCAACAGCTCCTCTAGAGTCGACCTGCAGGCATGCAAG
11. ptac + RBS F	ptac + RBS (ssDNA) for Gibson with pNV18.1-DypB	CCTGCAGGTCGACTCTAGAGGAGCTGTTGACAATTAATCATCGGCTCGTATAATGTGTGGAATTGTGAGCG GATAACAATTTCACACAGGAGATATCATATGCCAGGCCCAGTCGCGAG
12. ptac + RBS R		CTCGCGACTGGGCCTGGCATATGATATCTCCTGTGTGAAATTGTTATCCGCTCACAATTCCACACATTATA CGAGCCGATGATTAATTGTCAACAGCTCCTCTAGAGTCGACCTGCAGG
13. ptac gBlock	Ptac + RBS gBlock (dsDNA) for Gibson with pNV18.1-DypB	CCCAGTCACGACGTTGTAAAACGACGGCCAGTGCCAAGCTTGCATGCCTGCAGGTCGACTGAGCTGTTGA CAATTAATCATCGGCTCGTATAATGTGTGGAATTGTGAGCGGATAACAATTTCACACAGGAGATATCATCT AGAGATGCCAGGCCCAGTCGCGAGATTGGCACCACAAGCAGTCCTCACTCCGCCCAGC
14. SDM del F	Remove 6 base pairs between RBS and start codon (last 6)	5'phos-ATGCCAGGCCCAGTCGCGAG
15. SDM del R		5'phos-TACTATAGAGGACACACTTTAACAATAGGCGAGTGTTAAGGTGTG
16. SDM del2 F	Remove 6 base pairs between RBS and start codon (first 6)	5'phos-CTAGAGATGCCAGGCCCAGTC
17. SDM del2 R		5'phos-AGAGGACACACTTTAACAATAGGCGAG

3.7 Protein expression

Once plasmids had been constructed, expression of the DypB protein was attempted. The same methods of expression and analysis were used for TOP10 and BL21 *E. coli* strains and *R. opacus* PD630, as detailed here.

3.7.1 Growth, induction and cell lysis

10 ml cultures of the recombinant strains were grown overnight at 37 °C or 30 °C, 200 rpm in LB media containing kanamycin (*E. coli*) or neomycin (*R. opacus*). IPTG was added to a final concentration of 1 mM and incubated for a further 4, 6 or 22 hours at either 37 °C or 30 °C. Cells were harvested by centrifugation at 4000 rpm for 15 minutes. The supernatant was retained and concentrated using 30 kDa Amicon Ultra-0.5 Centrifugal Filter Units, then stored at -20 °C until analysis by SDS-PAGE analysis.

BugBuster Master Mix (Merck Millipore) was used to lyse the cells and extract soluble proteins. Cell pellets were resuspended in 500 µl BugBuster and incubated on a rotary shaker at room temperature for 20 minutes, then centrifuged at 16000 rpm for 20 minutes at 4 °C. The supernatant containing soluble proteins was transferred to an Eppendorf tube and stored at -20 °C until analysis by SDS-PAGE.

To isolate insoluble proteins from inclusion bodies, the remaining cell debris pellet was resuspended in 500 µl BugBuster Protein Extraction Reagent and 1:10 diluted Master Mix and mixed by vortexing. Tubes were centrifuged at 5000 rpm for 15 minutes and the supernatant discarded. Pellets were then resuspended in 500 µl 1:10 Master Mix and centrifuged as before. This washing step was repeated three times, and the samples then stored at -20 °C until SDS-PAGE analysis.

3.7.2 SDS-PAGE

SDS polyacrylamide gel electrophoresis was used to analyse the proteins. Samples of concentrated culture supernatant and of soluble protein extract were mixed with NuPAGE LDS Sample Buffer 4X and NuPAGE Reducing Agent 10X, then heated to 70 °C for 10 minutes. Insoluble protein samples were mixed with LDS Sample Buffer only and heated to 85 °C for 3 minutes. These were loaded into NuPAGE 4-12% Bis-Tris Protein Gels, and electrophoresis performed using MES running buffer at 200 V for 35 minutes. The PageRuler Unstained Protein Ladder was also loaded for molecular weight reference.

Gels were stained overnight with SYPRO Ruby Protein Gel Stain following the standard protocol and visualised using a Syngene Dyversity Imaging System.

3.8 Laccase experiments

Laccase from *Trametes versicolor* was dissolved in water at a concentration of 5 mg/ml and filter sterilised. The redox mediators syringaldehyde and 2,2′-azinobis(3-ethylbenzothiazoline-6-sulfonic acid) (ABTS) were dissolved in water to a concentration of 0.1 M and also filter sterilised.

3.8.1 Enzyme activity

The activity of the *T. versicolor* laccase was assessed by its ability to oxidise the mediators ABTS and syringaldehyde. The enzyme was incubated in 0.1 M sodium acetate (pH 5.0), and 0.5 mM mediator for 1 minute, and the change in absorbance was measured at 420 nm or 370 nm for ABTS and syringaldehyde respectively. Each was performed in triplicate. 1 unit of enzyme is defined as the amount of enzyme required to convert 1 µmol of substrate per minute ($\varepsilon_{420\,nm}$ = 36000 M^{-1} cm^{-1}, $\varepsilon_{370\,nm}$ = 8500 M^{-1} cm^{-1}).

3.8.2 Laccase treatment of Kraft lignin

Kraft lignin was treated with *T. versicolor* laccase before being used as a feedstock for PD630 cultures. 10 ml reactions were carried out in 125 ml baffled flasks to ensure adequate aeration and therefore availability of oxygen to the laccase as the electron donor. The reactions contained: 1 ml of 1 M sodium acetate pH 5.0, 2.13 ml of 5 mg/ml (4.7 U/ml) laccase stock solution, 0.1 ml of 0.1 M syringaldehyde stock solution, 0.5 g Kraft lignin and water to 10 ml. Control experiments containing no laccase enzyme were also carried out.

The flasks were incubated at 50 °C and 200 rpm for various lengths of time (12, 24, 48, 72, 96, 120 hours), then heated to 100 °C for 10 minutes to inactivate the enzyme. These reaction mixes were then used as feedstock for PD630 fermentation cultures, adding 1 ml of laccase/lignin reaction mix to 9 ml minimal media and nitrogen source. Growth experiments were then carried out as before (section 3.3).

A scaled-up reaction of 100 ml was carried out in a 1 l flask and incubated for 96 hours. This was used as the feedstock for lipid accumulation experiments.

3.8.3 Simultaneous depolymerisation and metabolism

Minimal growth media was prepared as in section 3.2, with the relevant nitrogen content and Kraft lignin added. 1 U/ml laccase and 1 mM mediator were then added directly to the media at the time of inoculation with PD630. Pre-adapted cells grown on laccase-treated lignin were harvested by centrifugation (4000 rpm for 10 minutes) and washed twice in minimal media containing no carbon source to remove all traces of degraded lignin. Growth and lipid accumulation experiments were carried out as before (sections 3.3 - 3.4).

Chapter 4

PD630 growth on lignin and lignin breakdown model compounds

4 PD630 growth on lignin and lignin breakdown model compounds

4.1 Introduction

Lignocellulosic biomass is increasingly being exploited as a feedstock for various sectors, including the biofuel industry where it is mostly used as a source of the polysaccharides cellulose and hemicellulose. These are fermented to produce bioethanol, while lignin is largely seen as a side product with inconvenient recalcitrant characteristics and is often just burned to produce energy. This underused resource therefore warrants research into higher value processing opportunities that could contribute to the energy industry.

Rhodococcus opacus PD630 is a species of oleaginous bacteria capable of accumulating large quantities of lipids in intracellular inclusion bodies, as described in chapter 1, figure 1.11 (Alvarez *et al*., 1996). These are mostly in the form of triacylglycerides (TAGs) which, once extracted and transesterified, could provide a sustainable alternative to diesel.

We set out to investigate the potential bioconversion of lignin to lipids using *Rhodococcus opacus* PD630. This strain has been reported to metabolise pre-treated lignin to some extent (Kosa and Ragauskas, 2013), though not as well as other strains of *Rhodococcus*, namely *R. jostii* RHA1 (Ahmad *et al*., 2011). Nevertheless, its TAG accumulation abilities make it highly attractive for use in biodiesel production. As discussed in chapter 1, lipid synthesis can be enhanced by depriving the cells of nitrogen, which limits protein synthesis and growth and instead encourages the storage of excess carbon as lipids. We used this method to maximise TAG accumulation in these experiments.

To assess the potential of PD630 to perform this conversion, we first looked at whether and how well it could grow and accumulate lipids when provided with Kraft lignin as a sole carbon source. Next, we performed similar experiments using lignin breakdown model compounds that resemble monolignols to see if the strain could grow on, and produce lipids from, lignin breakdown products. This simulates a scenario where lignin (or lignocellulosic biomass) is pre-treated to degrade the polymer and release the constituent monomers, which can then be metabolised by the bacteria.

4-hydroxybenzoic acid (4-HBA), vanillic acid (VanA) and vanillin were selected following reports of growth of PD630 and related strains on these substrates (Chen *et al*., 2012; Kosa and Ragauskas, 2012; Wang *et al*., 2014). Their structures are shown in figure 4.1.

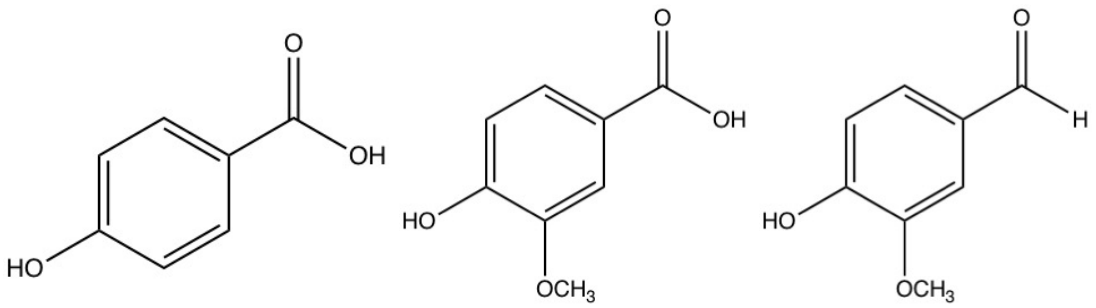


Figure 4.1: Structure of lignin model compounds used in these experiments. 4-hydroxybenzoic acid, vanillic acid and vanillin.

4.2 Results and discussion

4.2.1 PD630 and lignin

As discussed in chapter 2, section 2.6.2, Kraft lignin refers to waste lignin following extraction of cellulose from lignocellulosic biomass for paper production by the Kraft process. It is better characterised than other forms of lignin and is a "real life" potential feedstock, so provides a good starting point for investigation.

4.2.1.1 Growth experiments

PD630 (initially cultured in rich media starter cultures, as described in chapter 3) was grown in minimal media containing 0.5%, 1% or 5% (w/v) Kraft lignin as the sole carbon source and 0.1% nitrogen (in the form of ammonium chloride). As shown in figure 4.2 growth was extremely slow, taking a full week to show any increase in optical density, and still only reaching maximum OD of 0.28, 0.31 and 0.36 after 12-14 days for the three concentrations respectively. Growth on glucose is also shown for comparison, where it reaches a maximum OD of approximately 1.6 after only 3 days. Adaptation to growth on a particular carbon source explains the long lag time, but increased lignin concentration did not alter the growth profile.

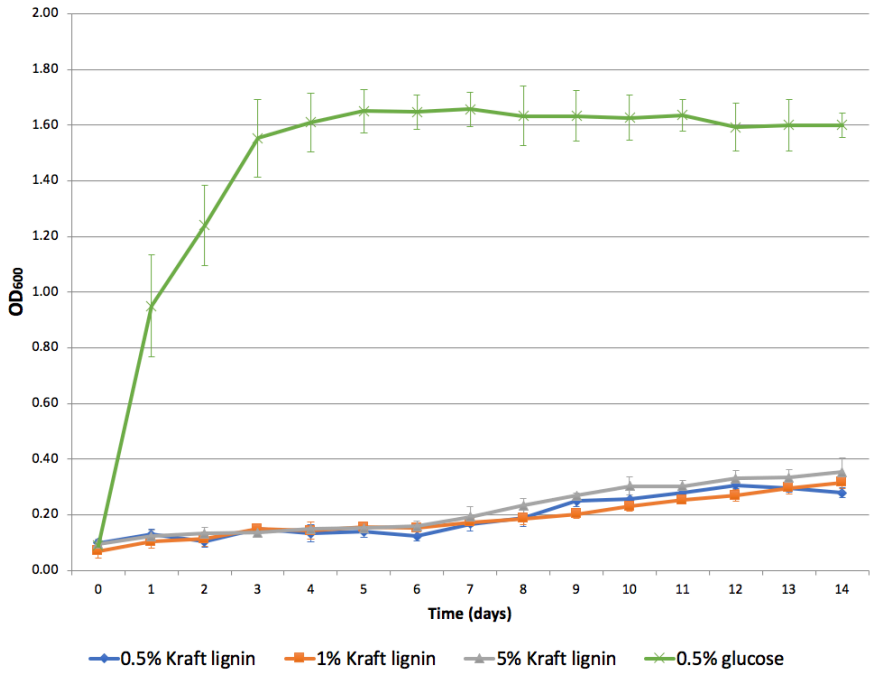


Figure 4.2: Growth of *R. opacus* PD630 on Kraft lignin and glucose as the sole carbon source. Minimal media was supplemented with 0.5%, 1% or 5% carbon and 0.1% nitrogen source. Error bars represent standard deviation (n=3).

4.2.1.2 Lipid accumulation

The intention was to grow cultures on Kraft lignin as above, then limit nitrogen availability to encourage cells to store lipid. However, repeated trials did not yield sufficient material for lipid extraction. Kosa *et al*., 2013 showed that PD630 also grew poorly on other forms of lignin (ethanol Organosolv) and partial breakdown to lower molecular weight lignin was required before the cells could grow (Kosa and Ragauskas, 2013).

4.2.2 PD630 and lignin breakdown model compounds

Having seen slow growth and therefore been unable to investigate lipid production when using Kraft lignin, we next looked at how PD630 performed when provided with the lignin breakdown model compounds 4-HBA, VanA and vanillin as the sole carbon source.

4.2.2.1 Growth experiments

Experiments were performed in the same format as for Kraft lignin, with starter cultures grown in rich media then used to inoculate minimal media supplemented with the relevant carbon source and 0.1% nitrogen. As these aromatic compounds are known inhibitory compounds to many microorganisms (Klinke, Thomsen and Ahring, 2004), preliminary tests were carried out to determine a suitable concentration for growth without any toxicity effects.

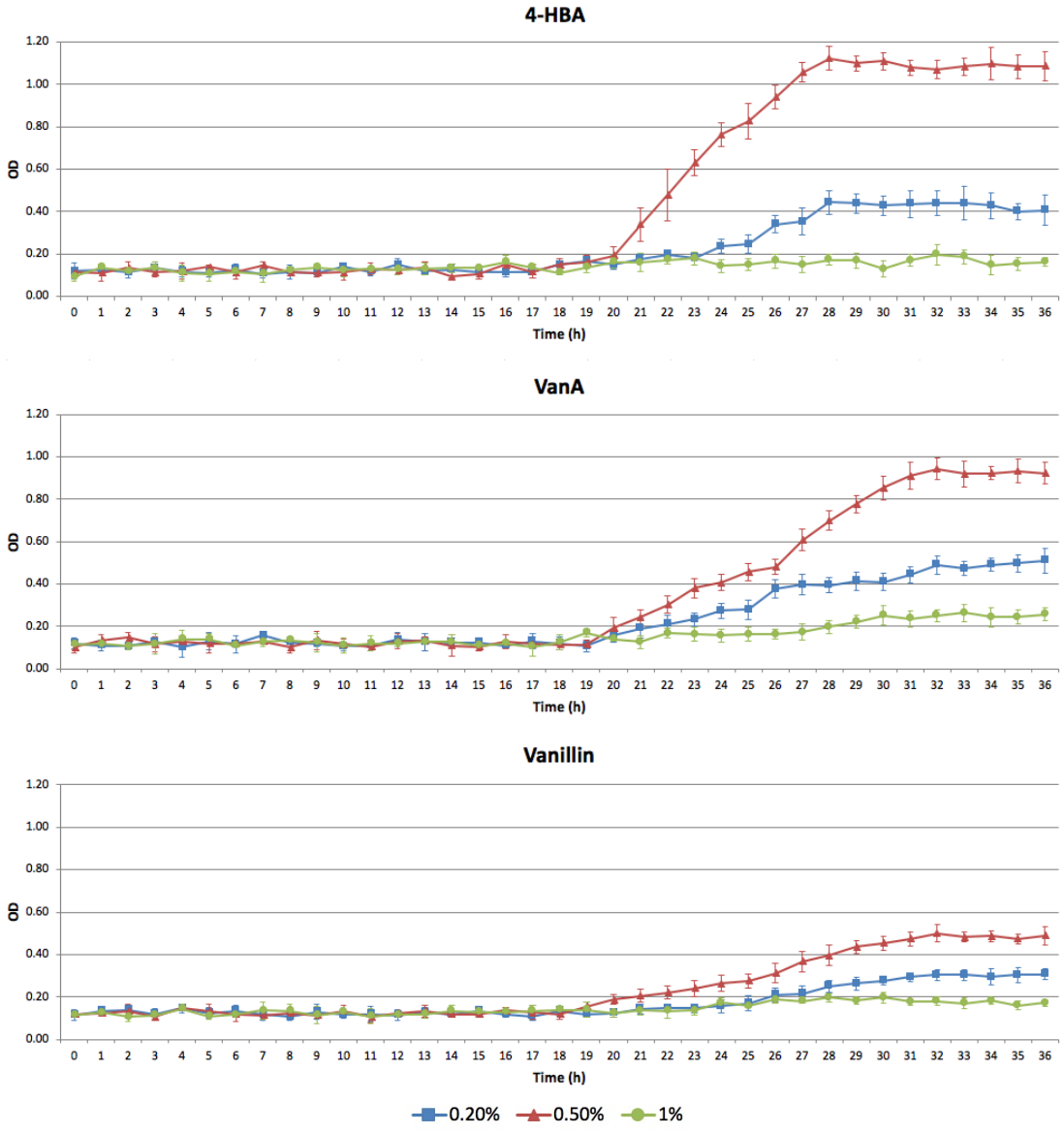


Figure 4.3: Growth of *R. opacus* PD630 on the lignin model compounds 4-HBA, VanA and vanillin as the sole carbon source. Cultures were grown in three different concentrations of carbon source and 0.1% nitrogen to assess the toxicity effect of these compounds. Error bars represent standard deviation (n=3).

Figure 4.3 shows that PD630 can grow on 4-HBA, VanA and vanillin as the only source of carbon. 0.2%, 0.5% and 1% media carbon content were tested and in all three cases the strongest growth was seen with 0.5%. At 0.2% it is likely that carbon availability is the limiting factor, while at 1% the inhibitory effects have begun to outweigh the benefit of a plentiful carbon supply. For all further experiments a media carbon content of 0.5% was used.

The strongest growth was observed on 4-HBA, reaching OD 1.12 in 28 hours. Using VanA it took 32 hours to reach a maximum OD of 0.94, while using vanillin only OD 0.50 was reached after 32 hours.

This difference could be due to vanillin being more toxic to the cells than the other two compounds. Vanillin has been shown to have inhibitory effects on the growth of *R. jostii* RHA1 while VanA did not (Chen *et al*., 2012). In this strain vanillin is converted to VanA by vanillin dehydrogenase, and then to protocatechuate by vanillate *O*-demethylase which feeds into the β-ketoadipate pathway for aromatic degradation (described in chapter 1, sections 1.7 and 1.7.1). It is possible that a similar degradation mechanism is used by PD630, and indeed Wang et al., 2014 also reported slower growth on vanillin compared with VanA (Wang *et al*., 2014). The toxicity of vanillin to microorganisms is well recognised, being observed, for example, in yeasts associated with food spoilage (Fitzgerald, Stratford and Narbad, 2003). Its aldehyde group is hypothesised to contribute to its antimicrobial properties by covalently bonding to biological molecules such as proteins and nucleic acids (Zaldivar, Martinez and Ingram, 1999; Fitzgerald *et al*., 2004; Lopachin and Gavin, 2014). This also limits its accessibility and therefore inhibits its degradation.

4-HBA lacks the methoxyl group that VanA and vanillin contain (figure 4.1), therefore fewer conversion steps are required before entering the β-ketoadipate pathway. This could explain the better growth seen on 4-HBA compared with the other two compounds.

Growth on all three compounds showed a long lag phase of 18-20 hours, where the cells are adapting to using the new substrate as their only source of carbon. This probably involves initiating gene expression of proteins required to metabolise these compounds before the cells resume growth and proliferation. 100 µl aliquots of these cultures were taken after 24 hours and used to inoculate 10 ml fresh minimal media. These new cultures began growing immediately with no lag time (figure 4.4), indicating they have already undergone the necessary adaptations.

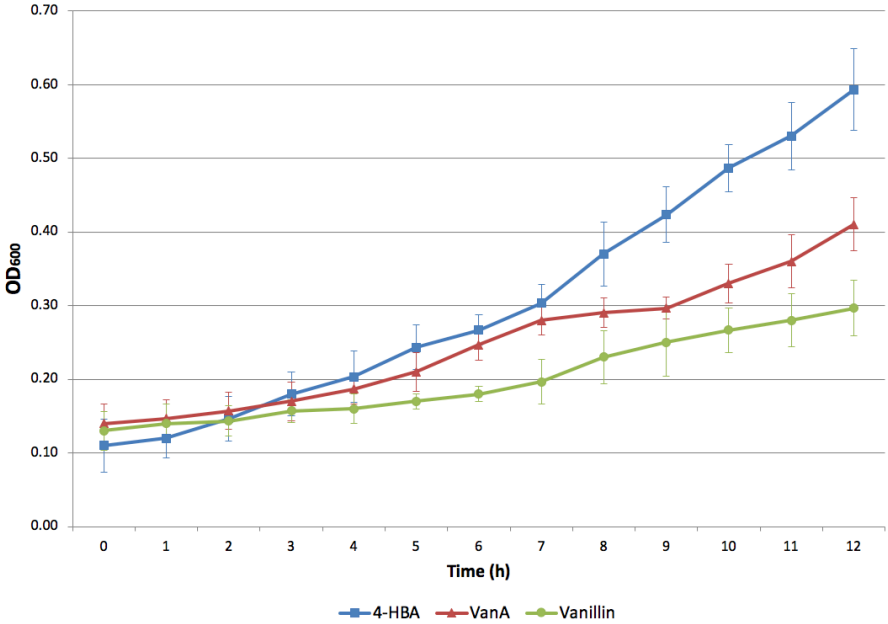


Figure 4.4: Growth of *R. opacus* PD630 cells already adapted to using lignin model compounds as a sole carbon source, eliminating the lag period. Minimal media contained 0.5% carbon source and 0.1% nitrogen source. Error bars represent standard deviation (n=3).

4.2.2.2 Lipid accumulation

Cultures were prepared for lipid accumulation experiments as described in chapter 3, section 3.4 (grown in minimal media containing 0.5% carbon and 0.1% nitrogen source to allow adaptation to the specific substrate, then transferred to 0.05% nitrogen to encourage lipid synthesis). Samples were taken every 12 hours and the cell dry weight (growth) and lipid content were analysed. Figure 4.5 shows PD630 growth and lipid content when cultured with glucose, 4-HBA, VanA and vanillin. Lipid content is expressed as a percentage of the cell dry weight (lipid mass divided by total lyophilised cell mass) and is plotted on the secondary y-axis. These results show that PD630 is able to grow on all four substrates, and accumulate lipids when grown on glucose, 4-HBA and VanA, but not vanillin.

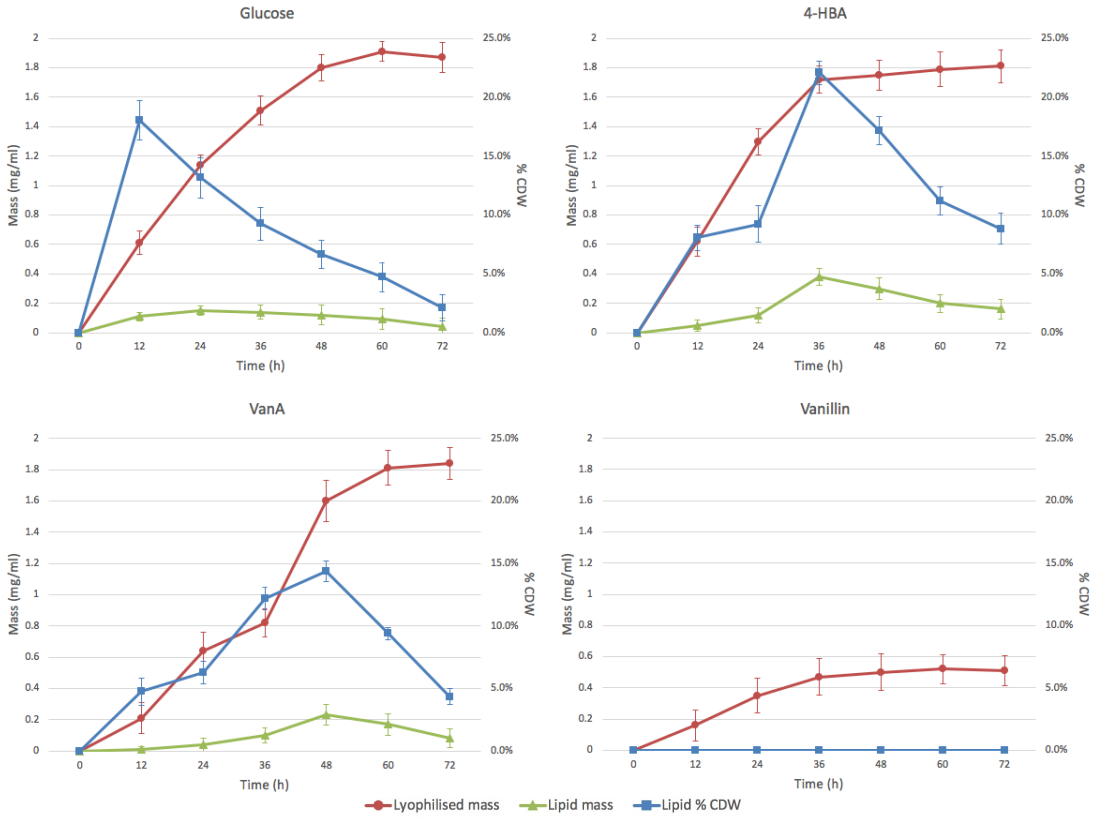


Figure 4.5: Growth and lipid accumulation of *R. opacus* PD630 on glucose and lignin breakdown model compounds. All were cultured in minimal media supplemented with 0.5% carbon source and 0.05% nitrogen source. Lyophilised cell mass (cell dry weight) and lipid mass are given in mg/ml (primary y-axis), while lipid content is given as % of the cell dry weight (secondary y-axis). Error bars represent standard deviation (n=3).

4-HBA and VanA cultures reach a similar maximum CDW of approximately 1.8 mg/ml, though this is reached more quickly for 4-HBA, as with the previous growth experiments. This maximum is also similar to glucose, showing the strain is able to grow just as well on these lignin breakdown model compounds. Once again, growth on vanillin is poor and the maximum CDW was 0.5 mg/ml.

Lipid levels in the glucose grown cells reached a maximum of 18% after 12 hours, before declining steadily. In 4-HBA the level increased more slowly, reaching a peak of 22% after 36 hours, while in VanA 14% was reached after 48 hours. Glucose is more straightforward to channel into the Krebs cycle (glycolysis to pyruvate and then acetyl-CoA) and so TAG synthesis from acetyl-CoA may begin sooner. As discussed above, aromatics require more complex degradation routes via the β-ketoadipate pathway (described in chapter 1, section 1.7.1) and TAG accumulation begins at a slower rate. As the media carbon content is declining the cells may be mobilising stored lipids to continue growth, despite the nitrogen limiting conditions, leading to the decrease in lipid content after the maximum is reached.

As well as poor growth, cultures grown on vanillin also failed to accumulate any detectable lipid. After sample lyophilisation, modified Folch extraction and solvent evaporation (chapter 3, section 3.4.1), almost no material was left to record as lipid mass. As discussed in the growth experiments, vanillin appears to be more toxic to the cells than the other model compounds, explaining the poor growth.

However, even the cells that did grow were not able to synthesise detectable quantities of lipid. To see whether vanillin toxicity plays a role here, cultures were grown in 0.25% glucose + 0.25% vanillin as shown in figure 4.6.

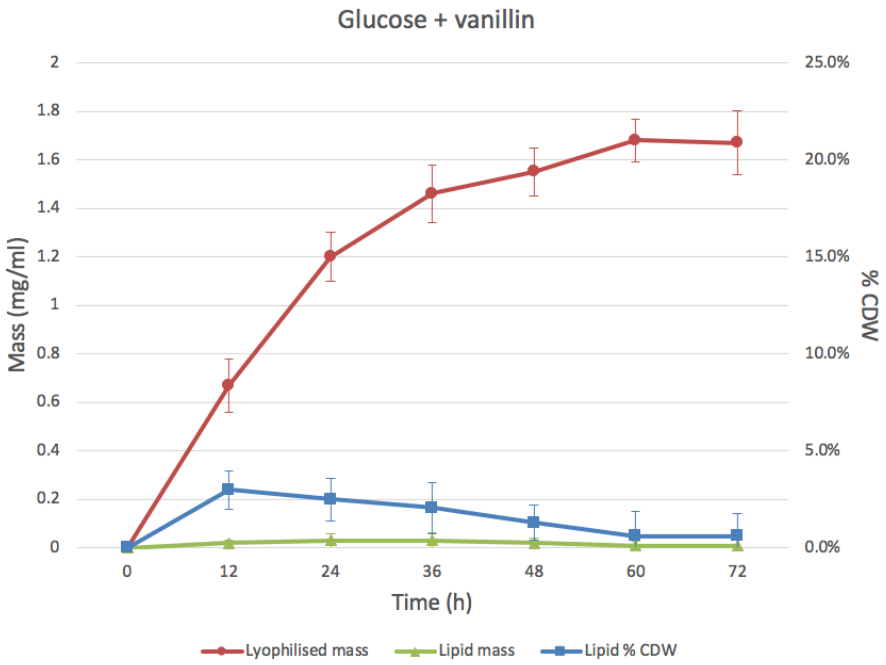


Figure 4.6: *R. opacus* PD630 growth and lipid accumulation in minimal media supplemented with 0.25% glucose, 0.25% vanillin and 0.05% nitrogen. Lyophilised cell mass (cell dry weight) and lipid mass are given in mg/ml (primary y-axis), while lipid content is given as % of the cell dry weight (secondary y-axis). Error bars represent standard deviation (n=3).

The cultures grew slower and to a lower maximum (1.7 mg/ml) than glucose alone (1.9 mg/ml), but far better than vanillin alone (0.5 mg/ml). Though the media contains half the concentration of glucose, the maximum reached is more than half of that when using glucose alone suggesting vanillin is also used as a carbon source for growth. The inhibitory properties of vanillin may contribute to this reduction, although the growth rate for the first 36 hours is comparable to that of glucose alone (~0.6 after 12 hours, ~1.2 after 24 hours and ~1.5 after 36 hours).

Lipid content is far lower than for glucose alone, reaching a maximum of just 3% after 12 hours before decreasing. This large difference suggests that vanillin's toxicity is affecting the cells' ability to synthesise lipids from glucose, rather than just inhibiting growth.

Given that the only structural difference between vanillin and VanA is the presence of an aldehyde group instead of a carboxylic acid group (figure 4.1) and that vanillin degradation proceeds via conversion to VanA, it is interesting to see such a marked disparity between their growth and lipid accumulation profiles. The experiment was repeated using a mixture of VanA and vanillin as the carbon source, shown in figure 4.7.

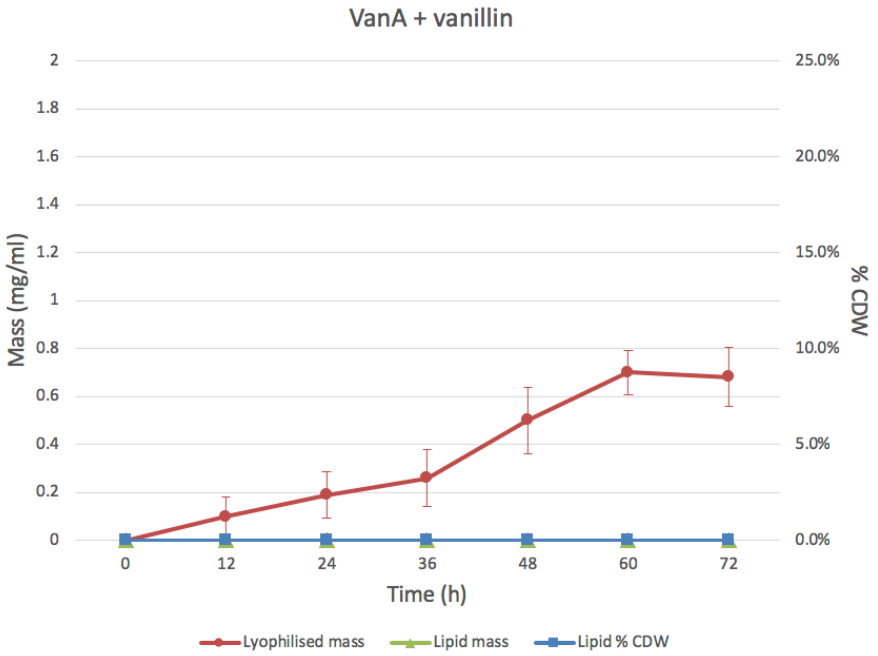


Figure 4.7: *R. opacus* PD630 growth and lipid accumulation in minimal media supplemented with 0.25% VanA, 0.25% vanillin and 0.05% nitrogen. Lyophilised cell mass (cell dry weight) and lipid mass are given in mg/ml (primary y-axis), while lipid content is given as % of the cell dry weight (secondary y-axis). Error bars represent standard deviation (n=3).

The presence of vanillin appears to negatively impact cell growth, with a much slower initial rate and a maximum of 0.7 mg/ml after 60 hours, compared with 1.8 mg/ml for VanA alone. No detectable lipid mass was recovered from the samples at all, suggesting vanillin severely inhibits lipid synthesis.

These results indicate that *R. opacus* PD630 is able to use vanillin as a carbon source for growth, but not to accumulate lipids. It appears to not significantly hinder growth when present in glucose-grown cultures but does inhibit the ability to synthesise TAGs. In contrast, vanillin has a detrimental effect on cell growth in VanA cultures and prevents lipid synthesis entirely.

These results are consistent with those of Kosa *et al.*, 2012, who observed poor growth on vanillin, and Wang *et al.*, 2014, who also saw that while vanillin could be metabolised and used for growth, TAG accumulation was not observed. Wang *et al.* also grew PD630 on the hydrolysates of three lignocellulose sources (treated by alkali hydrolysis with sodium hydroxide and enzymatic hydrolysis with cellulase and glucosidase), which contained varying levels of monolignols including the model compounds used here. The strain was able to grow well on these complex hydrolysates, also using them to accumulate lipids (Wang *et al.*, 2014). Their results validate the potential of PD630 to perform the bioconversion of lignin breakdown products to TAGs.

4.2.3 Relationship between growth and lipid storage

Cells grow and proliferate when carbon and nitrogen are both plentiful but, as discussed, nitrogen deficient conditions inhibit protein synthesis and shift metabolism away from growth and towards lipid accumulation. Growth rates decrease, and excess carbon is stored as TAGs. If nitrogen becomes available again the cells are likely to mobilise these lipids to allow growth to continue using endogenous carbon. To illustrate this, cultures were grown on 4-HBA as before and a dose of ammonium chloride added after 72 hours once the cells reached stationary phase (to a concentration of 0.1%), shown in figure 4.8.

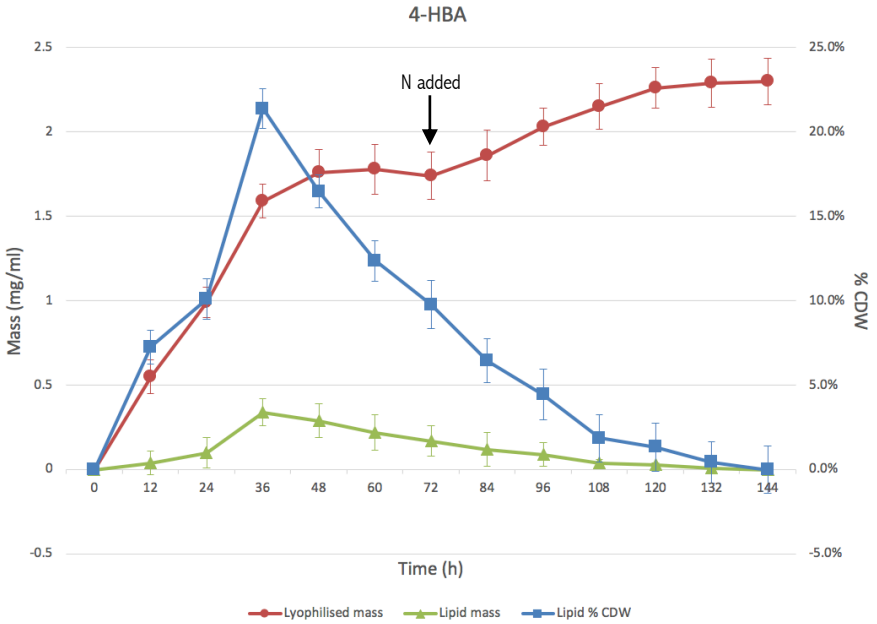


Figure 4.8: *R. opacus* PD630 growth and lipid accumulation in minimal media supplemented with 0.5% 4-HBA and 0.05% nitrogen. After 72 hours additional nitrogen was added. Lyophilised cell mass (cell dry weight) and lipid mass are given in mg/ml (primary y-axis), while lipid content is given as % of the cell dry weight (secondary y-axis). Error bars represent standard deviation (n=3).

Similar to before, cells grew to a maximum CDW of approximately 1.8 mg/ml after 48 hours, while the maximum lipid content of 21% was reached after 36 hours under nitrogen deficient conditions. As the carbon supply is used up, cell proliferation is reduced and the cultures enter stationary phase. Lipid content also decreases as cells use endogenous carbon for energy generation. When nitrogen is added back to the media at a non-limiting concentration of 0.1%, growth recommences and the CDW increases to 2.3 mg/ml after 120 hours. As no more carbon is added, it is assumed that stored lipids are oxidised and used for growth, and indeed the cell lipid content continues to decrease over this period and becomes undetectable after 144 hours.

4.3 Conclusions

The experimental results detailed in this chapter show that *R. opacus* PD630 is able to metabolise lignin breakdown model compounds and use them for lipid biosynthesis under nitrogen limiting conditions. In particular, cells grown on 4-HBA reached a lipid content of 22% after 36 hours, which exceeds the oleaginous threshold. VanA was also metabolised and used for lipid synthesis, reaching 14% after 48 hours. The strain was able to use vanillin for growth, but no TAGs were synthesised when using this substrate. PD630 therefore shows potential as a route for the conversion of lignocellulosic biomass to lipids for biodiesel production.

However, growth and lipid accumulation were poor or non-existent on polymeric Kraft lignin itself. This led to the decision to engineer a strain of *Rhodococcus* better able to carry out the whole bioconversion pathway. As lipid synthesis is extremely complex, we chose to engineer lignin degradation capabilities into PD630 by cloning and expressing the lignin peroxidase *DypB* gene, found in, *R. jostii* RHA1, a known lignin degrader.

Chapter 5

Expression of lignin peroxidase DypB in *R. opacus* PD630

5 Expression of lignin peroxidase DypB in *R. opacus* PD630

5.1 Introduction

In this chapter we describe attempts to engineer lignin depolymerisation capability into PD630 in order to create a strain able to break down lignin, use the aromatic monomers for growth and accumulate significant quantities of triglycerides.

Results presented in chapter 4 showed that *R. opacus* PD630 grows poorly on Kraft lignin as a sole carbon source, requiring long adaptation times. Cell growth was too slow to provide enough material for investigation of lipid accumulation. However, the strain did grow on the lignin breakdown model compounds 4-hydroxybenzoic acid, vanillic acid and vanillin, and could use the former two for lipid accumulation under nitrogen limiting conditions.

Although not as extensively studied and characterised as other bacterial strains, *Rhodococcus* species still offer potential for genetic manipulation and heterologous gene expression. Indeed, such is the interest in lipid accumulation in PD630, that metabolism of other lignocellulosic biomass components has been engineered into this strain. The ability to saccharify cellulose to cellobiose (Hetzler, Bröker and Steinbüchel, 2013) and subsequently metabolise cellobiose (Hetzler and Steinbüchel, 2013) was accomplished, and xylose metabolism (a hemicellulose monomer) has also been achieved (Xiong, Wang and Chen, 2012; Kurosawa, Wewetzer and Sinskey, 2013).

R. jostii RHA1 is a known lignin degrader, and a lignin peroxidase, DypB, has been identified (Ahmad *et al*., 2011). Degradation has been observed in the extracellular medium, suggesting this enzyme is transported out of the cell where it catalyses lignin depolymerisation. The breakdown products may then be transported into the cell and further degraded via the β-ketoadipate pathway before entering central carbon metabolism. Supposing the *DypB* gene contains an element targeting the enzyme for secretion, we intended to express this protein in PD630 where it would perform the same function of extracellular lignin depolymerisation.

5.2 Results and discussion

5.2.1 Approach

We decided to follow a similar approach to Xiong *et al*., who successfully engineered xylose metabolism into PD630 (Xiong, Wang and Chen, 2012). They used an *E. coli* – *Rhodococcus* shuttle

vector, pNV18, to express exogenous xylose isomerase and xylulokinase in the strain, which could then successfully use xylose for growth and could accumulate lipid levels of up to 68.3%.

Using a shuttle vector allows the plasmid construction to be executed in *E. coli*. With well-characterised laboratory strains and established genetic techniques, this appeared to be the best method. Very recently a molecular toolkit for genetic manipulation in PD630 was published by DeLorenzo *et al*., which includes a library of constitutive promoters of variable output level, a new antibiotic resistance marker, a system for genome modification by integration and tuneable gene repression (DeLorenzo *et al*., 2018). Although not available at the time these experiments were carried out, this work facilitates more reliable, predictable gene expression and greatly enhances the potential of *R. opacus* PD630 as a chassis for genetic engineering and industrial applications.

5.2.2 Plasmid construction

The pNV18.1 shuttle vector consists of the *E. coli* pK18 cloning plasmid with the mycobacterial pAL5000 origin of replication added, and is 4411 base pairs in length (Chiba *et al*., 2007). It contains a multiple cloning site and the *aph* gene conferring resistance to kanamycin and neomycin for antibiotic selection.

The 1053 bp DNA sequence coding for the DypB lignin peroxidase in *R. jostii* RHA1 was obtained from the published and annotated genome sequence (McLeod *et al*., 2006), and was synthesised and received in the *E. coli* expression vector, pUCIDT-AMP. Plasmid maps are shown in figure 5.1, and DNA sequences are given in the appendix.

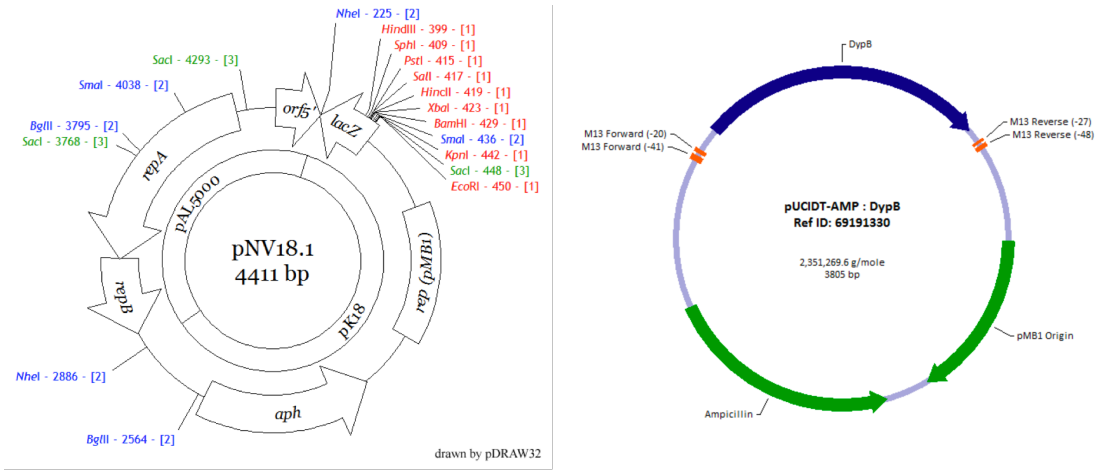


Figure 5.1: Plasmid maps of pNV18.1 (the *E. coli* – *Rhodococcus* shuttle vector), and pUCIDT-AMP containing the *DypB* gene.

5.2.2.1 Inserting DypB into pNV18.1

The Gibson assembly method was used to insert the *DypB* lignin peroxidase gene into the shuttle vector pNV18.1. This is a one-pot, isothermal, *in vitro* recombination method of DNA fragment assembly, as shown in figure 5.2. The fragments are designed to have overlapping sequences of around 40 base pairs and are incubated at 50 °C for one hour with three enzymes. T5 exonuclease degrades DNA from the 5' end to expose the overhangs and is then heat inactivated. Complementary sequences then anneal and the overhangs act as primers for Phusion DNA polymerase to fill in the gaps. Taq ligase then seals the nicks.

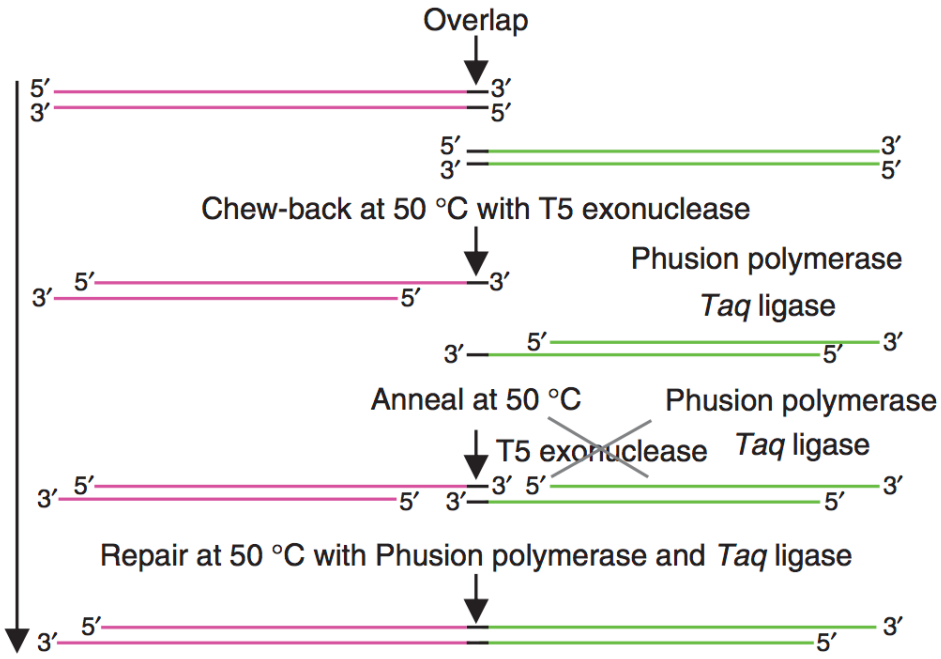


Figure 5.2: Gibson assembly method. DNA fragments with overlapping regions are incubated at 50 C for one hour with three enzymes: T5 exonuclease chews back the 5' end, exposing the overhangs and allowing complementary sequences to anneal. The overhangs act as primers for Phusion DNA polymerase to fill in the gaps, and the nicks are sealed by Taq ligase. T5 exonuclease is heat inactivated soon in the reaction, limiting the amount of DNA degradation. This method can be used to assemble several DNA fragments at once, or to create a circular plasmid from linear fragments. Reprinted with permission from Gibson *et al*. Copyright 2009, Nature America, Inc.

PCR was carried out to amplify the plasmid backbone and *DypB* ready for Gibson assembly. Primer sequences were designed to give the resulting DNA fragments overlapping sequences at both ends, so creating a circular plasmid. Primer were approximately 40 base pairs in length, had GC content of 40-60%, a G or C residue at the end to anchor to the template DNA, and pairs had melting temperatures within a few degrees of each other. Sequences for these primers are given in chapter 3, table 3.1.

Initially it was planned to insert *DypB* into pNV18.1 at the start of the multiple cloning site. Primers 1 and 2 were used to amplify *DypB* from pUCIDT-AMP and primers 3 and 4 to linearise and amplify the pNV18.1 backbone. Analytical agarose gels showed no specific DNA products at the expected fragment size. After a few attempts at varying the conditions (changing the polymerase enzyme, melting temperature, extension time, number of cycles, template DNA concentration, adding DMSO and magnesium chloride) a new site was chosen, the BamHI restriction site, and new primers synthesised (primers 5-8).

Again, many attempts were required to produce products of the expected band size, and the final optimised conditions are detailed in chapter 3, section 3.6.1. High primer melting temperatures specific to Phusion DNA polymerase from the NEB calculator recommended using a two-step thermocycling method, and the GC buffer provided was chosen due to the high GC content of both *DypB* and pNV18.1.

Figure 5.3 (left) shows the effect of varying DMSO concentration on the reaction. DNA products can be seen around the expected sizes of 1053 bp and 4411 bp, with the strongest and cleanest bands at 3% DMSO. Larger scale PCRs were carried out under these conditions, and the reactions then digested with DpnI. This enzyme digests methylated DNA, therefore removing the templates (which were propagated in a methylating strain of *E. coli*) and avoiding false positive colonies. The reaction was run on a gel for band excision and purification (figure 5.3, right).

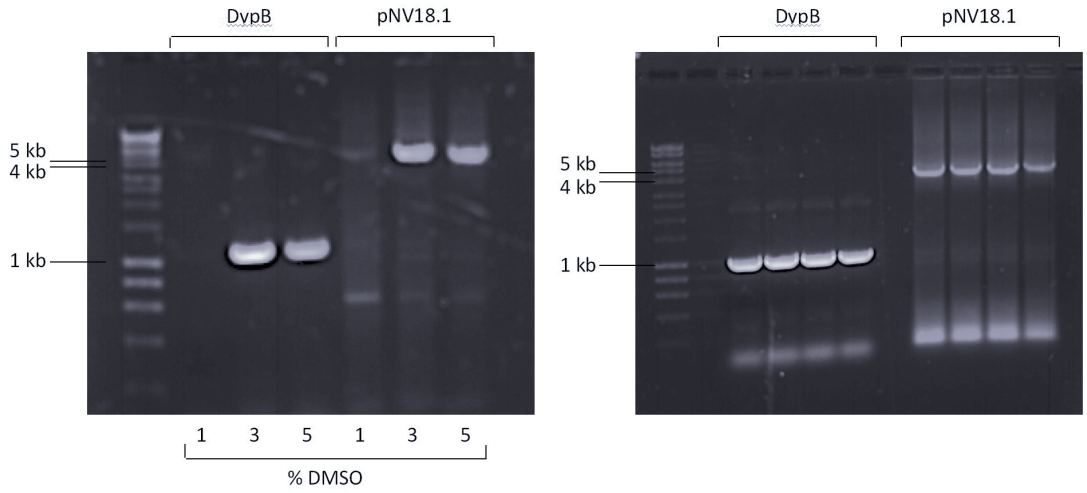


Figure 5.3: Agarose gels of PCR products. Left - varying DMSO concentration. Right - scaled up reactions with 3% DMSO for gel extraction, purification and Gibson assembly.

The purified fragments were then used for Gibson assembly as described in chapter 3, section 3.6.2. The resulting plasmid was transformed into *E. coli*, then the plasmid DNA isolated for sequencing to confirm the insertion was successful, as shown in figure 5.4.



Figure 5.4: Sequencing results. Alignment of the expected pNV18.1-DypB sequence (top line) and the actual sequencing results (bottom line). Highlighted green area shows *DypB* has been inserted into the pNV18.1 plasmid.

5.2.2.2 Addition of tac promoter

An upstream promoter sequence is required to drive transcription of DNA to mRNA once the plasmid has been transformed into a chassis organism. A ribosome binding site is also necessary for the ribosome to recruit tRNA for translation of mRNA to protein. The tac promoter (ptac) is a hybrid of the *E. coli* trp and lac promoters which can be induced using isopropyl β-D-1-thiogalactopyranoside (IPTG) for high levels of protein expression (de Boer, Comstock and Vasser, 1983). It is the promoter used by Xiong *et al*. for engineering xylose metabolism in PD630 using the same plasmid (Xiong, Wang and Chen, 2012).

In the initial attempt, ptac and a ribosome binding site were synthesised as a linear, single stranded DNA fragment (119 bp), flanked by overhangs for Gibson assembly into the backbone plasmid. The reverse complementary sequence was also synthesised, and the strands were annealed as described in chapter 3, section 3.6.3. Primers 9 and 10 were used to amplify pNV18.1-DypB and add appropriate overhangs, and Gibson assembly was carried out. After transformation into *E. coli,* the DNA was

isolated and sequenced, unfortunately not returning the expected sequence, despite agarose gels of the PCR products showing bands of the expected size.

The promoter and ribosome binding site sequences were then synthesised as a 199 bp gBlock (a linear, double stranded DNA) with complementary overlapping sequences for Gibson assembly with the backbone plasmid. pNV18.1-DypB was linearised by digestion with fast digest XbaI and the two fragments mixed for the Gibson reaction. Transformation, plasmid isolation and sequencing showed the insertion had been successful.

The resulting plasmid map (only showing the features of interest) is shown in figure 5.5.

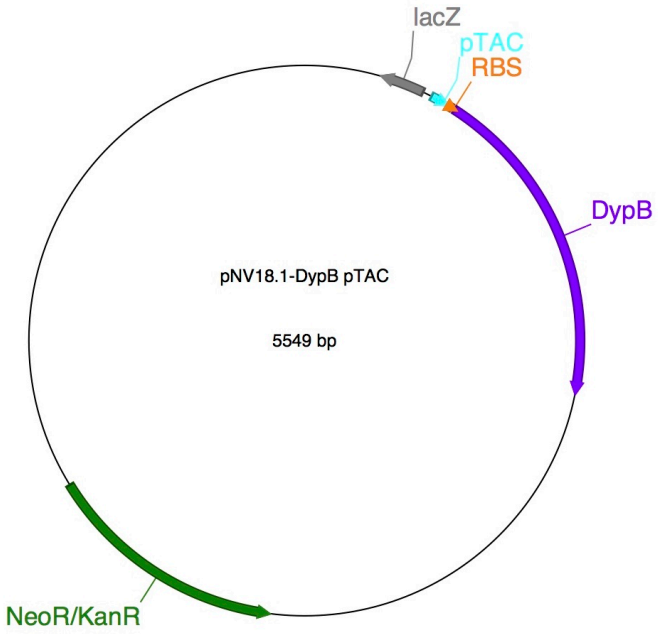


Figure 5.5: Plasmid map of pNV18.1-ptac-DypB. The *DypB* gene is under the control of the IPTG-inducible tac promoter. The plasmid also contains the aph gene conferring resistant to kanamycin (*E. coli*) and neomycin (PD630), and the lacZ gene for blue-white selection (not used in these experiments).

5.2.3 Protein expression

Once the plasmid had been constructed and transformed into TOP10 *E. coli*, expression of the DypB protein was attempted. The lignin degrading activity of RHA1 was observed extracellularly, therefore both the culture supernatant (secreted protein) and cell lysate (intracellular soluble protein) were analysed. The molecular weight of DypB is expected to be approximately 37 kDa (Ahmad *et al*., 2011).

Recombinant TOP10 cultures grown overnight at 37 °C were induced with IPTG and incubated for a further 4 hours. The culture media supernatant and lysed cell content were prepared for SDS polyacrylamide gel electrophoresis as described in chapter 3, section 3.7, and the gel is shown in figure

5.6. Lanes marked with a star contain IPTG induced cultures, while those without contain uninduced controls. Lanes 1, 2, 5 and 6 contain wildtype TOP10 (lacking the pNV18.1-DypB-ptac plasmid).

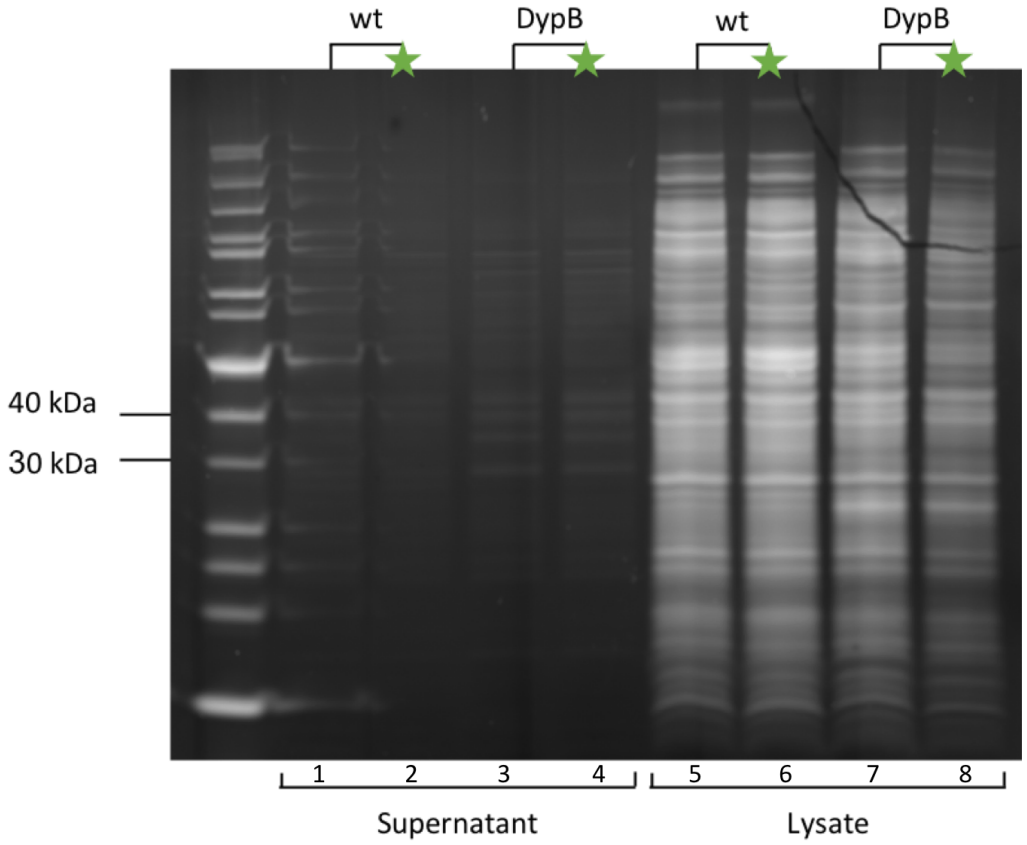


Figure 5.6: SDS-PAGE comparing wildtype (wt) and recombinant (DypB) TOP10 *E. coli*. Lanes 1-4 contain culture supernatant (secreted protein), while lanes 5-8 contain cell lysate (soluble protein). Lanes marked with a star indicate cells were induced with IPTG and incubated for a further 4 hours, while unmarked lanes contain uninduced control cultures.

No clear protein bands are seen at the expected 37 kDa in either the culture supernatant or cell lysate, and there is no obvious difference between uninduced/induced or wildtype/recombinant. The supernatant proteins are also very faint, so the experiment was repeated with an extended induction time of 6 hours, and the supernatant was concentrated before gel electrophoresis, as shown in figure 5.7.

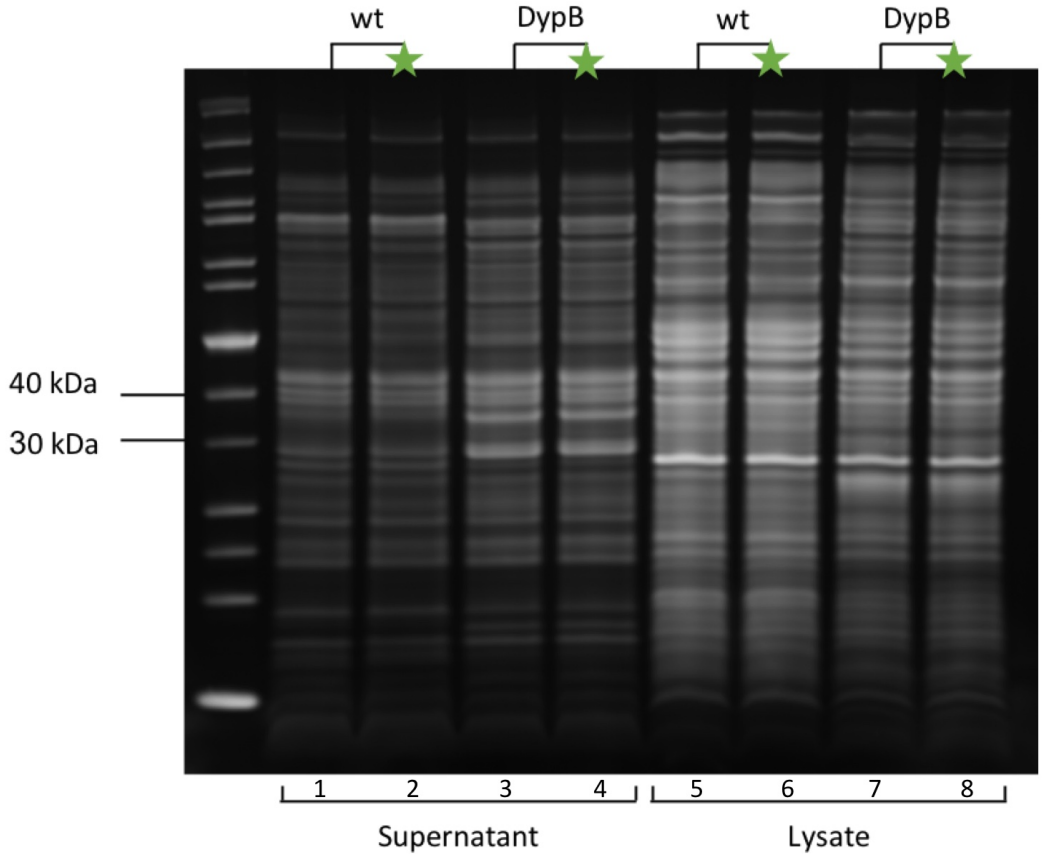


Figure 5.7: SDS-PAGE comparing wildtype (wt) and recombinant (DypB) TOP10 *E. coli* with longer induction time. Lanes 1-4 contain concentrated culture supernatant (secreted protein), while lanes 5-8 contain cell lysate (soluble protein). Lanes marked with a star indicate cells were induced with IPTG and incubated for a further 6 hours, while unmarked lanes contain uninduced control cultures.

This time there appear to be additional bands in the recombinant strain supernatant samples (lanes 3 and 4 compared with lanes 1 and 2), at approximately 35 kDa and just below 30 kDa. However, there is no clear difference between the uninduced and induced culture (comparing lanes 3 and 4) and so unless there is some leaky expression (for which there is little evidence in the literature) this is not due to the presence of the plasmid. The bands are also not as strong as would be expected from a recombinantly expressed protein.

This experiment was repeated using a specific expression strain of *E. coli*, BL21, to see if any stronger bands were present. Recombinant proteins prone to aggregation often show improved expression at lower temperatures for a longer period of time (Vasina and Baneyx, 1997), so the cells were incubated at 30 °C after induction for 22 hours. This is shown in figure 5.8.

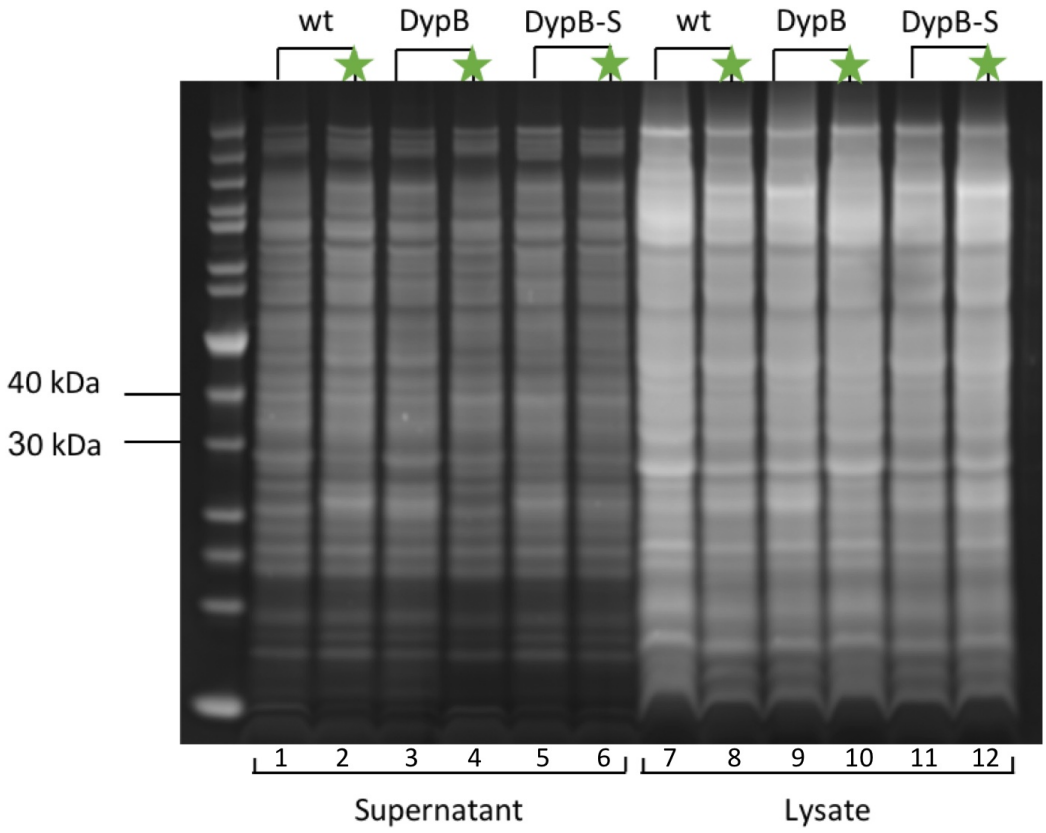


Figure 5.8: SDS-PAGE comparing wildtype (wt) and recombinant (DypB) BL21 *E. coli*. Lanes 1-6 contain concentrated culture supernatant (secreted protein), while lanes 7-12 contain cell lysate (intracellular soluble protein). Lanes marked with a star indicate cells were induced with IPTG and incubated further, while unmarked lanes contain uninduced control cultures. Lanes 5, 6, 11 and 12 (DypB-S) contain samples that were incubated at 30 °C instead of 37 °C for 22 hours instead of 6.

As with TOP10, the proteins of recombinant BL21 cultures appear no different to the wildtype strain at 37 kDa, and induced cultures seem the same as uninduced. Slow induction at 30 °C for 22 hours also appears to have no impact on protein expression.

It is possible that recombinant DypB could be contained in inclusion bodies with insoluble protein, so this experiment was repeated once again, this time also analysing the cell debris pellet following cell lysis. The induction was carried out at 37 °C for 6 hours. The gel is shown in figure 5.9.

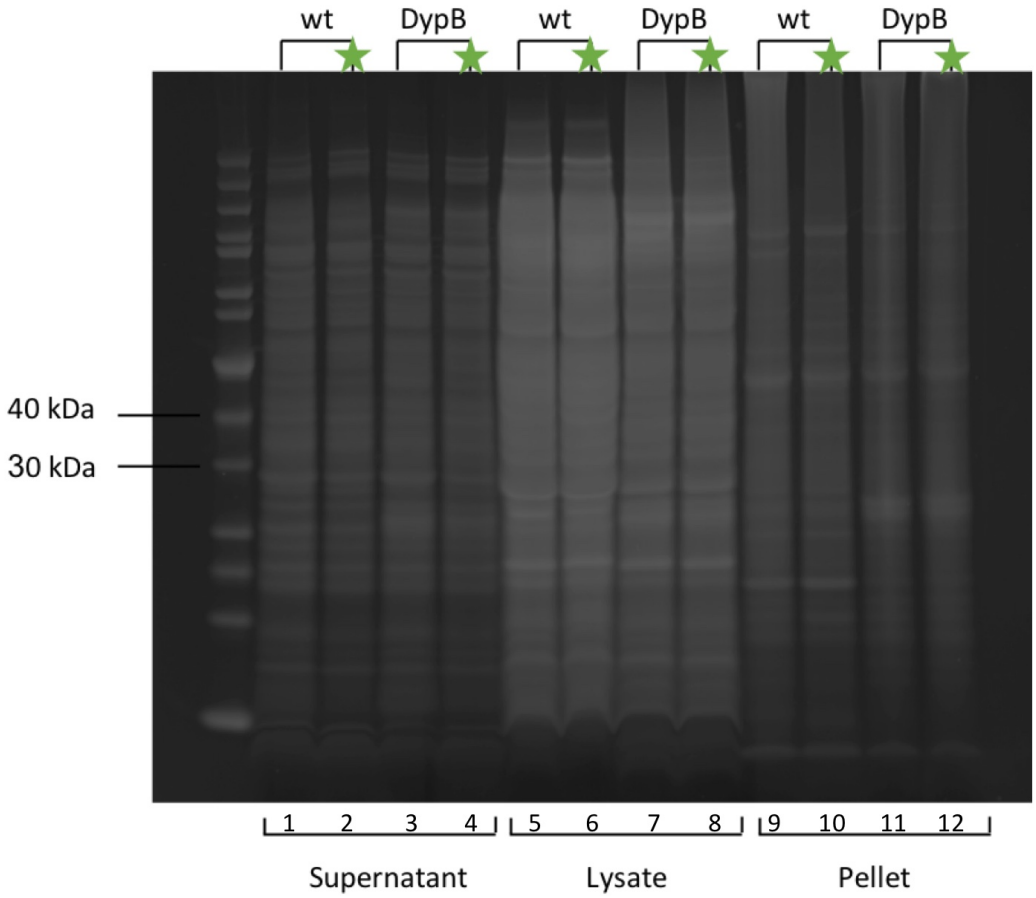


Figure 5.9: SDS-PAGE comparing wildtype (wt) and recombinant (DypB) BL21 *E. coli*. Lanes 1-4 contain concentrated culture supernatant (secreted protein), lanes 5-8 contain cell lysate (intracellular soluble protein) and lanes 9-12 contain inclusion bodies (insoluble protein). Lanes marked with a star indicate cells were induced with IPTG and incubated for a further 6 hours, while unmarked lanes contain uninduced control cultures.

Unfortunately, the insoluble fraction also did not show any protein at 37 kDa (lanes 9-12), indicating expression of DypB had been unsuccessful. The problem should not be caused by species differences between *E. coli* and PD630 as a shuttle vector was used, and DypB has previously been heterologously expressed in *E. coli* (Ahmad *et al*., 2011). To confirm this, the plasmid was transformed into PD630 and the above experiment repeated, but with the same result shown in figure 5.10.

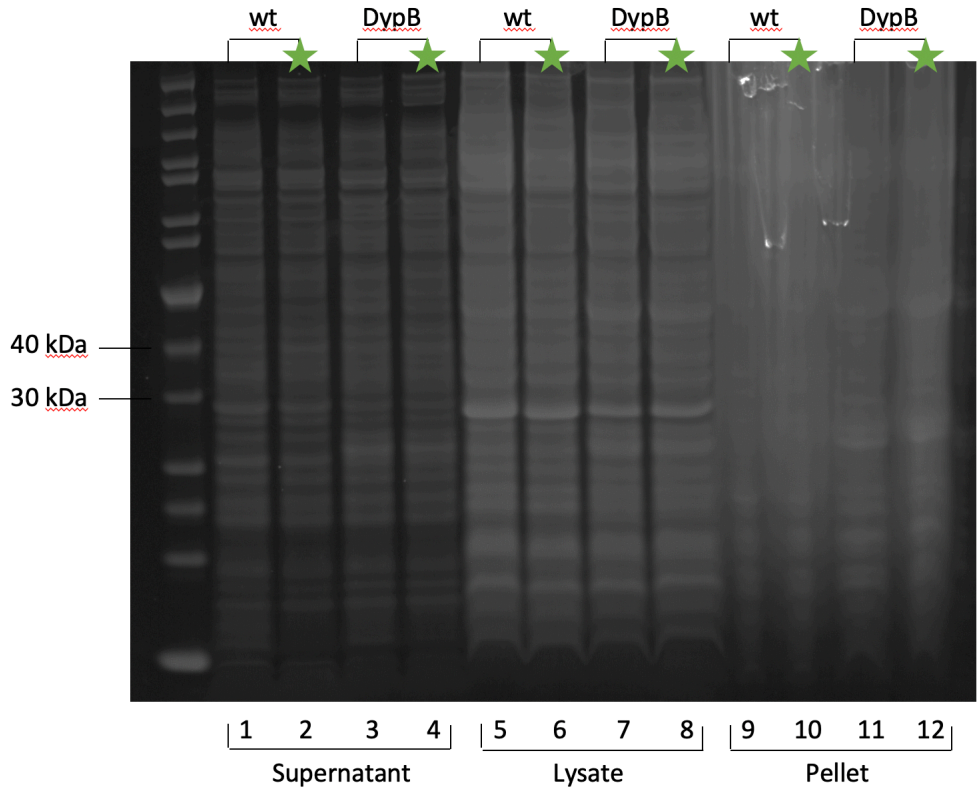


Figure 5.10: SDS-PAGE comparing wildtype (wt) and recombinant (DypB) PD630. Lanes 1-4 contain concentrated culture supernatant (secreted protein), lanes 5-8 contain cell lysate (intracellular soluble protein) and lanes 9-12 contain inclusion bodies (insoluble protein). Lanes marked with a star indicate cells were induced with IPTG and incubated for a further 6 hours, while unmarked lanes contain uninduced control cultures.

5.2.4 Plasmid alteration: site directed mutagenesis

After adding the gBlock to the plasmid, there were 12 base pairs separating the ribosome binding site and start codon of *DypB* due to the location of the XbaI restriction site. The optimal spacing for the ribosome to bind and initiate protein expression is 6-7, so site directed mutagenesis was performed to remove 6 of them. Figure 5.11 shows the strategy used.



Figure 5.11: DNA sequence of region targeted for site directed mutagenesis to remove 6 base pairs between the ribosome binding site and the DypB start codon. The blue residues are the end of the tac promoter, green is the ribosome binding site and red is the start of the DypB gene. Primers 14 and 15 were used for the first attempt, primers 16 and 17 for the second. Sequences are given in chapter 3, table 3.1.

Inverse PCR was carried out using 5' phosphorylated primers that flank and amplify away from the desired deletion site. In the first attempt, this was the last 6 base pairs of the spacer sequence using primers 14 and 15 (chapter 3, table 3.1). The reaction conditions are detailed in chapter 3, section 3.6.5. DpnI digestion removed template DNA and gel electrophoresis, band excision and gel purification removed non-specific bands and other reaction components. The linear PCR product was circularised by ligation, with the use of 5' phosphorylated primers avoiding the need for a phosphorylation step. As a size difference of only 6 base pairs is impossible to distinguish on a gel, the plasmid was transformed into *E. coli* and the DNA isolated from three separate transformants and sent for sequencing.

The results showed either the deletion had not occurred and the 12 base pair spacing was still present, or the sequence was disordered and alignment with the original sequence was difficult in this region (figure 5.12). This could perhaps be a sequencing artefact, or that some secondary structure in the plasmid DNA caused the reactions to not proceed as expected. A second attempt was made to remove the first 6 base pairs of the spacer using new primers (16 and 17), but the sequencing results returned a similar outcome.

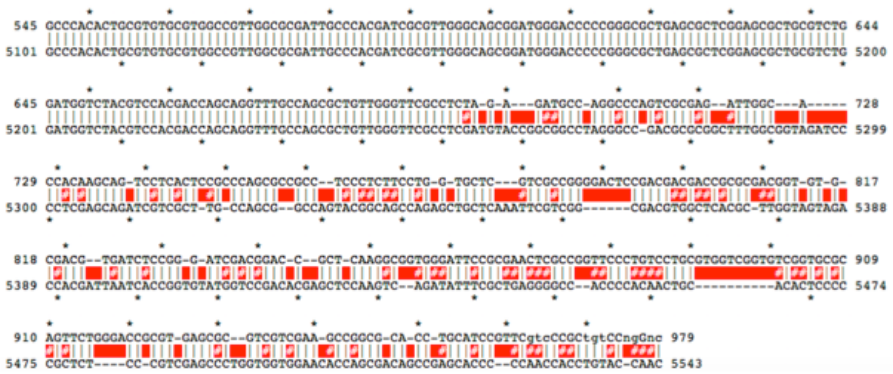


Figure 5.12: SDM sequencing results. Poor alignment of the expected pNV18.1-ptac-DypB sequence after SDM and actual sequencing results, suggesting the sequencing reaction did not work as expected.

5.3 Conclusions

In this chapter we set out to engineer lignin degrading activity into *R. opacus* PD630 by expressing the DypB lignin peroxidase gene from *R. jostii* RHA1. A plasmid was selected that had previously been used for heterologous gene expression in PD630 and the Gibson assembly method was used to insert the *DypB* gene at the multiple cloning site. The tac promoter and a ribosome binding site were then added by synthesising a gBlock DNA fragment and using Gibson assembly upstream of the *DypB* gene.

Subsequent efforts to express the protein in *E. coli* and PD630 were unsuccessful, and the protein could not be located in the culture supernatant (secreted protein), the cell lysate (soluble protein) or the remaining cell debris (insoluble protein in inclusion bodies).

Therefore, we attempted to optimise the spacing between the ribosome binding site and *DypB* start codon for expression in *E. coli*. Site directed mutagenesis was performed to try to remove 6 base pairs, but this proved difficult and many attempts returned sequencing results without the desired genetic change.

The recent publication of the aforementioned molecular toolkit for gene expression in PD630 (DeLorenzo *et al*., 2018) makes revisiting this work in the future an interesting prospect. However, rather than pursue and troubleshoot further, we decided to look into different options for enhancing PD630's lignin degradation. As well as peroxidases, laccases also catalyse the depolymerisation of lignin under certain conditions, and so we explored this further in chapter 6.

Chapter 6

Degradation of Kraft lignin using laccase and *R. opacus* PD630

6 Degradation of Kraft lignin using laccase and PD630

6.1 Introduction

Engineering DypB into *R. opacus* PD630 proved difficult and we were unable to express the enzyme in *E. coli* or PD630. Rather than pursue and troubleshoot further, we decided to look at an alternative enzymatic lignin degradation system using a laccase rather than a peroxidase. Instead of a single microorganism able to perform the whole bioconversion of lignin to lipids, we explore the possibility of a mixed system where polymeric lignin is treated with laccase to release monolignols, which are then accessible to PD630 for growth and lipid synthesis.

Earlier this year, Liu *et al*. investigated a combination of pre-treatments to significantly increase lipid yield in *R. opacus* PD630 grown on corn stover biomass (Liu *et al*., 2018). These involved heating with dilute sulphuric acid and sodium hydroxide, laccase enzyme treatment, detoxification processes to remove inhibitory compounds (heating, activated carbon or gas stripping), and optimisation of fermentation conditions (inoculum density, adding more carbon source by refreshing media periodically, oxygen content control in a fermenter). Xie *et al*. have also used laccase treatment to increase the solubility of lignin, improving its fermentation potential by PD630 (Xie *et al*., 2017). Here, we use the potential waste product Kraft lignin and assess the effect of laccase treatment on its degradation and bioconversion to lipids by PD630.

Laccases are multicopper oxidase enzymes found in plants, fungi and, more recently discovered, bacteria. They are typically secreted and extracellularly catalyse the oxidation of phenolic compounds, including lignin. Laccases use molecular oxygen as the electron acceptor, producing water as the by-product. This is in contrast to peroxidases that require the industrially unattractive hydrogen peroxide (Mate and Alcalde, 2016).

As discussed in chapter 1, laccase-catalysed reactions are complex and can result in both polymerisation and depolymerisation of lignin. The addition of a mediator compound generally encourages depolymerisation, and increases the redox potential by shuttling between the laccase and large lignin polymer, continuously undergoing oxidation and reduction (Christopher, Yao and Ji, 2014; Munk *et al*., 2015). Synthetic mediators, such as 2,2′-azinobis(3-ethylbenzothiazoline-6-sulfonic acid) (ABTS), are effective but can be costly and toxic. Natural mediators include small aromatic compounds such as the breakdown products of lignin itself, and would therefore be of interest in a degradation system such as this. Syringaldehyde (figure 6.1) has been shown to enhance the activity of *P. cinnabarinus* laccase on Kraft paper pulp (Camarero *et al*., 2005, 2007; Gutiérrez *et al*., 2007).

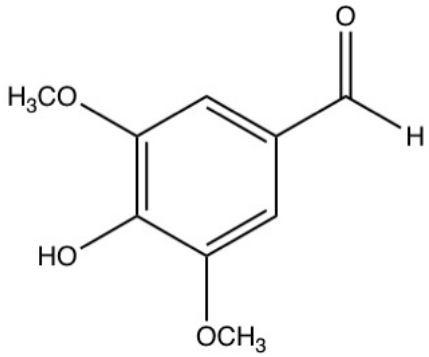


Figure 6.1: Structure of syringaldehyde, the laccase mediator used for these experiments.

Bacterial laccases are generally more thermostable and operate at less acidic pH than fungal laccases, but tend to have lower redox potential (Margot *et al*., 2013). Additionally, fungal laccases have been better characterised and some are available commercially. One such enzyme is that of *Trametes versicolor*, which was selected for these experiments (structure shown and more detail described in chapter 1, figures 1.6 and 1.7). It has been shown to catalyse lignin polymerisation when acting alone, but depolymerisation in the presence of the mediator ABTS (Bourbonnais *et al*., 1995).

We first assessed laccase oxidation of ABTS and syringaldehyde to select the mediator for subsequent experiments, then investigated growth of PD630 on Kraft lignin that has been treated with laccase. The optimal conditions for *T. versicolor* laccase activity are not conducive to PD630 growth, therefore we performed the experiment in two stages: first treat Kraft lignin with laccase to cause depolymerisation, then use this as a feedstock for PD630 and assess its growth and lipid synthesis.

Finally, we explored the potential for a "one pot" process of simultaneous lignin depolymerisation by laccase and metabolism of the degradation products by PD630.

6.2 Results and discussion

6.2.1 Laccase activity

The activity of *T. versicolor* laccase was tested by its ability to oxidise the mediator compounds ABTS (synthetic) or syringaldehyde (natural). A mediator concentration of 1 mM was used (Bourbonnais *et al*., 1995). Reduced ABTS and syringaldehyde are colourless, while the oxidised forms are dark green and yellow respectively. Absorption was measured at 420 nm or 370 nm, as the wavelengths at which there is greatest difference between the reduced and oxidised forms (Childs and Bardsley, 1975; Bourbonnais *et al*., 1995; Pardo *et al*., 2013).

Enzyme activity increased in the presence of both ABTS and syringaldehyde, as shown in figure 6.2. A higher mean change in absorbance for ABTS (1.40) versus syringaldehyde (1.33) was not significantly different according to t test analysis. The natural mediator, syringaldehyde, was therefore selected for subsequent experiments.

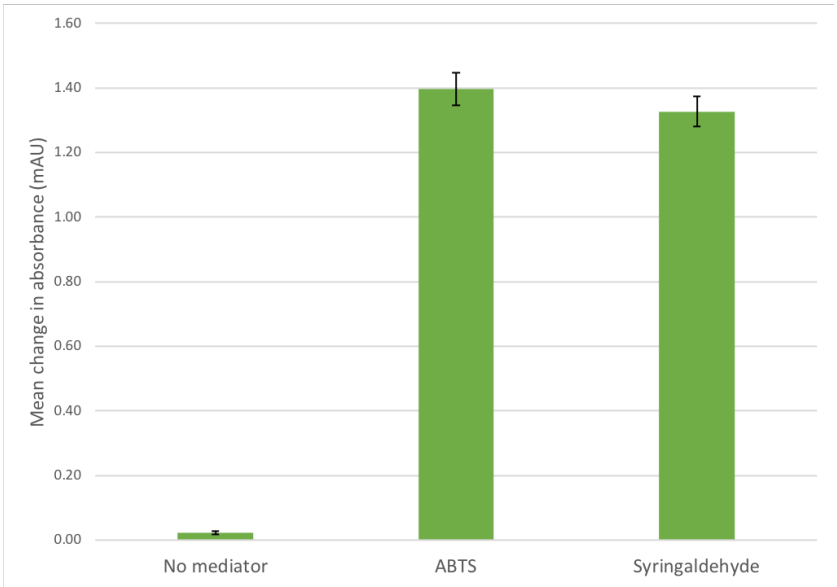


Figure 6.2: *T. versicolor* laccase enzyme activity. Change in absorbance was measured after incubation with mediator/substrate for 1 minute. Absorbance measurements were made at 420 nm for ABTS and 370 nm for syringaldehyde. Error bars represent standard deviation (n=3).

6.2.2 Laccase oxidation of Kraft lignin

Kraft lignin was treated with laccase, mediated by syringaldehyde, as described in chapter 3, section 3.8.2. The enzymes were heat inactivated after various time periods (12-120 hours) to assess the effect of laccase treatment time on the ability of PD630 cultures to metabolise Kraft lignin.

6.2.3 PD630 growth on laccase-treated Kraft lignin

After heat inactivation, 1 ml laccase reaction mix was used to supplement 9 ml minimal growth media and inoculated with PD630. This corresponds to a carbon content of 0.5% (as for experiments in chapter 4), and nitrogen was non-limiting at 0.1%. Cell growth was monitored over the following 48 hours, shown in figure 6.3. The growth curves indicate that PD630 can grow on Kraft lignin pre-treated with laccase as its sole carbon source.

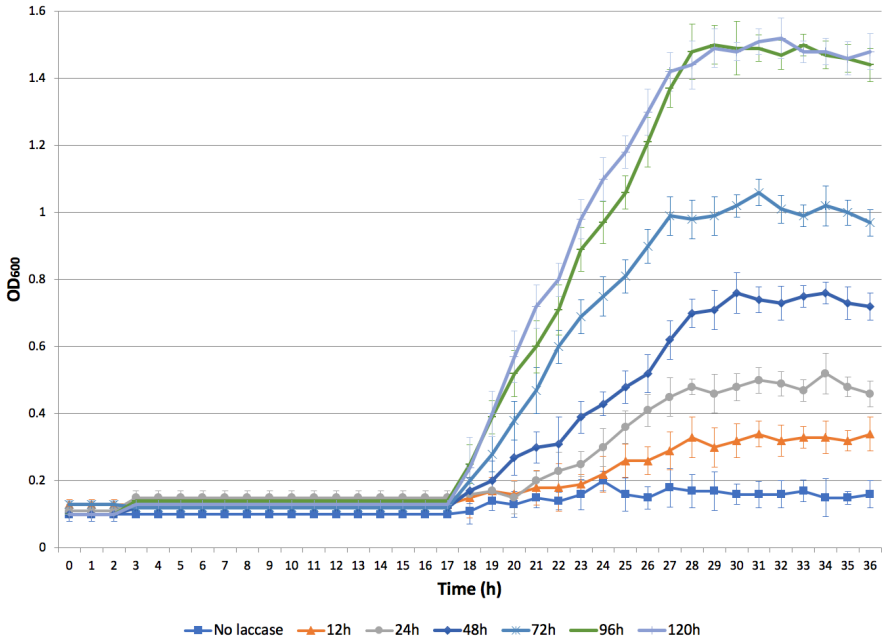


Figure 6.3: Growth of *R. opacus* PD630 on Kraft lignin treated with *T. versicolor* laccase mediated with syringaldehyde for various time periods. Higher maximum OD at longer treatment times indicates more carbon has been made accessible for growth. Error bars represent standard deviation (n=3).

Increased incubation time of Kraft lignin and laccase increased the growth rate and maximum OD of PD630. The results in chapter 4 showed growth on untreated Kraft lignin was very poor, therefore this suggests the laccase treatment has caused lignin depolymerisation, releasing lower molecular weight lignin fragments and/or monolignols that the PD630 cells are able to metabolise and use for growth. Little difference in growth is apparent between treatment for 96 and 120 hours (both reach a maximum OD or 1.5 after 28 hours) indicating lignin degradation by the laccase has reached its maximum level. This may be that the polymer is fully degraded, or that a steady state between depolymerisation and repolymerisation has been reached. 96-hour treatment was used for subsequent experiments. PD630 may also be able to grow on the mediator, syringaldehyde, and the laccase protein itself. However, these are constant between the various reaction times and growth experiments, therefore differences in growth must be due to the breakdown of lignin and not growth on syringaldehyde.

All cultures showed a long lag phase of 17 hours, indicating the cells need to adapt to growth on this new substrate as the sole carbon source. This is consistent with results in chapter 4, where the same lag was seen when cultures were provided with the lignin breakdown model compounds 4-HBA, vanillic acid and vanillin. This was confirmed by taking a 100 µl sample of cells grown on 96-hour treated lignin after 24 hours and inoculating fresh media, also containing 96-hour treated lignin. The cultures began to grow with no lag time (figure 6.4).

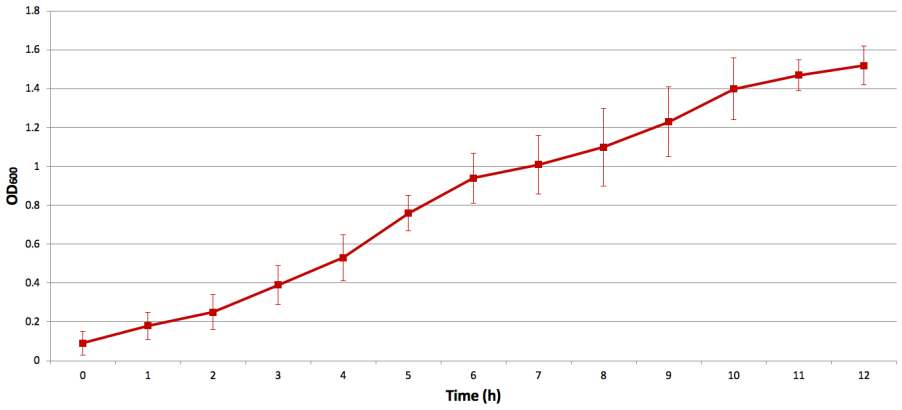


Figure 6.4: Growth of PD630 cultures already adapted to growth on Kraft lignin that has been treated with *T. versicolor* laccase for 96 hours. This minimal media also contained 96-hour treated Kraft lignin and 0.1% nitrogen source. Error bars represent standard deviation (n=3).

6.2.4 PD630 lipid accumulation on laccase-treated Kraft lignin

Having established that pre-treatment of Kraft lignin with laccase and syringaldehyde enables PD630 to metabolise it, we next looked at whether it could use it to accumulate lipids. Cells grown for 24 hours on 96-hour treated lignin, and therefore already adapted, were used to inoculate fresh media containing the same treated lignin but only 0.05% nitrogen. Samples were taken every 12 hours and the cell dry weight (growth) and lipid content were analysed, as described in chapter 3, sections 3.4 and 3.4.1, and shown in figure 6.5. Lipid content is expressed as a percentage of the cell dry weight (lipid mass divided by total lyophilised cell mass) and is plotted on the secondary y-axis.

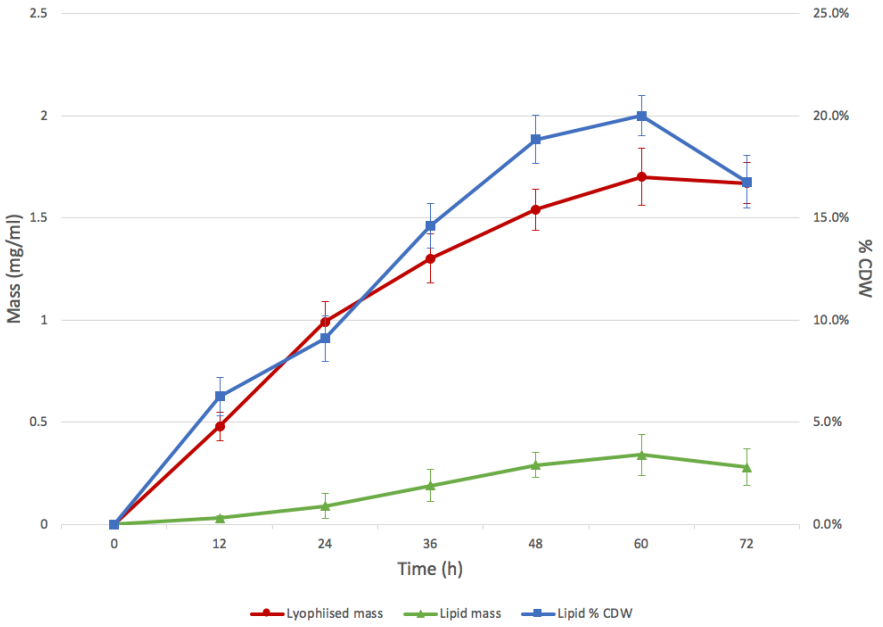


Figure 6.5: *R. opacus* PD630 growth and lipid accumulation in minimal media supplemented with 0.5% Kraft lignin that had been treated with *T. versicolor* laccase for 96 hours, and 0.05% nitrogen. Lyophilised cell mass (cell dry weight) and lipid mass are given in mg/ml (primary y-axis), while lipid content is given as % of the cell dry weight (secondary y-axis). Error bars represent standard deviation (n=3).

These results show that PD630 can indeed use laccase-treated Kraft lignin to accumulate lipids. A maximum lipid content of 20% is reached after 60 hours, also coinciding with the maximum CDW of 1.7 mg/ml. After this point the accessible carbon in the media may be depleted and the cells may be mobilising stored lipids, therefore decreasing lipid content.

When compared with the results in chapter 4, maximum CDW is slightly lower than cells grown on 4-HBA or VanA (1.8 mg/ml), and lipid content is lower than 4-HBA (22%) but greater than VanA (14%) (chapter 4, section 4.2.2.2, figure 4.5). Growth was slower and lipid accumulation also took longer (lipid content peaked after 36 and 48 hours for 4-HBA and VanA respectively).

It is probable that laccase treatment does not depolymerise lignin entirely to monolignols, with a steady state reached between depolymerisation and repolymerisation and a mixture of monomers and oligomers remaining (Shleev *et al*., 2006). This would cause some of the carbon to be less accessible to PD630, possibly explaining these observations.

6.2.5 Simultaneous depolymerisation and metabolism

Rather than a two-step method of (1) lignin depolymerisation by treatment with laccase, followed by (2) growth and lipid production by PD630, we investigated the potential for a single process where these stages occur simultaneously. This would also test a hypothesis that removal of lignin degradation products (by way of metabolism by PD630) may push the reaction towards depolymerisation by the laccase (Munk *et al*., 2015), increasing availability to the cells and enhancing growth and lipid synthesis.

6.2.5.1 PD630 growth

The two processes were previously carried out under different conditions: 50 °C and pH 5.0 for the laccase reaction and 30 °C and pH 7.0 for PD630 fermentation. However, laccase should show some activity at suboptimal temperature and pH, and so it was added to minimal growth media along with syringaldehyde at the time of PD630 inoculation. Concentrations were the same as those used for the two-step experiments (1 U/ml laccase, 1 mM syringaldehyde, 0.5% Kraft lignin, 0.1% nitrogen), and the cells used for inoculation were already adapted to growth on laccase-treated lignin. Cells were harvested and washed in minimal media to ensure all traces of treated lignin were removed. Growth was monitored over the following 48 hours.

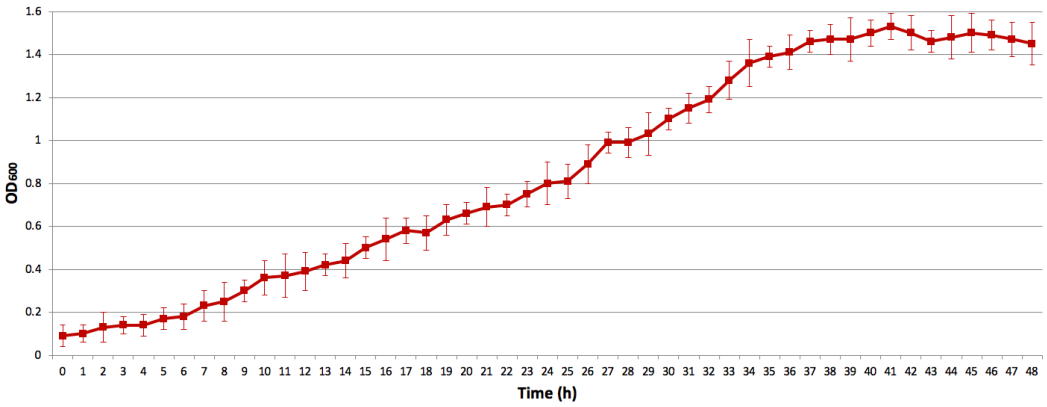


Figure 6.6: Growth of *R. opacus* PD630 in minimal growth media supplemented with 0.5% Kraft lignin, 0.1% nitrogen, 1 U/ml *T. versicolor* laccase and 1 mM syringaldehyde. Error bars represent standard deviation (n=3).

Figure 6.6 shows PD630 cultures have grown on this substrate, indicating that depolymerisation of lignin has occurred through treatment with laccase and the cells are then able to metabolise the degradation products. A maximum OD of 1.5 is reached after 41 hours, which is comparable to that of cultures grown on 96- or 120-hour treated lignin in the two-step process, though there is no significant lag time as the cells are already adapted. The cultures took 41 hours of exponential growth to reach the maximum OD compared with only 10 hours in the two-step process. However, the laccase treatment in that case was carried out for 96 hours, and so substrate availability may be limiting the growth rate in this present experiment. The fact that a similar OD is achieved after 41 hours rather than 96 may suggest that removal of the degradation products by PD630 uptake favours depolymerisation by the laccase. Additionally, the laccase is operating at suboptimal conditions and so its activity may be even slower.

6.2.5.2 PD630 lipid accumulation

The above was repeated under nitrogen-limiting conditions to see if lipids could be synthesised as part of the simultaneous degradation and metabolism process. Figure 6.7 shows that lipids are indeed accumulated by PD630, indicating that lignin depolymerisation by laccase and metabolism and lipid synthesis by PD630 have occurred simultaneously in this one step processes.

The growth and lipid content profiles are similar to those seen in the two-step method. CDW reached a comparable level of 1.7 mg/ml, though this took 96 hours rather than 60. Lipid content actually peaked higher than the two-step process at 23% compared with 20%, though this also took a longer time period (72 hours rather than 60).

The similar maximum CDW may indicate that no additional carbon was made available to PD630 in this one-step process, and the laccase reaction was not driven towards depolymerisation by removal of the breakdown products. However, it would be interesting to see if this holds true at higher lignin concentrations.

On the other hand, lipid content was higher and well over the oleaginous threshold, at 23%, indicating simultaneous depolymerisation and metabolism somehow encouraged carbon storage in the form of TAGs. If carbon is made accessible more slowly in this method, this seems counter intuitive, given that a high carbon to nitrogen ratio should enhance lipid synthesis rather than the other way around.

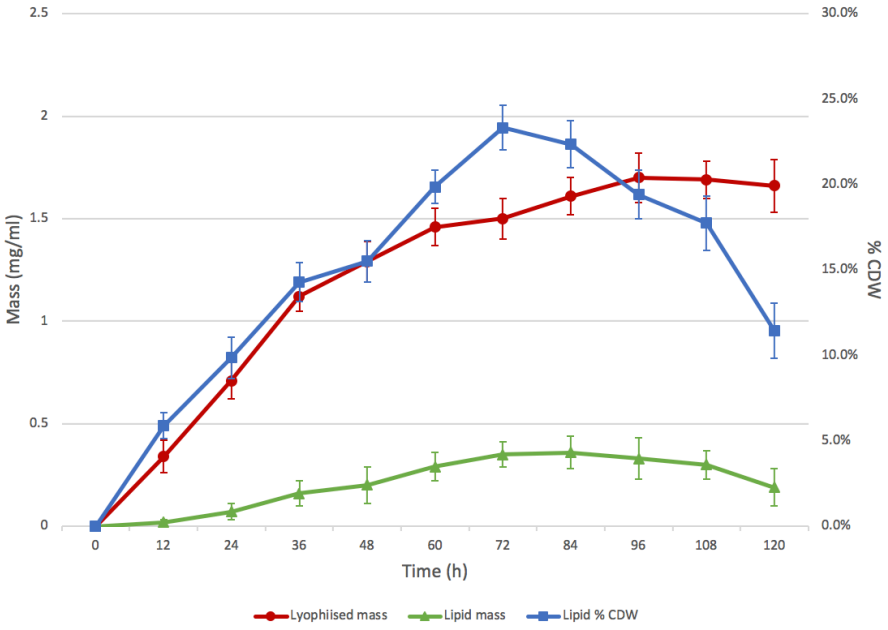


Figure 6.7: *R. opacus* PD630 growth and lipid accumulation in minimal media supplemented with 0.5% Kraft lignin, 0.05% nitrogen, 1 U/ml *T. versicolor* laccase and 1 mM syringaldehyde. Lyophilised cell mass (cell dry weight) and lipid mass are given in mg/ml (primary y-axis), while lipid content is given as % of the cell dry weight (secondary y-axis). Error bars represent standard deviation (n=3).

6.3 Conclusions

In this chapter we have demonstrated that a mixed enzymatic and microbial system is possible for the bioconversion of lignin to lipid. Treatment of Kraft lignin with *T. versicolor* laccase in the presence of syringaldehyde allowed *R. opacus* PD630 to use it as the sole carbon source for growth and lipid accumulation to oleaginous levels.

In the two-step process, lipid content reached 20% after 60 hours. The single-step process showed slower growth and lipid accumulation rates, but seemed to enhance lipid storage, with 23% lipid content achieved after 72 hours.

The use of a natural mediator, syringaldehyde, has environmental and economic advantages over the synthetic mediator, ABTS. It may also be that after depolymerisation is initiated, the released monolignols themselves act as mediators, so creating an autocatalytic system. This raises the question of whether a mediator is even necessary in the single-step process. This, and a comparison of other mediators, would be interesting follow up experiments.

Monitoring the lignin depolymerisation process would also be of interest, perhaps by assessing the average molecular weight of lignin at different time points during the reaction using gel permeation chromatography, or by performing NMR spectroscopy to identify the breakdown products.

As mentioned, Liu *et al*. recently screened a variety of biomass pre-treatment strategies to enhance lipid production by *R. opacus* PD630 (Liu *et al*., 2018), including chemical and thermal methods, detoxification processes, laccase treatment and optimised fermentation strategies. It is likely that adding some of these other approaches to our system would enhance lipid yield further.

Overall, the conversion of lignin to lipid using *T. versicolor* laccase and *R. opacus* PD630 by simultaneous depolymerisation, fermentation and lipid synthesis is a potential method for the bioconversion of lignin to lipids. This assay, monitoring PD630 growth, could be useful for screening the activity of engineered enzymes or different mediator compounds.

Chapter 7

Conclusions and future work

7 Conclusions and future work

7.1 Summary

There is a pressing need for sustainable liquid transportation fuels to address climate change concerns and meet increasing global energy demand. Biofuels offer a low carbon alternative to fossil fuels, and microbial biodiesel has the potential to play a key role in their future. The work presented in this thesis demonstrates the possibility of producing biodiesel from lignin using *Rhodococcus* bacteria.

The recalcitrant, heterogenous lignin polymer is a component of lignocellulosic biomass and is abundant, renewable and often wasted, therefore providing an underutilised feedstock for conversion by ligninolytic bacteria that have evolved to depolymerise and metabolise it. Other microorganisms can accumulate high levels of intracellular lipids in the form of triacylglycerols, which are readily processed to biodiesel by transesterification to fatty acid alkyl esters. Making use of both these capabilities, by employing microorganisms to convert lignin into value-added products such as biodiesel, could help to challenge the industry saying: "you can make anything out of lignin, except money" (Graichen *et al*., 2017).

Chapter 2 considered the feasibility of producing biodiesel from lignin on a large scale by addressing both environmental and economic factors, concluding that it could be commercially viable under the right circumstances. Sourcing waste lignin as a feedstock and using the existing infrastructure of biorefineries or pulp mills brings costs in line with cellulosic bioethanol production, at around $140 per barrel of oil equivalent. While this is still costlier than petroleum-derived diesel, policy support and technology advances should reduce this in the coming years. Furthermore, there is a compelling argument for addressing carbon emissions and striving to meet the Paris 2015 Agreement's 2 °C target even at a higher monetary cost than current conventional fuels.

The approach followed here was to identify a bacterial strain able to synthesise and store high levels of intracellular lipids. The chosen strain, *Rhodococcus opacus* PD630, is highly oleaginous, especially under nitrogen limiting conditions (Alvarez *et al*., 1996) and has also demonstrated some lignin degrading capability (Kosa and Ragauskas, 2013), albeit to a lesser extent than related species such as *R. jostii* RHA1 (Ahmad *et al*., 2011).

We first cultured *R. opacus* PD630 with Kraft lignin, where it showed very slow growth with little improvement at higher lignin concentrations, demonstrating a limited ability for lignin degradation. Therefore we provided the strain with lignin breakdown model compounds to see whether it can metabolise pre-treated (depolymerised) lignin. The chosen compounds were 4-HBA, vanillic acid and vanillin, which the cultures were able to use as sole carbon source for growth and lipid accumulation. The highest levels were observed for 4-HBA, where cells reached 22% lipid content (percentage of the

dry cell weight) after 36 hours with limited nitrogen. VanA was also metabolised and used for lipid synthesis, reaching 14% after 48 hours. The strain performed less well on vanillin, with limited growth and no lipid detected. The presence of vanillin also hindered growth and lipid synthesis on both glucose and vanillic acid, indicating the likely effect was due to toxicity and/or inhibition of lipid biosynthesis rather than a simple inability to metabolise vanillin.

Based on these results, which demonstrated that PD630 can grow and produce lipids on monolignols but not Kraft lignin, we chose to enhance lignin depolymerisation by expressing the DypB enzyme, a lignin peroxidase from *R. jostii* RHA1.

A shuttle plasmid was selected in which to clone the *DypB* gene using the Gibson assembly method, along with a promoter and ribosome binding site. Protein expression experiments in both *E. coli* and PD630 were unsuccessful, as were subsequent efforts to alter the plasmid sequence by site directed mutagenesis to overcome the issues.

We therefore decided to investigate an alternative lignin depolymerising enzyme. *Trametes versicolor* laccase was used to pre-treat and depolymerise Kraft lignin in the presence of syringaldehyde, a redox mediator compound. The breakdown products after 96 hours of treatment were provided as a carbon source for PD630 cultures, which grew and reached 20% lipid content after 60 hours. Combining the depolymerisation and fermentation steps into a single process slowed but did not prevent growth, and even seemed to enhance lipid storage levels, with cells reaching a lipid content of 23% after 72 hours.

These results demonstrate the feasibility of a mixed enzymatic and microbial system for the bioconversion of lignin to lipid, with cells able to reach oleaginous lipid content using lignin as a sole carbon source. This work supports research into the production of biodiesel from microorganisms, and efforts to provide a sustainable alternative to fossil fuels.

7.2 Commercial potential

Pursuing a single step microbial conversion process may be the most desirable and cost-effective option in the long term. However, based on our results the mixed enzymatic and microbial approach offers a more immediate route to commercialisation.

Developing and optimising our research to a level attracting investment for large scale production would take many years. However, adding a waste lignin processing stream to an existing cellulose biorefinery would incur only the incremental cost of a parallel process with different specific technologies, sharing resources and reducing unit costs, as discussed in chapter 2. If such biorefineries are already successfully operating (at a scale of around 2000 barrels per day), it follows that an additional process could also operate to a similar extent, given the same cost and policy influences.

Some of the world's leading companies are choosing to collaborate in pursuit of mixed enzymatic and microbial conversion technology, as illustrated by the recent joint venture between ExxonMobil, Renewable Energy Group and Clariant. The combination of Clariant's biomass conversion technology (which uses proprietary enzymes to convert cellulose into sugars) and REG/ExxonMobil's fermentation and biodiesel production technologies is hoped to streamline the overall bioconversion process at commercial scale.

Using the system developed in this thesis in partnership with such industrial set ups could lead to commercialisation in a shorter time. Lignin waste product could be converted into biodiesel in a parallel enzymatic and microbial process, using enzymes and microbes that build on our research.

7.3 Future work

7.3.1 PD630 lignin depolymerisation

Engineering the lignin peroxidase, DypB, into *R. opacus* PD630 proved to be more difficult than anticipated. We were unable to express the enzyme, and subsequent plasmid modification attempts were unsuccessful. The lack of well-characterised, reliable genetic tools compared to other bacterial species made troubleshooting challenging. Earlier this year a molecular toolkit was published specifically for genetic manipulation in PD630 (DeLorenzo *et al*., 2018). This provides a library of constitutive and inducible promoters with a 45-fold span of expression levels, and available plasmids were characterised in detail. The combination facilitates more controlled, predictable expression of heterologous genes in PD630, and makes revisiting this work in the future an interesting prospect. The toolkit also introduces a new antibiotic resistance marker, a system for genome modification and tuneable gene repression, all of which greatly expand the potential of PD630 for genetic engineering and industrial applications.

7.3.2 Combined enzymatic and microbial approach

7.3.2.1 Mediator compounds and monitoring lignin breakdown

Mediator compounds increase the redox potential of laccase-catalysed depolymerisation by shuttling between the enzyme and bulky lignin polymer. We chose a natural mediator, syringaldehyde, having environmental and economic advantages over synthetic compounds and being a lignin breakdown product itself setting up the possibility of an autocatalytic reaction. However, we only compared its

effect on enzyme activity with one other compound, ATBS, so it may be worthwhile screening a wider variety of redox mediators at different concentrations.

Additionally, the single-step process where depolymerisation and fermentation occur simultaneously may not require a mediator at all. Once depolymerisation has been initiated, the liberated monolignols may act as redox mediators, so creating a self-fulfilling system. This could also potentially minimise the inhibitory effects of syringaldehyde or other compounds (discussed below).

It would be interesting to identify the products of lignin depolymerisation by laccase, to give a greater understanding of the compounds PD630 is able to use for growth and lipid accumulation. It may be that partial breakdown to oligomers is enough to allow metabolism. This could be broadly assessed by monitoring the average molecular weight of lignin over time using gel permeation chromatography (Gellerstedt, 1992; Lange, Rulli and Crestini, 2016), where a higher molecular weight would indicate that smaller lignin fragments are being taken up and metabolised. NMR spectroscopy would give a detailed structural picture of the products of lignin depolymerisation (Ralph and Landucci, 2010).

7.3.2.2 Inhibitory effect of lignin breakdown compounds

As discussed in chapter 4 and in many other studies, lignin breakdown products can be toxic to microorganisms and inhibit growth (Fitzgerald *et al*., 2004; Klinke, Thomsen and Ahring, 2004; Chen *et al*., 2012). Growth of PD630 on 4-HBA, VanA and vanillin all showed long lag times, though vanillin in particular was a poor substrate and inhibited lipid storage.

Growth rates and lipid levels could be enhanced if the strain were less susceptible to these compounds, which has already been demonstrated in similar situations. Yoneda *et al*. adaptively evolved PD630 to improve resistance to phenol, increasing its growth by 373% and lipid production 2-fold (Yoneda *et al*., 2016). Kurosawa *et al*. used a similar method to improve the tolerance of *R. opacus* MITXM-61 to lignin, 4-hydroxybenzaldehyde, and syringaldehyde (Kurosawa, Laser and Sinskey, 2015). The evolved strain showed a 2- to 3-fold increase in resistance, and shortened lag times when grown on hydrolysed lignocellulosic biomass containing these compounds. Henson *et al*. produced 35 adapted strains of PD630 able to grow on combinations of lignin model compounds, some of which showed 1900% improvement in OD after 43 hours and reached lipid content of 44%. These strains had mutations in both the chromosome and endogenous plasmids related to redox reactions, as well as upregulated pathways for by-product detoxification. They were used to elucidate parts of the β-ketoadipate pathway described in chapter 1, section 1.7.1 (Henson, Campbell, *et al*., 2018).

This is particularly relevant, as we used syringaldehyde as the redox mediator for laccase treatment of Kraft lignin. A study of PD630 growth on syringaldehyde, alone and in combination with lignin and other monolignols, followed by an adaptive evolution strategy could improve lipid yields.

7.3.2.3 Other lignin pre-treatments

Increased lipid yield in PD630 could be achieved by combining a number of lignin pre-treatments, including thermal and chemical processes, detoxification, laccase treatment and optimised fermentation methods. Liu *et al*. increased lipid content by up to 75% by heating corn stover biomass with dilute sulphuric acid and sodium hydroxide to fractionate the lignin, then treating with laccase enzyme and using a fed-batch fermentation strategy (Liu *et al*., 2018). It is likely that adding these or other pre-treatment methods would enhance lignin depolymerisation and therefore PD630 growth and lipid accumulation. However, there is a trade-off between the value of the additional lipid production and the additional materials required for these processes, especially at larger scale.

7.3.2.4 Fatty acid profile analysis

In these experiments we only measured total cell lipid content. It would be interesting to carry out a transesterification reaction on the isolated TAGs and assess the chain length, branching and degree of unsaturation of the resulting fatty acid alkyl esters. This could be done by gas chromatography (Kalscheuer, Stölting and Steinbüchel, 2006; Kurosawa *et al*., 2010; Kosa and Ragauskas, 2012) or possibly capillary electrophoresis (Vergara-Barberán *et al*., 2011; de Oliveira *et al*., 2014).

This would also provide a way to assess the effect of various growth substrates, lignin pre-treatment methods and fermentation strategies on the profile of fatty acids synthesised. In turn, it may then be possible to optimise these methods to enhance production of fatty acids that are most suited to use as biodiesel.

7.4 Concluding remarks

This work set out to investigate the conversion of lignin waste to biodiesel using oleaginous bacteria. While attempts to engineer a single organism to perform the entire pathway were challenging, a combined enzymatic and microbial approach achieved the overall concept and demonstrates the potential for producing biodiesel from renewable feedstocks. This approach could have potential for scale up and commercial application in the medium term, in combination with technologies focussed on producing biodiesel from the cellulose component of biomass, while utilising waste lignin and shared facilities. Recently published works highlight the interest in *R. opacus* PD630 as a tool for industrial applications and offer motivation for revisiting some of these experiments in the future.

8 References

ABB Communications (2011) *ABB helps pulp mill become fossil-free energy supplier*. Available at: http://www.abb.com/cawp/seitp202/bb675f2338f94e2ac1257933002f71ad.aspx (Accessed: 28 May 2018).

Ahmad, M. *et al*. (2010) 'Development of novel assays for lignin degradation: comparative analysis of bacterial and fungal lignin degraders.', *Molecular BioSystems*, 6(5), pp. 815–21. Available at: http://www.ncbi.nlm.nih.gov/pubmed/20567767 (Accessed: 11 July 2014).

Ahmad, M. *et al*. (2011) 'Identification of DypB from Rhodococcus jostii RHA1 as a lignin peroxidase.', *Biochemistry*, 50(23), pp. 5096–107.

Alcalde, M. (2007) 'Laccases: Biological Functions, Molecular Structure and Industrial Applications', in Polaina, J. and MacCabe, A. P. (eds). Dordrecht: Springer Netherlands, pp. 461–476. Available at: https://doi.org/10.1007/1-4020-5377-0_26.

Alternative Fuels Data Center (2018a) *Biodiesel Benefits and Considerations*. Available at: https://www.afdc.energy.gov/fuels/biodiesel_benefits.html (Accessed: 2 June 2018).

Alternative Fuels Data Center (2018b) *Ethanol Benefits and Considerations*. Available at: https://www.afdc.energy.gov/fuels/ethanol_benefits.html (Accessed: 1 June 2018).

Alvarez, H. M. *et al*. (1996) 'Formation of intracytoplasmic lipid inclusions by Rhodococcus opacus strain PD630.', *Archives of Microbiology*, 165(6), pp. 377–86. Available at: http://www.ncbi.nlm.nih.gov/pubmed/8661931.

Alvarez, H. M. *et al*. (2001) 'Biosynthesis of fatty acids and triacylglycerols by 2,6,10,14-tetramethyl pentadecane-grown cells of Nocardia globerula 432', *FEMS Microbiology Letters*, 200(2), pp. 195–200.

Alvarez, H. M. *et al*. (2013) 'Metabolism of triacylglycerols in Rhodococcus species: insights from physiology and molecular genetics', *Journal of Molecular Biochemistry*, 2(1), pp. 69–78.

Alvarez, H. M. and Steinbüchel, A. (2002) 'Triacylglycerols in prokaryotic microorganisms.', *Applied Microbiology and Biotechnology*, 60(4), pp. 367–76. Available at: http://www.ncbi.nlm.nih.gov/pubmed/12466875 (Accessed: 18 June 2014).

Amara, S. *et al*. (2016) 'Characterization of key triacylglycerol biosynthesis processes in rhodococci', *Scientific Reports*, 6, p. 24985. Available at: http://dx.doi.org/10.1038/srep24985.

Argonne National Laboratory (2017) *The Greenhouse gases, Regulated Emissions, and Energy use in Transportation Model*. Available at: https://greet.es.anl.gov (Accessed: 1 June 2018).

Atsumi, S. *et al*. (2008) 'Metabolic engineering of Escherichia coli for 1-butanol production', *Metabolic Engineering*, 10(6), pp. 305–311. Available at:

https://www.sciencedirect.com/science/article/pii/S109671760700047X (Accessed: 6 June 2018).

Balan, V. (2014) 'Current Challenges in Commercially Producing Biofuels from Lignocellulosic Biomass', *ISRN Biotechnology*, 2014(i), pp. 1–31. Available at: http://www.hindawi.com/journals/isrn/2014/463074/.

Balat, M., Balat, H. and Öz, C. (2008) 'Progress in bioethanol processing', *Progress in Energy and Combustion Science*, 34(5), pp. 551–573. Available at: https://www.sciencedirect.com/science/article/pii/S0360128507000706 (Accessed: 6 June 2018).

Bell *et al*. (1998) 'The Genus Rhodococcus', *Journal of Applied Microbiology*. Wiley/Blackwell (10.1111), 85(2), pp. 195–210. Available at: https://doi.org/10.1046/j.1365-2672.1998.00525.x.

Betts, W. B. *et al*. (1991) 'Biosynthesis and Structure of Lignocellulose', in Betts, W. B. (ed.) *Biodegradation: Natural and Synthetic Materials*. London: Springer London, pp. 139–155. Available at: https://doi.org/10.1007/978-1-4471-3470-1_7.

Biermann, C. J. (1993) *Essentials of pulping and papermaking*. San Diego, California, USA: Academic Press.

Biochemtex (2009) *Cellulosic Ethanol PROSEA*. Available at: http://www.betarenewables.com/en/proesa/what-is-it (Accessed: 27 May 2018).

BioGrace Project (2012) *Harmonised Calculations of Biofuel Greenhouse Gas Emissions in Europe*. Available at: http://www.biograce.net (Accessed: 31 May 2018).

de Boer, H. A., Comstock, L. J. and Vasser, M. (1983) 'The tac promoter: a functional hybrid derived from the trp and lac promoters.', *Proceedings of the National Academy of Sciences of the United States of America*, 80(1), pp. 21–25. Available at: http://www.ncbi.nlm.nih.gov/pmc/articles/PMC393301/.

Boerjan, W., Ralph, J. and Baucher, M. (2003) 'Lignin Biosynthesis', *Annual Review of Plant Biology*, 54(1), pp. 519–546. Available at: https://doi.org/10.1146/annurev.arplant.54.031902.134938.

Bourbonnais, R. *et al*. (1995) 'Lignin Oxidation by Laccase Isozymes from Trametes versicolor and Role of the Mediator 2,2'-Azinobis(3-Ethylbenzthiazoline-6-Sulfonate) in Kraft Lignin Depolymerisation', *Applied and Environmental Microbiology*, 61(5), pp. 1876–1880.

Bourbonnais, R. and Paice, M. G. (1990) 'Oxidation of non-phenolic substrates: An expanded role for laccase in lignin biodegradation', *FEBS*, 267(1), pp. 99–102.

BP (2017) *BP Statistical Review of World Energy 2017*. Available at: https://www.bp.com/content/dam/bp/en/corporate/pdf/energy-economics/statistical-review-2017/bp-statistical-review-of-world-energy-2017-full-report.pdf (Accessed: 3 February 2018).

BP (2018) *BP Energy Outlook 2018*. Available at: https://www.bp.com/content/dam/bp/en/corporate/pdf/energy-economics/energy-outlook/bp-energy-

outlook-2018.pdf (Accessed: 3 May 2018).

Bracmort, K. (2018) *The Renewable Fuel Standard (RFS): An Overview*, *Congressional Research Service*. Available at: https://fas.org/sgp/crs/misc/R43325.pdf (Accessed: 7 May 2018).

Brandt-Talbot, A. *et al*. (2017) 'An economically viable ionic liquid for the fractionation of lignocellulosic biomass', *Green Chemistry*. The Royal Society of Chemistry, 19(13), pp. 3078–3102. doi: 10.1039/c7gc00705a.

Brown, M. E. and Chang, M. C. Y. (2014) 'Exploring bacterial lignin degradation.', *Current Opinion in Chemical Biology*, 19, pp. 1–7. Available at: http://www.sciencedirect.com/science/article/pii/S1367593113002342 (Accessed: 10 July 2014).

Brownbridge, G. *et al*. (2013) 'The future viability of algae-derived biodiesel under economic and technical uncertainties', *Bioresource Technology*, 151, pp. 166–173. Available at: http://dx.doi.org/10.1016/j.biortech.2013.10.062.

Brunecky, R. *et al*. (2013) 'Revealing Nature's Cellulase Diversity: The Digestion Mechanism of Caldicellulosiruptor bescii CelA', *Science*, 342, pp. 1513–1516.

Brunecky, R. *et al*. (2017) 'The Multi Domain Caldicellulosiruptor bescii CelA Cellulase Excels at the Hydrolysis of Crystalline Cellulose', *Scientific Reports*, 7(1), pp. 1–17. Available at: http://dx.doi.org/10.1038/s41598-017-08985-w.

Bugg, T. D. H., Ahmad, M., Hardiman, E. M. and Rahmanpour, R. (2011) 'Pathways for degradation of lignin in bacteria and fungi.', *Natural Product Reports*, 28(12), pp. 1883–96. Available at: http://www.ncbi.nlm.nih.gov/pubmed/21918777 (Accessed: 10 July 2014).

Bugg, T. D. H., Ahmad, M., Hardiman, E. M. and Singh, R. (2011) 'The emerging role for bacteria in lignin degradation and bio-product formation.', *Current Opinion in Biotechnology*, 22(3), pp. 394–400. Available at: http://www.sciencedirect.com/science/article/pii/S0958166910001977 (Accessed: 11 July 2014).

Camarero, S. *et al*. (2005) 'Lignin-Derived Compounds as Efficient Laccase Mediators of Different Types of Recalcitrant Dyes', *Applied and Environmental Microbiology*, 71(4), pp. 1775–1784.

Camarero, S. *et al*. (2007) 'Paper pulp delignification using laccase and natural mediators', *Enzyme and Microbial Technology*, 40(5), pp. 1264–1271. Available at: https://www.sciencedirect.com/science/article/pii/S014102290600487X (Accessed: 27 May 2018).

Carrington, D. (2012) *Leaked data: Palm biodiesel as dirty as fuel from tar sands*, *The Guardian*. Available at: https://www.theguardian.com/environment/damian-carrington-blog/2012/jan/27/biofuels-biodiesel-ethanol-palm-oil.

Carriquiry, M. A., Du, X. and Timilsina, G. R. (2011) 'Second generation biofuels: Economics and policies', *Energy Policy*, 39(7), pp. 4222–4234. Available at:

https://www.sciencedirect.com/science/article/pii/S0301421511003193 (Accessed: 10 May 2018).

Chakar, F. S. and Ragauskas, A. J. (2004) 'Review of current and future softwood kraft lignin process chemistry', *Industrial Crops and Products*. Elsevier, 20(2), pp. 131–141. doi: 10.1016/J.INDCROP.2004.04.016.

Chen, H.-P. P. *et al*. (2012) 'Vanillin catabolism in Rhodococcus jostii RHA1', *Applied and Environmental Microbiology*, 78(2), pp. 586–588.

Chiba, K. *et al*. (2007) 'Construction of a pair of practical Nocardia-Escherichia coli shuttle vectors', *Japanese Journal of Infectious Diseases*, 60(10), pp. 45–47.

Childs, R. E. and Bardsley, W. G. (1975) 'The steady-state kinetics of peroxidase with 2,2'-azino-di-(3-ethyl-benzthiazoline-6-sulphonic acid) as chromogen.', *Biochemical Journal*, 145(1), pp. 93–103. Available at: http://www.ncbi.nlm.nih.gov/pmc/articles/PMC1165190/.

Christopher, L. P., Yao, B. and Ji, Y. (2014) 'Lignin Biodegradation with Laccase-Mediator Systems', *Frontiers in Energy Research*, 2, pp. 1–13. Available at: http://journal.frontiersin.org/article/10.3389/fenrg.2014.00012/abstract.

Conca, J. (2014) *It's final - corn ethanol is of no use*, *Forbes*. Available at: https://www.forbes.com/sites/jamesconca/2014/04/20/its-final-corn-ethanol-is-of-no-use/#593db22567d3 (Accessed: 8 June 2018).

Constant, S. *et al*. (2016) 'New insights into the structure and composition of technical lignins: a comparative characterisation study', *Green Chemistry*, 18(9), pp. 2651–2665. Available at: http://xlink.rsc.org/?DOI=C5GC03043A.

Costenoble, O. (2017) *Worldwide Fuels Standards: Overview of specifications and regulations on (bio)fuels*. Available at: http://task39.sites.olt.ubc.ca/files/2013/05/Worldwide-fuels-standards-Overview-of-specifications-and-regulations-on-biofuels.pdf (Accessed: 1 June 2018).

Crooks, E. (2018) *Ethanol hopes rise as crude oil prices surge*, *Financial Times*. New York. Available at: https://accounts.ft.com/login?location=https%3A%2F%2Fwww.ft.com%2Fcontent%2F4f1164fc-589c-11e8-bdb7-f6677d2e1ce8.

Davis, R. *et al*. (2013) *Process Design and Economics for the Conversion of Lignocellulosic Biomass to Hydrocarbons: Dilute-Acid and Enzymatic Deconstruction of Biomass to Sugars and Biological Conversion of Sugars to Hydrocarbons*, *National Renewable Energy Laboratory, U.S. Department of Energy*. doi: 10.2172/1107470.

Davis, R. *et al*. (2014) *Process Design and Economics for the Conversion of Algal Biomass to Biofuels: Algal Biomass Fractionation to Lipid- and Carbohydrate-Derived Fuel Products*, *National Renewable Energy Laboratory, U.S. Department of Energy*. doi: 10.2172/1159351.

DeLorenzo, D. M. *et al*. (2018) 'Molecular Toolkit for Gene Expression Control and Genome

Modification in Rhodococcus opacus PD630', *ACS Synthetic Biology*, 7(2), pp. 727–738.

Demirbas, A. (2008) 'Biofuels sources, biofuel policy, biofuel economy and global biofuel projections', *Energy Conversion and Management*, 49(8), pp. 2106–2116. Available at: http://linkinghub.elsevier.com/retrieve/pii/S0196890408000770 (Accessed: 23 May 2014).

Demirbaş, A. (2002) 'Fuel Characteristics of Olive Husk and Walnut, Hazelnut, Sunflower, and Almond Shells', *Energy Sources*, 24(3), pp. 215–221. Available at: http://www.tandfonline.com/doi/abs/10.1080/009083102317243601 (Accessed: 9 September 2014).

Duan, Y. *et al*. (2011) 'De novo biosynthesis of biodiesel by Escherichia coli in optimized fed-batch cultivation.', *PloS one*, 6(5). Available at: http://www.pubmedcentral.nih.gov/articlerender.fcgi?artid=3100327&tool=pmcentrez&rendertype=abstract (Accessed: 5 October 2014).

Dutta, A. *et al*. (2011) *Process Design and Economics for Conversion of Lignocellulosic Biomass to Ethanol: Thermochemical Pathway by Indirect Gasification and Mixed Alcohol synthesis*, *National Renewable Energy Laboratory, U.S. Department of Energy*. doi: 10.2172/1015885.

Ethanol Europe Renewables (2018) *Failed E.U. Commission advanced biofuel policy wastes billions of Euros*, *Euractiv*. Available at: https://www.euractiv.com/section/climate-environment/opinion/failed-eu-commission-advanced-biofuel-policy-wastes-billions-of-euros/ (Accessed: 27 May 2018).

Eulberg, D. *et al*. (1998) 'Characterization of a protocatechuate catabolic gene cluster from Rhodococcus opacus 1CP: Evidence for a merged enzyme with 4-carboxymuconolactone-decarboxylating and 3-oxoadipate enol-lactone- hydrolyzing activity', *Journal of Bacteriology*, 180(5), pp. 1072–1081.

ExxonMobil (2018) *ExxonMobil and Synthetic Genomics Algae Biofuels Program Targets 10,000 Barrels Per Day by 2025*. Available at: http://news.exxonmobil.com/press-release/exxonmobil-and-synthetic-genomics-algae-biofuels-program-targets-10000-barrels-day-202 (Accessed: 1 June 2018).

Fitzgerald, D. J. *et al*. (2004) 'Mode of antimicrobial of vanillin against Escherichia coli, Lactobacillus plantarum and Listeria innocua', *Journal of Applied Microbiology*, 97(1), pp. 104–113.

Fitzgerald, D. J., Stratford, M. and Narbad, A. (2003) 'Analysis of the inhibition of food spoilage yeasts by vanillin.', *International Journal of Food Microbiology*. Netherlands, 86(1–2), pp. 113–122.

Folch, J., Lees, M. and Sloane Stanley, G. H. (1957) 'A simple method for the isolation and purification of total lipides from animal tissues', *Journal of Biological Chemistry*, 226, pp. 497–509. doi: 10.1016/j.ultrasmedbio.2011.03.005.

Froass, P. M., Ragauskas, A. J. and Jiang, J. (1996) 'Chemical Structure of Residual Lignin from Kraft Pulp', *Journal of Wood Chemistry and Technology*. Taylor & Francis, 16(4), pp. 347–365. doi: 10.1080/02773819608545820.

Fuchs, G., Boll, M. and Heider, J. (2011) 'Microbial degradation of aromatic compounds- From one strategy to four', *Nature Reviews Microbiology*, 9(11), pp. 803–816. Available at: http://dx.doi.org/10.1038/nrmicro2652.

Fukuda, H., Kondo, A. and Noda, H. (2001) 'Biodiesel fuel production by transesterification of oils', *Journal of Bioscience and Bioengineering*, pp. 405–416. Available at: https://www.sciencedirect.com/science/article/pii/S1389172301802887 (Accessed: 9 May 2018).

Ge, Y., Dababneh, F. and Li, L. (2017) 'Economic Evaluation of Lignocellulosic Biofuel Manufacturing Considering Integrated Lignin Waste Conversion to Hydrocarbon Fuels', *Procedia Manufacturing*, 10, pp. 112–122. Available at: http://dx.doi.org/10.1016/j.promfg.2017.07.037.

Gebremariam, S. N. and Marchetti, J. M. (2018) 'Economics of biodiesel production: Review', *Energy Conversion and Management*, 168, pp. 74–84. Available at: http://linkinghub.elsevier.com/retrieve/pii/S0196890418304655 (Accessed: 10 May 2018).

Van Der Geize, R. and Dijkhuizen, L. (2004) 'Harnessing the catabolic diversity of rhodococci for environmental and biotechnological applications', *Current Opinion in Microbiology*, 7(3), pp. 255–261. Available at: https://www.sciencedirect.com/science/article/pii/S1369527404000384 (Accessed: 9 May 2018).

Gellerstedt, G. (1992) 'Gel Permeation Chromatography', in Lin, S. Y. and Dence, C. W. (eds) *Methods in Lignin Chemistry*. Springer Berlin Heidelberg.

Gellerstedt, G. and Henriksson, G. (2008) 'Lignins: Major Sources, Structure and Properties', in *Monomers, Polymers and Composites from Renewable Resources*, pp. 201–224. Available at: http://linkinghub.elsevier.com/retrieve/pii/B9780080453163000090 (Accessed: 7 June 2018).

Generoso, W. C. *et al*. (2015) 'Metabolic engineering of Saccharomyces cerevisiae for production of butanol isomers', *Current Opinion in Biotechnology*, pp. 1–7. Available at: https://www.sciencedirect.com/science/article/pii/S0958166914001645 (Accessed: 6 June 2018).

de Gonzalo, G. *et al*. (2016) 'Bacterial enzymes involved in lignin degradation', *Journal of Biotechnology*, 236, pp. 110–119. Available at: http://dx.doi.org/10.1016/j.jbiotec.2016.08.011.

Gosselink, R. (2011) 'Lignin as a renewable aromatic resource for the chemical industry', in *Mini-symposium organised by Wageningen UR Lignin Platform, December 2011*. Available at: https://www.wur.nl/upload_mm/d/7/f/35cbaa28-e1d6-4d6a-88f1-bfa1265b9af0_Mini-symp 6-12-2011 Gosselink_Lignin as a renewable aromatic resource for the chem ind.pdf.

Graichen, F. H. M. *et al*. (2017) 'Yes, we can make money out of lignin and other bio-based resources', *Industrial Crops and Products*, 106, pp. 74–85. Available at: https://www.sciencedirect.com/science/article/pii/S092666901630721X#bib0060 (Accessed: 12 June 2018).

Growth Energy (2018) *Growth Energy Statement: More Biofuels Vital to Improving U.S. Energy Outlook*. Available at: https://growthenergy.org/2018/02/14/growth-energy-statement-biofuels-vital-improving-u-s-energy-outlook/ (Accessed: 8 June 2018).

Guo, D., Pan, H. and Li, X. (2015) 'Metabolic engineering of Escherichia coli for production of biodiesel from fatty alcohols and acetyl-CoA', *Applied Microbiology and Biotechnology*, 99(18), pp. 7805–7812.

Gutiérrez, A. *et al*. (2007) 'Removal of lipophilic extractives from paper pulp by laccase and lignin-derived phenols as natural mediators', *Environmental Science and Technology*, 41(11), pp. 4124–4129.

Hammerschlag, R. (2006) 'Ethanol's Energy Return on Investment: A Survey of the Literature 1990–Present', *Environmental Science & Technology*, 40(6), pp. 1744–1750. Available at: https://doi.org/10.1021/es052024h.

Harwood, C. S. and Parales, R. E. (1996) 'The β-Ketoadipate pathway and the biology of self-identity', *Annual Review of Microbiology*, 50(1), pp. 553–590. Available at: http://www.annualreviews.org/doi/10.1146/annurev.micro.50.1.553.

Heitner, C., Dimmel, D. and Schmidt, J. (2010) *Lignin and Lignans: Advances in Chemistry*. CRC Press.

Henson, W. R., Hsu, F.-F., *et al*. (2018) 'Lipid metabolism of phenol-tolerant Rhodococcus opacus strains for lignin bioconversion', *Biotechnology for Biofuels*, 11(1), p. 339. doi: 10.1186/s13068-018-1337-z.

Henson, W. R., Campbell, T., *et al*. (2018) 'Multi-omic elucidation of aromatic catabolism in adaptively evolved Rhodococcus opacus', *Metabolic Engineering*. Academic Press, 49, pp. 69–83. doi: 10.1016/j.ymben.2018.06.009.

Hernández, M. A. *et al*. (2008) 'Biosynthesis of storage compounds by Rhodococcus jostii RHA1 and global identification of genes involved in their metabolism', *BMC Genomics*, 9, pp. 1–14.

Hetzler, S., Bröker, D. and Steinbüchel, A. (2013) 'Saccharification of cellulose by recombinant Rhodococcus opacus PD630 strains.', *Applied and Environmental Microbiology*, 79(17), pp. 5159–66. Available at: http://www.pubmedcentral.nih.gov/articlerender.fcgi?artid=3753941&tool=pmcentrez&rendertype=abstract (Accessed: 8 July 2014).

Hetzler, S. and Steinbüchel, A. (2013) 'Establishment of cellobiose utilization for lipid production in Rhodococcus opacus PD630.', *Applied and Environmental Microbiology*, 79(9), pp. 3122–5. Available at: http://www.pubmedcentral.nih.gov/articlerender.fcgi?artid=3623151&tool=pmcentrez&rendertype=abstract (Accessed: 23 September 2014).

Holder, J. W. *et al*. (2011) 'Comparative and functional genomics of Rhodococcus opacus PD630 for biofuels development.', *PLoS genetics*, 7(9). Available at: http://www.pubmedcentral.nih.gov/articlerender.fcgi?artid=3169528&tool=pmcentrez&rendertype=abstract (Accessed: 30 May 2014).

Hossain, M. Z. *et al*. (2014) 'Chemical composition of date-pits and its potential for developing value-added product - A review', *Polish Journal of Food and Nutrition Sciences*, 64(4), pp. 215–226.

Humbird, D. *et al*. (2011) *Process Design and Economics for Biochemical Conversion of Lignocellulosic Biomass to Ethanol: Dilute-Acid Pretreatment and Enzymatic Hydrolysis of Corn Stover*, *National Renewable Energy Laboratory, U.S. Department of Energy*. doi: 10.2172/1013269.

Humphreys, J. M. and Chapple, C. (2002) 'Rewriting the lignin roadmap.', *Current Opinion in Plant Biology*, 5(3), pp. 224–229.

International Energy Agency (2017) *Energy Technology Perspectives 2017*. Available at: https://www.iea.org/etp2017/summary/ (Accessed: 8 June 2018).

International Energy Agency (2018) *Bioenergy and Biofuels*. Available at: https://www.iea.org/topics/renewables/bioenergy/ (Accessed: 31 May 2018).

International Energy Agengy (2008) *From 1st- to 2nd-generation biofuel technologies: an overview of current industry and R&D activities*. Available at: https://www.iea.org/publications/freepublications/publication/2nd_Biofuel_Gen.pdf.

Islam, M. A. *et al*. (2013) 'Influence of Fatty Acid Structure on Fuel Properties of Algae Derived Biodiesel', *Procedia Engineering*, 56, pp. 591–596. Available at: http://linkinghub.elsevier.com/retrieve/pii/S1877705813005183 (Accessed: 4 June 2014).

Kalscheuer, R., Stölting, T. and Steinbüchel, A. (2006) 'Microdiesel: Escherichia coli engineered for fuel production.', *Microbiology*, 152(Pt 9), pp. 2529–36. Available at: http://www.ncbi.nlm.nih.gov/pubmed/16946248 (Accessed: 29 May 2014).

Kan, T., Strezov, V. and Evans, T. J. (2016) 'Lignocellulosic biomass pyrolysis: A review of product properties and effects of pyrolysis parameters', *Renewable and Sustainable Energy Reviews*, 57, pp. 126–1140. Available at: https://www.sciencedirect.com/science/article/pii/S1364032115015683#bib4 (Accessed: 7 May 2018).

Kim, D. H. *et al*. (2011) 'Engine performance and toxix gas analysis of biobutanol-blended gasoline as a vehicle fuel', *International Journal of Automotive Technology*, 12(3), pp. 409–16. Available at: http://link.springer.com/article/10.1007/s12239-012-0027-2.

Klinke, H. B., Thomsen, A. B. and Ahring, B. K. (2004) 'Inhibition of ethanol-producing yeast and bacteria by degradation products produced during pre-treatment of biomass', *Applied Microbiology and Biotechnology*, 66(1), pp. 10–26.

Knothe, G. (2005) 'Dependence of biodiesel fuel properties on the structure of fatty acid alkyl esters', *Fuel Processing Technology*, 86(10), pp. 1059–1070. Available at: http://linkinghub.elsevier.com/retrieve/pii/S0378382004001894 (Accessed: 26 May 2014).

Knothe, G. (2008) '"Designer" Biodiesel: Optimizing Fatty Ester Composition to Improve Fuel Properties', *Energy & Fuels*, 22(2), pp. 1358–1364. Available at: http://pubs.acs.org/doi/abs/10.1021/ef700639e.

Knothe, G. and Steidley, K. R. (2005) 'Kinematic viscosity of biodiesel fuel components and related compounds. Influence of compound structure and comparison to petrodiesel fuel components', *Fuel*, 84(9), pp. 1059–1065. Available at: http://linkinghub.elsevier.com/retrieve/pii/S0016236105000475 (Accessed: 25 May 2014).

Kosa, M. and Ragauskas, A. J. (2012) 'Bioconversion of lignin model compounds with oleaginous Rhodococci.', *Applied Microbiology and Biotechnology*, 93(2), pp. 891–900. Available at: http://www.ncbi.nlm.nih.gov/pubmed/22159607 (Accessed: 3 July 2014).

Kosa, M. and Ragauskas, A. J. (2013) 'Lignin to lipid bioconversion by oleaginous Rhodococci', *Green Chemistry*, 15(8), p. 2070. Available at: http://xlink.rsc.org/?DOI=c3gc40434j (Accessed: 3 July 2014).

Kuhad, R. C., Singh, A. and Eriksson, K.-E. L. (1997) 'Microorganisms and enzymes involved in the degradation of plant fiber cell walls', in Eriksson, K.-E. L. et al. (eds) *Biotechnology in the Pulp and Paper Industry*. Berlin, Heidelberg: Springer Berlin Heidelberg, pp. 45–125. Available at: https://doi.org/10.1007/BFb0102072.

Kurosawa, K. *et al*. (2010) 'High-cell-density batch fermentation of Rhodococcus opacus PD630 using a high glucose concentration for triacylglycerol production.', *Journal of Biotechnology*, 147(3–4), pp. 212–8. Available at: http://www.ncbi.nlm.nih.gov/pubmed/20412824 (Accessed: 14 June 2014).

Kurosawa, K., Laser, J. and Sinskey, A. J. (2015) 'Tolerance and adaptive evolution of triacylglycerol-producing Rhodococcus opacus to lignocellulose-derived inhibitors', *Biotechnology for Biofuels*, 8, p. 76.

Kurosawa, K., Wewetzer, S. J. and Sinskey, A. J. (2013) 'Engineering xylose metabolism in triacylglycerol-producing Rhodococcus opacus for lignocellulosic fuel production', *Biotechnology for Biofuels*, 6(1), p. 134. Available at: http://biotechnologyforbiofuels.biomedcentral.com/articles/10.1186/1754-6834-6-134.

Lane, J. (2012) *DuPont breaks ground on world's largest cellulosic biorefinery*, *Biofuels Digest*. Available at: http://www.biofuelsdigest.com/bdigest/2012/11/30/dupont-breaks-ground-on-worlds-largest-cellulosic-biorefinery/.

Lange, H., Rulli, F. and Crestini, C. (2016) 'Gel Permeation Chromatography in Determining Molecular Weights of Lignins: Critical Aspects Revisited for Improved Utility in the Development of

Novel Materials', *ACS Sustainable Chemistry and Engineering*, 4(10), pp. 5167–5180.

Lange, J. (2007) 'Lignocellulose conversion: an introduction to chemistry, process and economics', *Biofuels, Bioproducts and Biorefining*, 1, pp. 39–48. Available at: https://onlinelibrary.wiley.com/doi/abs/10.1002/bbb.7.

Laskar, D. D. *et al*. (2013) 'Pathways for biomass-derived lignin to hydrocarbon fuels', *Biofuels, Bioproducts & Biorefining*, pp. 602–626.

Lee, S. Y. *et al*. (2008) 'Fermentative butanol production by clostridia', *Biotechnology and Bioengineering*, 101(2), pp. 209–228.

Lewandowski, I. *et al*. (2000) 'Miscanthus: European experience with a novel energy crop', *Biomass and Bioenergy*, 19(4), pp. 209–227. Available at: https://www.sciencedirect.com/science/article/pii/S0961953400000325 (Accessed: 7 May 2018).

Lewis, N. G., Davin, L. B. and Sarkanen, S. (1998) 'Lignin and Lignan Biosynthesis: Distinctions and Reconciliations', in *Lignin and Lignan Biosynthesis*. American Chemical Society (ACS Symposium Series), p. 1. Available at: https://doi.org/10.1021/bk-1998-0697.ch001.

Liliana, R. *et al*. (2008) 'Microalgae for oil: Strain selection, induction of lipid synthesis and outdoor mass cultivation in a low-cost photobioreactor', *Biotechnology and Bioengineering*, 102(1), pp. 100–112. Available at: https://onlinelibrary.wiley.com/doi/abs/10.1002/bit.22033.

Liu, Q., Luo, L. and Zheng, L. (2018) 'Lignins: Biosynthesis and biological functions in plants', *International Journal of Molecular Sciences*, 19(2).

Liu, Z. H. *et al*. (2018) 'Combinatorial pretreatment and fermentation optimization enabled a record yield on lignin bioconversion', *Biotechnology for Biofuels*, 11(1), pp. 1–20. Available at: https://doi.org/10.1186/s13068-018-1021-3.

Lopachin, R. M. and Gavin, T. (2014) 'Molecular mechanisms of aldehyde toxicity: A chemical perspective', *Chemical Research in Toxicology*, 27(7), pp. 1081–1091.

Low Carbon Technology Partnerships (2015) *Low Carbon Transport Fuels*. Available at: https://www.wbcsd.org/contentwbc/download/1884/23978 (Accessed: 1 June 2018).

Mäki-Arvela, P. *et al*. (2010) 'Dissolution of lignocellulosic materials and its constituents using ionic liquids - A review', *Industrial Crops and Products*, pp. 175–201. Available at: https://www.sciencedirect.com/science/article/pii/S0926669010000841 (Accessed: 14 June 2018).

Malherbe, S. and Cloete, T. E. (2002) 'Lignocellulose biodegradation: Fundamentals and applications', *Reviews in Environmental Science and Biotechnology*, 1(2), pp. 105–114. Available at: https://doi.org/10.1023/A:1020858910646.

Mansfield, S. D. (2009) 'Solutions for dissolution-engineering cell walls for deconstruction', *Current*

Opinion in Biotechnology, 20, pp. 286–294. Available at: https://www.sciencedirect.com/science/article/pii/S0958166909000585 (Accessed: 8 May 2018).

Margot, J. *et al*. (2013) 'Bacterial versus fungal laccase: potential for micropollutant degradation', *AMB Express*, 3(1), p. 63. Available at: https://doi.org/10.1186/2191-0855-3-63.

Mate, D. M. and Alcalde, M. (2016) 'Laccase: a multi-purpose biocatalyst at the forefront of biotechnology', *Microbial Biotechnology*, 10(6), pp. 1457–1467.

Matos, M., Barreiro, M. F. and Gandini, A. (2010) 'Olive stone as a renewable source of biopolyols', *Industrial Crops and Products*, 32(1), pp. 7–12. Available at: http://dx.doi.org/10.1016/j.indcrop.2010.02.010.

Mayer, A. M. and Staples, R. C. (2002) 'Laccase: New functions for an old enzyme', *Phytochemistry*, 60(6), pp. 551–565. Available at: https://www.sciencedirect.com/science/article/pii/S0031942202001711 (Accessed: 31 May 2018).

McLeod, M. P. *et al*. (2006) 'The complete genome of Rhodococcus sp. RHA1 provides insights into a catabolic powerhouse', *Proceedings of the National Academy of Sciences*, 103(42), pp. 15582–15587. Available at: http://www.pnas.org/cgi/doi/10.1073/pnas.0607048103.

Meher, L., Vidyasagar, D. and Naik, S. (2006) 'Technical aspects of biodiesel production by transesterification—a review', *Renewable and Sustainable Energy Reviews*, 10(3), pp. 248–268. Available at: http://www.sciencedirect.com/science/article/pii/S1364032104001236 (Accessed: 10 July 2014).

Mekhilef, S., Siga, S. and Saidur, R. (2011) 'A review on palm oil biodiesel as a source of renewable fuel', *Renewable and Sustainable Energy Reviews*, 15(4), pp. 1937–1949. Available at: https://www.sciencedirect.com/science/article/pii/S1364032110004478 (Accessed: 6 June 2018).

Miki, K., Renganathan, V. and Gold, M. H. (1986) 'Mechanism of β-aryl ether dimeric lignin model compound oxidation by lignin peroxidase by Phanerochaete chrysosporium', *Biochemistry*, 25(17), pp. 4790–4796. Available at: https://doi.org/10.1021/bi00365a011.

Miller, J. (2016) *Lignin: Technology, Applications and Markets*. *Special Market Analysis Study*, *RISI*. Available at: http://mktintell.com/files/LigninTechnologyApplicationsandMarkets.pdf (Accessed: 27 May 2018).

Mohr, A. and Raman, S. (2013) 'Lessons from first generation biofuels and implications for the sustainability appraisal of second generation biofuels', *Energy Policy*, 63, pp. 114–122. Available at: https://www.sciencedirect.com/science/article/pii/S0301421513008264 (Accessed: 6 June 2018).

Mosier, N. *et al*. (2005) 'Features of promising technologies for pretreatment of lignocellulosic biomass', *Bioresource Technology*. Elsevier, 96(6), pp. 673–686. doi: 10.1016/j.biortech.2004.06.025.

Mullis, K. *et al*. (1986) 'Specific enzymatic amplification of DNA in vitro: The polymerase chain

reaction', *Cold Spring Harbor Symposia on Quantitative Biology*, 51(1), pp. 263–273. doi: 10.1101/SQB.1986.051.01.032.

Munk, L. *et al*. (2015) 'Can laccases catalyze bond cleavage in lignin?', *Biotechnology Advances*, 33(1), pp. 13–24. Available at: http://dx.doi.org/10.1016/j.biotechadv.2014.12.008.

Nagarajan, S. *et al*. (2013) 'An updated comprehensive techno-economic analysis of algae biodiesel', *Bioresource Technology*, 145, pp. 150–156. Available at: http://dx.doi.org/10.1016/j.biortech.2012.11.108.

de Oliveira, M. A. L. *et al*. (2014) '20 Years of Fatty Acid Analysis By Capillary Electrophoresis.', *Molecules*, 19(9), pp. 14094–113. Available at: http://www.ncbi.nlm.nih.gov/pubmed/25207715 (Accessed: 23 October 2014).

Olukoshi, E. R. and Packter, N. M. (1994) 'Importance of stored triacylglycerols in Streptomyces : possible carbon source for anti biot ics', *Microbiology*, 140, pp. 931–943.

Pardo, I. *et al*. (2013) 'New colorimetric screening assays for the directed evolution of fungal laccases to improve the conversion of plant biomass', *BMC Biotechnology*, 13(90).

Paulson, N. D. and Ginder, R. G. (2007) *Growth and Direction of the Biodiesel Industry in the United States*. 07–WP 448.

Piontek, K., Antorini, M. and Choinowski, T. (2002) 'Crystal structure of a laccase from the fungus Trametes versicolor at 1.90-Å resolution containing a full complement of coppers', *Journal of Biological Chemistry*, 277(40), pp. 37663–37669.

Pollegioni, L., Tonin, F. and Rosini, E. (2015) 'Lignin-degrading enzymes', *FEBS Journal*, 282(7), pp. 1190–1213.

Ragauskas, A. J. *et al*. (2014) 'Lignin valorization: Improving lignin processing in the biorefinery', *Science*, 344(6185).

Ragnar, M. *et al*. (2014) 'Pulp', in *Ullmann's Encyclopedia of Industrial Chemistry*, pp. 1–92. Available at: http://doi.wiley.com/10.1002/14356007.a18_545.pub4%0Ahttp://dx.doi.org/10.1002/14356007.a18_545.pub4%5Cnhttp://doi.wiley.com/10.1002/14356007.a18_545.pub4.

Rahmanpour, R. and Bugg, T. D. H. (2013) 'Assembly in vitro of Rhodococcus jostii RHA1 encapsulin and peroxidase DypB to form a nanocompartment', *FEBS Journal*, 280(9), pp. 2097–2104.

Ralph, J. and Landucci, L. L. . (2010) 'NMR of Lignins', in Heitner, C., Dimmel, D., and Schmidt, J. (eds) *Lignins and Lignans*. CRC Press.

Reboredo, F. H. *et al*. (2016) 'The Fall of Oil Prices and the Effects on Biofuels', *Trends in Biotechnology*, 34(1), pp. 3–6. Available at:

https://www.sciencedirect.com/science/article/pii/S0167779915002206 (Accessed: 7 May 2018).

REN21 (2017) *Renewables 2017 Global Status Report*, *Paris: REN21 Secretariat*. Available at: http://www.ren21.net/gsr-2017/ (Accessed: 8 June 2018).

Renewable Fuels Association (2018) *31 States Broke Through the "Blend Wall" in 2016*. Available at: http://www.ethanolrfa.org/wp-content/uploads/2018/02/2016-state-ethanol-blends.pdf (Accessed: 6 May 2018).

Rinaldi, R. *et al*. (2016) 'Paving the Way for Lignin Valorisation: Recent Advances in Bioengineering, Biorefining and Catalysis', *Angewandte Chemie International Edition*, pp. 2–54. Available at: http://doi.wiley.com/10.1002/anie.201510351.

Roberts, J. N. *et al*. (2011) 'Characterization of Dye-Decolorizing Peroxidases from Rhodococcus jostii RHA1', *Biochemistry*, 50, pp. 5108–5119. Available at: http://www.ncbi.nlm.nih.gov/pubmed/21534568 (Accessed: 11 July 2014).

Sainsbury, P. D. *et al*. (2013) 'Breaking down lignin to high-value chemicals: the conversion of lignocellulose to vanillin in a gene deletion mutant of Rhodococcus jostii RHA1.', *ACS Chemical Biology*, 8(10), pp. 2151–6. Available at: http://www.ncbi.nlm.nih.gov/pubmed/23898824.

Schlegel, H. G., Kaltwasser, H. and Gottschalk, G. (1961) 'Ein Submersverfahren zur Kultur wasserstoffoxydierender Bakterien: Wachstumsphysiologische Untersuchungen', *Archiv für Mikrobiologie*, 38(3), pp. 209–222.

Searchinger, T. and Heimlich, R. (2015) *'Avoiding Bioenergy Competition for Food Crops and Land.' Working Paper, Installment 9 of Creating a Sustainable Food Future*. Washington, DC. Available at: http://www.wri.org/sites/default/files/avoiding_bioenergy_competition_food_crops_land.pdf (Accessed: 6 June 2018).

Shell (2018) *Shell Scenarios Sky: Meeting the Goals of the Paris Agreement*. Available at: https://www.shell.com/energy-and-innovation/the-energy-future/scenarios/shell-scenario-sky.html (Accessed: 4 June 2018).

Shell Energy and Innovation (no date) *Biofuels*. Available at: https://www.shell.com/energy-and-innovation/the-energy-future/future-transport/biofuels.html (Accessed: 8 June 2018).

Shleev, S. *et al*. (2006) 'Interaction of fungal laccases and laccase-mediator systems with lignin', *Enzyme and Microbial Technology*, 39(4), pp. 841–847. Available at: https://www.sciencedirect.com/science/article/pii/S0141022906000275 (Accessed: 30 May 2018).

Silva, E. A. A. B. da *et al*. (2009) 'An integrated process to produce vanillin and lignin-based polyurethanes from Kraft lignin', *Chemical Engineering Research and Design*, 87(9), pp. 1276–1292. Available at: https://www.sciencedirect.com/science/article/pii/S0263876209001798 (Accessed: 11 June 2018).

Singh, R. *et al*. (2013) 'Improved manganese-oxidizing activity of DypB, a peroxidase from a lignolytic bacterium.', *ACS Chemical Biology*, 8(4), pp. 700–6. Available at: http://www.pubmedcentral.nih.gov/articlerender.fcgi?artid=3631457&tool=pmcentrez&rendertype=abstract.

Singh, R. and Eltis, L. D. (2015) 'The multihued palette of dye-decolorizing peroxidases', *Archives of Biochemistry and Biophysics*, pp. 56–65. Available at: https://www.sciencedirect.com/science/article/pii/S0003986115000399 (Accessed: 27 May 2018).

Skolrud, T. D. *et al*. (2016) 'The role of federal Renewable Fuel Standards and market structure on the growth of the cellulosic biofuel sector', *Energy Economics*, 58, pp. 141–151. Available at: https://www.sciencedirect.com/science/article/pii/S0140988316301736 (Accessed: 10 May 2018).

Souza, G. M. *et al*. (2015a) *Bioenergy & Sustainability: bridging the gaps*, *SCOPE Scientific Committee on Problems of the Environment*. Edited by G. M. Souza et al. Paris Cedex, France.

Souza, G. M. *et al*. (2015b) *Bioenergy and Sustainability: Bridging the Gaps*, *SCOPE briefing*. Paris. doi: 10.1017/CBO9781107415324.004.

Staffel, I. (2011) *The Energy and Fuel Data Sheet*. Available at: http://www.claverton-energy.com/wordpress/wp-content/uploads/2012/08/the_energy_and_fuel_data_sheet1.pdf.

Stewart, D. (2008) 'Lignin as a base material for materials applications: Chemistry, application and economics', *Industrial Crops and Products*, 27(2), pp. 202–207. Available at: https://www.sciencedirect.com/science/article/pii/S0926669007001094 (Accessed: 6 May 2018).

Sutcliffe, I. C. and Dover, L. G. (2010) 'The Rhodococcal Cell Envelope: Composition, Organisation and Biosynthesis', in *Biology of Rhodococcus*, pp. 29–72.

Tajparast, M. and Frigon, D. (2015) 'Genome-scale metabolic model of Rhodococcus jostii RHA1 (iMT1174) to study the accumulation of storage compounds during nitrogen-limited condition', *BMC Systems Biology*, 9(1), p. 43. Available at: https://doi.org/10.1186/s12918-015-0190-y.

Timilsina, G. R. and Shrestha, A. (2010) 'Biofuels: Markets, Targets and Impacts', *Policy Research Working Paper; no. WPS 5364*. doi: 10.1596/1813-9450-5364.

U.S. Department of Energy (2016) *2016 Billion-Ton Report: Advancing Domestic Resources for a Thriving Bioeconomy, Volume 1: Economic Availability of Feetstocks*. Available at: http://energy.gov/eere/bioenergy/2016-billion-ton-report.

U.S. Energy Information Administration (2018) *Annual Energy Outlook 2018 with projections to 2050*. Available at: www.eia.gov/aeo (Accessed: 3 June 2018).

Valentine, J. *et al*. (2012) 'Food vs. fuel: the use of land for lignocellulosic "next generation" energy crops that minimize competition with primary food production', *GCB Bioenergy*, 4(1), pp. 1–19. Available at: https://onlinelibrary.wiley.com/doi/abs/10.1111/j.1757-1707.2011.01111.x.

Valle-Rodríguez, J. O. *et al*. (2014) 'Metabolic engineering of Saccharomyces cerevisiae for production of fatty acid ethyl esters, an advanced biofuel, by eliminating non-essential fatty acid utilization pathways', *Applied Energy*, 115, pp. 226–232. Available at: https://www.sciencedirect.com/science/article/pii/S0306261913008234 (Accessed: 6 June 2018).

Vanholme, R. *et al*. (2010) 'Lignin Biosynthesis and Structure', *Plant Physiology*, 153(3), p. 895 LP-905. Available at: http://www.plantphysiol.org/content/153/3/895.abstract.

Vasina, J. A. and Baneyx, F. (1997) 'Expression of aggregation-prone recombinant proteins at low temperatures: A comparative study of the Escherichia coli cspA and tac promoter systems', *Protein Expression and Purification*, 9(2), pp. 211–218. Available at: https://www.sciencedirect.com/science/article/pii/S1046592896906786 (Accessed: 18 May 2018).

Vergara-Barberán, M. *et al*. (2011) 'Capillary electrophoresis of free fatty acids by indirect ultraviolet detection: application to the classification of vegetable oils according to their botanical origin.', *Journal of Agricultural and Food Chemistry*, 59(20), pp. 10775–80. Available at: http://www.ncbi.nlm.nih.gov/pubmed/21905655.

Wang, B. *et al*. (2014) 'Cultivation of lipid-producing bacteria with lignocellulosic biomass: effects of inhibitory compounds of lignocellulosic hydrolysates.', *Bioresource Technology*, 161, pp. 162–170.

Wang, H. *et al*. (2015) 'Biomass-derived lignin to jet fuel range hydrocarbons via aqueous phase hydrodeoxygenation', *Green Chem.*, 17(12), pp. 5131–5135. Available at: http://xlink.rsc.org/?DOI=C5GC01534K.

Wang, Z. *et al*. (2016) 'Demand for Ethanol in the Face of Blend Wall: Is it a Complement or a Substitute for Conventional Transportation Fuel in the United States?', *2016 Annual Meeting, February 6-9, 2016, Southern Agricultural Economics Association, San Antonio, Texas*, p. 22.

Weng, J. K. *et al*. (2008) 'Emerging strategies of lignin engineering and degradation for cellulosic biofuel production', *Current Opinion in Biotechnology*, 19, pp. 166–172. Available at: https://www.sciencedirect.com/science/article/pii/S0958166908000268 (Accessed: 8 May 2018).

De Wild, P. J., Huijgen, W. J. J. and Gosselink, R. J. A. (2014) 'Lignin pyrolysis for profitable lignocellulosic biorefineries', *Biofuels, Bioproducts and Biorefining*, 8, pp. 645–6578.

Wong, D. W. S. (2009) 'Structure and Action Mechanism of Ligninolytic Enzymes', *Applied Biochemistry and Biotechnology*, 157(2), pp. 174–209. Available at: http://link.springer.com/10.1007/s12010-008-8279-z.

Xie, S. *et al*. (2017) 'Advanced Chemical Design for Efficient Lignin Bioconversion', *ACS Sustainable Chemistry and Engineering*, 5(3), pp. 2215–2223.

Xiong, X., Wang, X. and Chen, S. (2012) 'Engineering of a xylose metabolic pathway in Rhodococcus strains', *Applied and Environmental Microbiology*, 78(16), pp. 5483–91. Available at:

http://www.pubmedcentral.nih.gov/articlerender.fcgi?artid=3406118&tool=pmcentrez&rendertype=abstract (Accessed: 10 June 2014).

Yoneda, A. *et al*. (2016) 'Comparative transcriptomics elucidates adaptive phenol tolerance and utilization in lipid-accumulating Rhodococcus opacus PD630', *Nucleic Acids Research*, 44(5), pp. 2240–2254.

Yu, K. O. *et al*. (2012) 'Synthesis of FAEEs from glycerol in engineered Saccharomyces cerevisiae using endogenously produced ethanol by heterologous expression of an unspecific bacterial acyltransferase', *Biotechnology and Bioengineering*, 109(1), pp. 110–115.

Zaldivar, J., Martinez, A. and Ingram, L. O. (1999) 'Effect of Selected Aldehydes on the Growth and Fermentation of Ethanologeic Escherichia coli', *Biotechnology and Bioengineering*, 65(1), pp. 24–33.

9 Appendix

9.1 Plasmid DNA sequences

Gene Name: pUCIDT-AMP:DypB

Gene Size: 1053 bp Plasmid Weight: 2,351,269.6 g/mole

Sequence Detail

```
00001  TCGCGCGTTT CGGTGATGAC GGTGAAAACC TCTGACACAT GCAGCTCCCG GAGACGGTCA CAGCTTGTCT GTAAGCGGAT
00081  GCCGGGAGCA GACAAGCCCG TCAGGGCGCG TCAGCGGGTG TTGGCGGGTG TCGGGGCTGG CTTAACTATG CGGCATCAGA
00161  GCAGATTGTA CTGAGAGTGC ACCAAATGCG GTGTGAAATA CCGCACAGAT GCGTAAGGAG AAAATACCGC ATCAGGCGCC
00241  ATTCGCCATT CAGGCTGCGC AACTGTTGGG AAGGGCGATC GGTGCGGGCC TCATCGCTAT TACGCCAGCT GGCGAAAGGG
00321  GGATGTGCTG CAAGGCGATT AAGTTGGGTA ACGCCAGGGT TTTCCCAGTC ACGACGTTGT AAAACGACGG CCAGTGCAAC
00401  GCGATGACGA TGGATAGCGA TTCATCGATG AGCTGACCCG ATCGCCGCCG CCGGAGGGTT GCGTTTGAGA CGGGCGACAG
00481  ATATGCCAGG CCCAGTCGCG AGATTGGCAC CACAAGCAGT CCTCACTCCG CCCAGCGCCG CCTCCCTCTT CCTGGTGCTC
00561  GTCGCCGGGG ACTCCGACGA CGACCGCGCG ACGGTGTGCG ACGTGATCTC CGGGATCGAC GGACCGCTCA AGGCGGTGGG
00641  ATTCCGCGAA CTCGCCGGTT CCCTGTCCTG CGTGGTCGGT GTCGGTGCGC AGTTCTGGGA CCGCGTGAGC GCGTCGTCGA
00721  AGCCGGCGCA CCTGCATCCG TTCGTCCCGC TGTCCGGGCC GGTCCACAGC GCGCCCTCCA CGCCGGGTGA CCTCCTGTTC
00801  CACATCAAGG CCGCCCGCAA GGATCTGTGC TTCGAACTGG GCCGCCAGAT CGTCTCCGCG CTGGGCTCCG CCGCCACCGT
00881  GGTCGACGAG GTGCACGGCT TCCGCTATTT CGACTCCCGC GACCTCCTCG GATTCGTCGA CGGCACCGAG AATCCCACCG
00961  ACGACGACGC CGCGGACTCC GCCCTGATCG GCGACGAGGA CCCCGACTTC CGGGGCGGCA GTTACGTGAT CGTGCAGAAG
01041  TACCTGCACG ACATGAGCGC GTGGAACACG CTGAGCACCG AGGAACAGGA ACGGGTCATC GGGCGCACCA AGCTCGAGAA
01121  CGTCGAACTC GACGACGACG CCCAGCCCAG CAATTCGCAC GTCACCCTCA ACACCATCGT CGACGACGAC GGCGTCGAAC
01201  ACGACATCCT CCGCGACAAC ATGGCATTCG GCAGCCTCGG CGAGGCGGAA TACGGCACCT ACTTCATCGG GTACGCCAAG
01281  GACCCCGCCG TCACCGAGCT GATGTTGCGA CGCATGTTTC TCGGCGAGCC GCCCGGCAAC TACGACCGCG TCCTCGACTT
01361  CTCCACGGCG GCCACCGGCA CATTGTTCTT CGTGCCGAGC CGGGACGTGC TCGAATCGCT CGGCGACGAG CCGGCCGGCG
01441  CGGAGTCGGC ACCCGAAGAC CCGGTCGAGC CCGCCGCGGC CGGCCCGTAC GACCTGTCCC TGAAAATCGG TGGTCTCAAA
01521  GGAGTATCGC AATGAATCAG TTCTGGACCA GCGAGCTGTG CTGCGACTCG TGGCGTAATC ATGGTCATAG CTGTTTCCTG
01601  TGTGAAATTG TTATCCGCTC ACAATTCCAC ACAACATACG AGCCGGAAGC ATAAAGTGTA AAGCCTGGGG TGCCTAATGA
01681  GTGAGCTAAC TCACATTAAT TGCGTTGCGC TCACTGCCCG CTTTCCAGTC GGGAAACCTG TCGTGCCAGC TGCATTAATG
01761  AATCGGCCAA CGCGCGGGGA GAGGCGGTTT GCGTATTGGG CGCTCTTCCG CTTCCTCGCT CACTGACTCG CTGCGCTCGG
01841  TCGTTCGGCT GCGGCGAGCG GTATCAGCTC ACTCAAAGGC GGTAATACGG TTATCCACAG AATCAGGGGA TAACGCAGGA
01921  AAGAACATGT GAGCAAAAGG CCAGCAAAAG GCCAGGAACC GTAAAAAGGC CGCGTTGCTG GCGTTTTTCC ATAGGCTCCG
02001  CCCCCCTGAC GAGCATCACA AAAATCGACG CTCAAGTCAG AGGTGGCGAA ACCCGACAGG ACTATAAAGA TACCAGGCGT
02081  TTCCCCCTGG AAGCTCCCTC GTGCGCTCTC CTGTTCCGAC CCTGTCGCTT ACCGGATACC TGTCCGCCTT TCTCCCTTCG
02161  GGAAGCGTGG CGCTTTCTCA TAGCTCACGC TGTAGGTATC TCAGTTCGGT GTAGGTCGTT CGCTCCAAGC TGGGCTGTGT
02241  GCACGAACCC CCCGTTCAGC CCGACCGCTG CGCCTTATCC GGTAACTATC GTCTTGAGTC CAACCCGGTA AGACACGACT
02321  TATCGCCACT GGCAGCAGCC ACTGGTAACA GGATTAGCAG AGCGAGGTAT GTAGGCGGTG CTACAGAGTT CTTGAAGTGG
02401  TGGCCTAACT ACGGCTACAC TAGAAGAACA GTATTTGGTA TCTGCGCTCT GCTGAAGCCA GTTACCTTCG GAAAAAGAGT
02481  TGGTAGCTCT TGATCCGGCA AACAAACCAC CGCTGGTAGC GGTGGTTTTT TTGTTTGCAA GCAGCAGATT ACGCGCAGAA
02561  AAAAAGGATC TCAAGAAGAT CCTTTGATCT TTTCTACGGG GTCTGACGCT CAGTGGAACG AAAACTCACG TTAAGGGATT
02641  TTGGTCATGA GATTATCAAA AAGGATCTTC ACCTAGATCC TTTTAAATTA AAAATGAAGT TTTAAATCAA TCTAAAGTAT
02721  ATATGAGTAA ACTTGGTCTG ACAGTTACCA ATGCTTAATC AGTGAGGCAC CTATCTCAGC GATCTGTCTA TTTCGTTCAT
02801  CCATAGTTGC CTGACTCCCC GTCGTGTAGA TAACTACGAT ACGGGAGGGC TTACCATCTG GCCCCAGTGC TGCAATGATA
02881  CCGCGAGACC CACGCTCACC GGCTCCAGAT TTATCAGCAA TAAACCAGCC AGCCGGAAGG GCCGAGCGCA GAAGTGGTCC
02961  TGCAACTTTA TCCGCCTCCA TCCAGTCTAT TAATTGTTGC CGGGAAGCTA GAGTAAGTAG TTCGCCAGTT AATAGTTTGC
03041  GCAACGTTGT TGCCATTGCT ACAGGCATCG TGGTGTCACG CTCGTCGTTT GGTATGGCTT CATTCAGCTC CGGTTCCCAA
03121  CGATCAAGGC GAGTTACATG ATCCCCCATG TTGTGCAAAA AAGCGGTTAG CTCCTTCGGT CCTCCGATCG TTGTCAGAAG
03201  TAAGTTGGCC GCAGTGTTAT CACTCATGGT TATGGCAGCA CTGCATAATT CTCTTACTGT CATGCCATCC GTAAGATGCT
03281  TTTCTGTGAC TGGTGAGTAC TCAACCAAGT CATTCTGAGA ATAGTGTATG CGGCGACCGA GTTGCTCTTG CCCGGCGTCA
03361  ATACGGGATA ATACCGCGCC ACATAGCAGA ACTTTAAAAG TGCTCATCAT TGGAAAACGT TCTTCGGGGC GAAAACTCTC
03441  AAGGATCTTA CCGCTGTTGA GATCCAGTTC GATGTAACCC ACTCGTGCAC CCAACTGATC TTCAGCATCT TTTACTTTCA
03521  CCAGCGTTTC TGGGTGAGCA AAAACAGGAA GGCAAAATGC CGCAAAAAAG GGAATAAGGG CGACACGGAA ATGTTGAATA
03601  CTCATACTCT ACCTTTTTCA ATATTATTGA AGCATTTATC AGGGTTATTG TCTCATGAGC GGATACATAT TTGAATGTAT
03681  TTAGAAAAAT AAACAAATAG GGGTTCCGCG CACATTTCCC CGAAAAGTGC CACCTGACGT CTAAGAAACC ATTATTATCA
03761  TGACATTAAC CTATAAAAAT AGGCGTATCA CGAGGCCCTT TCGTC
```

Figure 9.1: DNA sequence of pUCIDT-AMP-DypB, as synthesised by Integrated DNA technologies. The *DypB* gene is shown in blue. A plasmid map is given in chapter 5, figure 5.1.

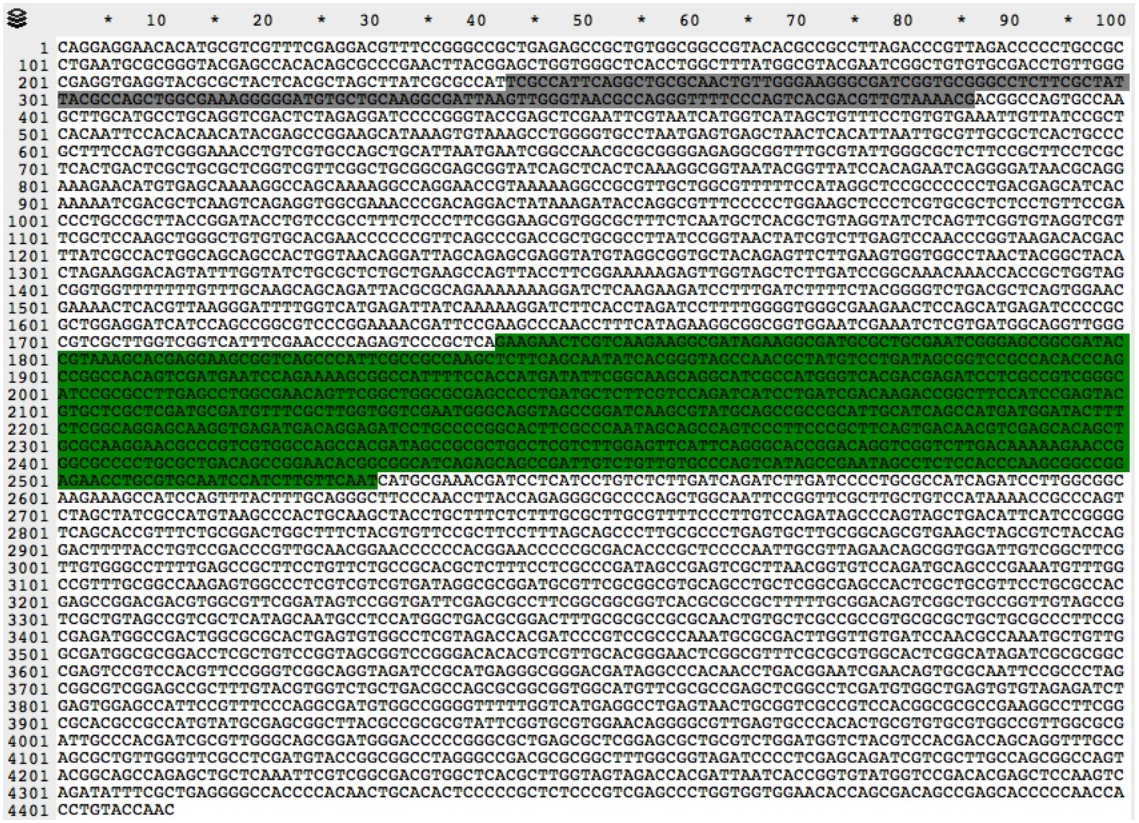


Figure 9.2: DNA sequence of pNV18.1, the *E. coli – Rhodococcus* shuttle vector as provided by Dr Jun Ishikawa, National Institute for Infectious Diseases, Tokyo (Chiba et al., 2007). The green sequence is *aph* (kanamycin/neomycin resistance) and grey is *lacZ*. A plasmid map is given in chapter 5, figure 5.1.